Vol. 64 • No. 1

January 2021

Microwave Journal

horizon house®

Founded in 1958

mwjournal.com


ANALOG DEVICES
AHEAD OF WHAT'S POSSIBLE™
COMMUNICATIONS
RADAR
ELECTRONIC WARFARE
We Have You Covered from RF to Bits
The industry's most complete portfolio of ICs and modules.
RF/µW Amplifiers/ TR Modules
Analog Beamforming
Frequency Conversion
Converters and Transceivers
ADC
DAC
Power
Find your competitive advantage at analog.com/ADEF

Designed For
5G MIMO Active Antenna!!!
The World First SMT Microstrip Patented Isolator/Circulator at 28GHz & 38GHz

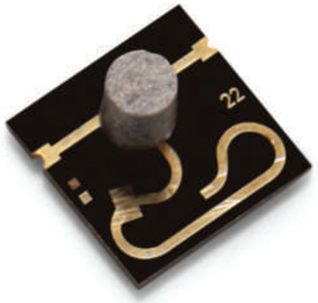

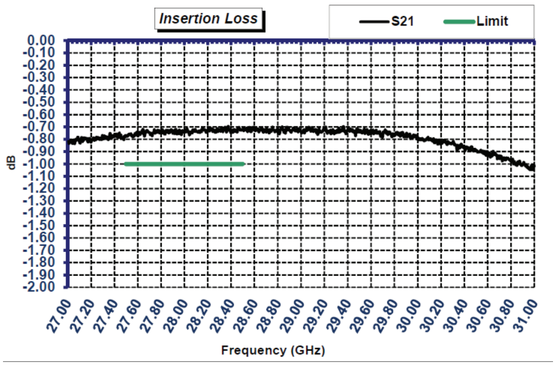

- No Metal Bias Needed
- Easy Reflow Assembly
- No Expensive Wire Bonding

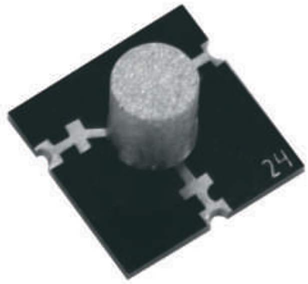

- 200kpcs Sold For Similar Array Application
- Proven Technology

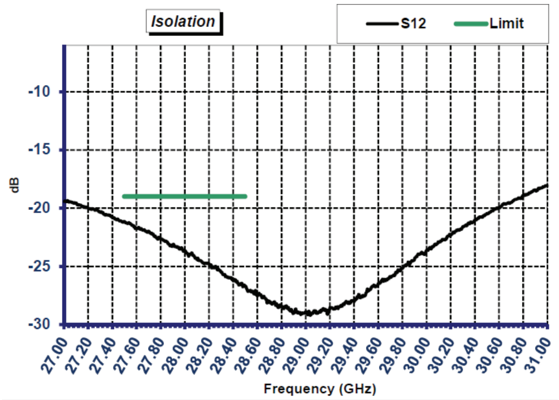


Waveguide Isolators


Surface Mount Circulators


Coaxial Circulators


Cavity Filters


Ceramic Filters

JQL

Tel:1(888)236-9828(US&Canada)

www.jqlelectronics.com sales@jqlelectronics.com

DC TO MMWAVE

Preferred by 20,000+

More than Just a Supplier

Selection and Solutions

- 27 product lines from one source
- 7500+ models in stock and growing
- Coverage from VHF to mmWave
- Custom components, integrated systems and test solutions with fast turnaround

Service

- Global presence, local service
- Accessible engineering and support
- Same-day shipping and on-time delivery
- Short lead times and low minimums

Peace of Mind

- Award-winning quality excellence
- Easy troubleshooting and RMA process
- Supply chain security through the life of your system—no EOL target

Constant Innovation

- Relentless investment in new products and design capabilities
- 400+ catalog introductions per year
- Patented technologies

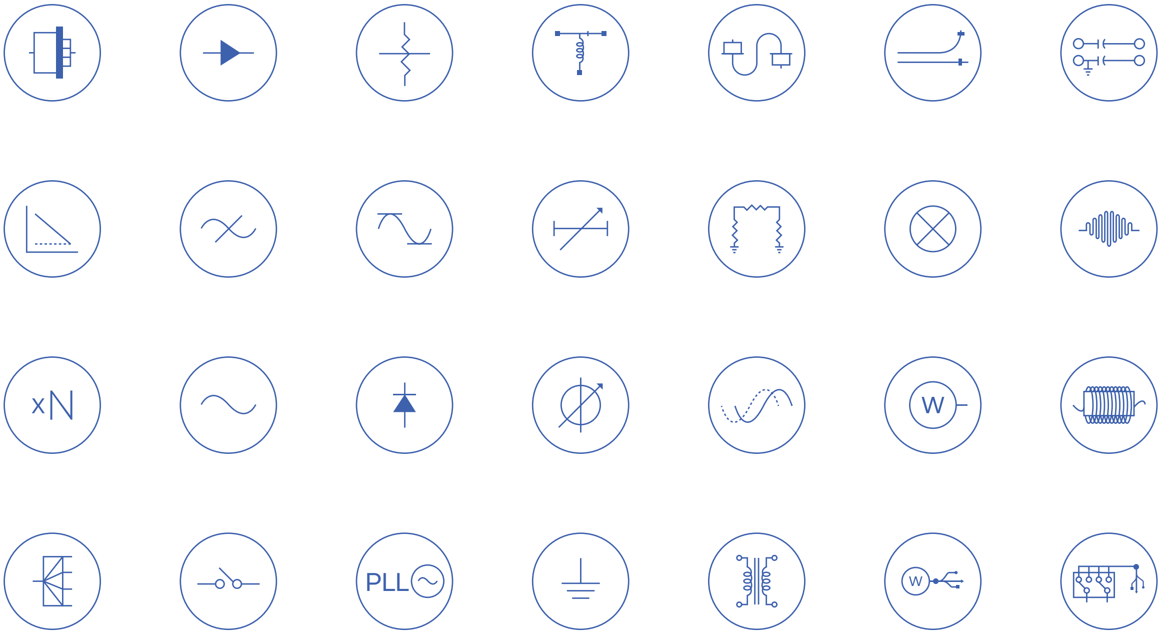

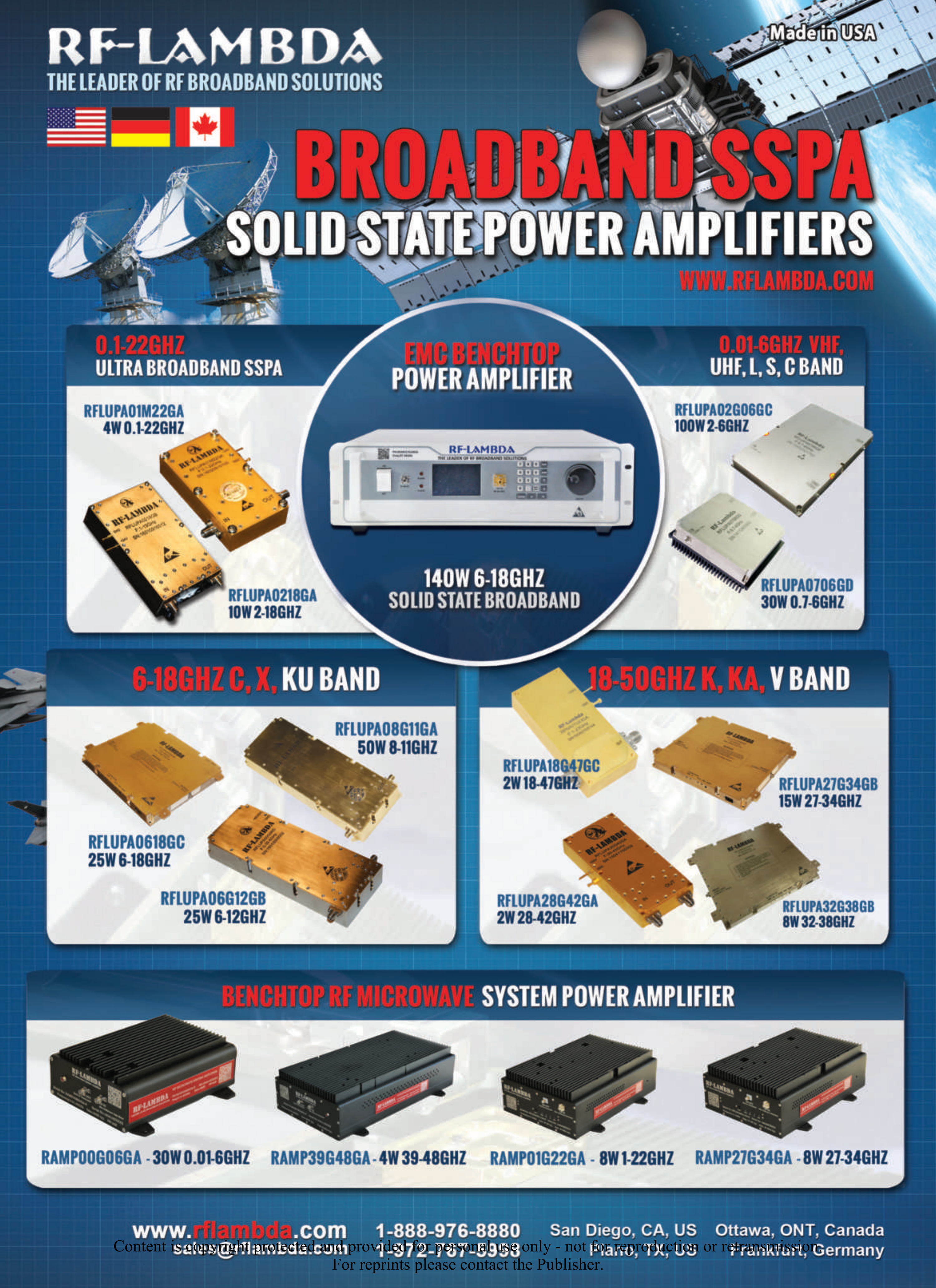

RF-LAMBDA
THE LEADER OF RF BROADBAND SOLUTIONS
Made in USA
BROADBAND SSPA
SOLID STATE POWER AMPLIFIERS
WWW.RFLAMBDA.COM
0.1-22GHZ
ULTRA BROADBAND SSPA
RFLUPA01M22GA
4W 0.1-22GHZ
RFLUPA0218GA
10W 2-18GHZ
EMC BENCHTOP
POWER AMPLIFIER
140W 6-18GHZ
SOLID STATE BROADBAND
0.01-6GHZ VHF,
UHF, L, S, C BAND
RFLUPA02G06GC
100W 2-6GHZ
RFLUPA0706GD
30W 0.7-6GHZ
6-18GHZ C, X, KU BAND
RFLUPA08G11GA
50W 8-11GHZ
RFLUPA0618GC
25W 6-18GHZ
RFLUPA06G12GB
25W 6-12GHZ
18-50GHZ K, KA, V BAND
RFLUPA18G47GC
2W 18-47GHZ
RFLUPA27G34GB
15W 27-34GHZ
RFLUPA28G42GA
2W 28-42GHZ
RFLUPA32G38GB
8W 32-38GHZ
BENCHTOP RF MICROWAVE SYSTEM POWER AMPLIFIER
RAMP00G06GA - 30W 0.01-6GHZ
RAMP39G48GA - 4W 39-48GHZ
RAMP01G22GA - 8W 1-22GHZ
RAMP27G34GA - 8W 27-34GHZ
www.rflambda.com 1-888-976-8880 San Diego, CA, US Ottawa, ONT, Canada
Frankfurt, Germany


Get Where You're Going with...
K&L MICROWAVE
a DOVER company
K&L's pre-filtered GPS LNAs
• Covers L1, L2, L5 and combinations
• Gains available 16 to 40 dB
• Low Noise Figure - Typically 1.8 dB or less
• Available with or without internal limiter
• Rugged design for harsh military environments
• Other frequencies available
Microwave Products Group
a DOVER company
K&L MICROWAVE
POLE ZERO
BSC
Dow-Key Microwave
ENABLING COMMUNICATION AND SIGNAL CONTROL
www.klmicrowave.com • www.klfilterwizard.com • 410-749-2424 • sales@klmicrowave.com •


Relax
We've got you covered
NOISEWAVE
NW18G-23CS
NW346B Precision
NW6G-D
NW18G-15CS
NW2G-15CS
NW3G-M
Your supplier of high performance, precise equipment for AWGN
NOISEWAVE
The new wave in NOISE
Ph. (973) 386-1119 • Fax (973) 386-1131 • info@noisewave.com • www.noisewave.com

Planar Monolithics Industries, Inc.

Limiting Amplifiers, up to 20 GHz

PMI offers a variety of Limiting Amplifiers that cover narrow to multi octave bandwidths up to 20 GHz. These Amplifiers are designed for Military and Industrial applications that require a stable, limited output level. More models are available at: https://www.pmi-rf.com/categories/limiting-amplifiers

- Amplifiers - Solid State
- Attenuators - Variable/ Programmable
- Bi-Phase Modulators
- Couplers (Quadrature, 180, Directional)
- Detectors - RF / Microwave
- DLVAs, ERLVAs & SDLVAs
- Filters & Switched Filter Banks
- Form, Fit, Functional Products & Services
- Frequency Converters
- Frequency Sources
- Frequency Discriminators & IFM
- Frequency Synthesizers
- Gain & Loss Equalizers
- Integrated MIC/MMIC Assemblies (IMAs)
- IQ Vector Modulators
- Limiters - RF / Microwave
- Log Amps
- Miscellaneous Products
- Monopulse Comparators
- Multifunction Integrated Assemblies (IMAs)
- Phase Shifters & Bi-Phase Modulators
- Power Dividers/Combiners (Passive & Active)
- Pulse Modulators - SPST
- Rack & Chassis Mount Products
- Receiver Front Ends & Transceivers
- Single Side Band Modulators
- SMT & QFN Products
- Switch Matrices
- Switch Filter Banks
- Switches - Solid-State
- Systems - Radar Sense & Avoid
- Systems - Fly Eye Radar
- Threshold Detectors
- USB Products

PEC2-50M2500M-2DBM-LM-SFF

PEC-150M6G-17LM-SFF
PEC-100M20D1G-20LM-SFF
PEC-100M16G-17LM-SFF

PEC-85-0R32R5-15LM-12-SFF

PEC2-1G12G-60-21DBM-LM-PP

PMI Model No.	Freq Range (GHz)	Noise Figure (dB)	Input Power (dBm)	Output Power (dBm)	Output Power Flatness (dB)	Size (Inches) / Connectors
PEC2-50M2500M-2DBM-LM-SFF https://www.pmi-rf.com/product-details/pec2-50m2500m-2dbm-lm-sff	50 MHz - 2.5	10 dB Typ above 500 MHz	-50 to +30	+2 Nom	±3.5	2.98" x 0.78" x 0.26" SMA (F)
PEC-100M16G-17LM-SFF https://www.pmi-rf.com/product-details/pec-100m16g-17lm-sff	100 MHz - 16	< 6 dB Above 1 GHz, < 9 dB Below 1 GHz	-12 to +16	+16 Min, +21 Max	±2.0 Max	1.91" x 0.70" x 0.36" SMA (F)
PEC-100M20D1G-20LM-SFF https://www.pmi-rf.com/product-details/pec-100m20d1g-20lm-sff	100 MHz - 20.1	< 6 dB Above 1 GHz, < 9 dB Below 1 GHz	-12 to +16	+19 Min, +24 Max	±2.5 Max	1.91" x 0.70" x 0.36" SMA (F)
PEC-150M6G-17LM-SFF https://www.pmi-rf.com/product-details/pec-150m6g-17lm-sff	150 MHz - 6.1	< 6 dB Above 1 GHz, < 9 dB Below 1 GHz	-12 to +16	+16 Min, +21 Max	±2.0 Max	1.91" x 0.70" x 0.36" SMA (F)
PEC-85-0R32R5-15LM-12-SFF https://www.pmi-rf.com/product-details/pec-85-0r32r5-15lm-12-sff	300 MHz - 2.5	5.0 dB Typ	-65 to +10	+15	± 2.5	5.0" x 1.5" x 0.51" SMA (F)
PEC2-1G12G-60-21DBM-LM-PP https://www.pmi-rf.com/product-details/pec2-1g12g-60-21dbm-lm-pp	1 - 12	8 dB Typ	-61 to +15	21 Min	±2.0 Nom	2.98" x 0.78" x 0.26" RF PIN / PIN
PEC2-1G18G-60-9DBM-LM-SFF https://www.pmi-rf.com/product-details/pec2-1g18g-60-9dbm-lm-sff	1 - 18	8 dB Typ	-61 to +30	+7 to +11 Max	±2.0	2.98" x 0.78" x 0.26" SMA (F)
PEC3-40-1D6G2D7G-15LM-SFF https://www.pmi-rf.com/product-details/pec3-40-1d6g2d7g-15lm-sff	1.6 - 2.7	5.5 dB Max	-25 to +5 Min, -30 to +5 Typ	+15 Min	±1.5	1.91" x 0.78" x 0.36" SMA (F)
PEC3-40-2G6G-15LM-SFF-HS https://www.pmi-rf.com/product-details/pec3-40-2g6g-15lm-sff-hs	1.85 - 6.25	5.5 dB Max	-15 to +17	+15 Min	±1.5 Max	1.91" x 0.78" x 0.36" SMA (F)
PEC2-2G18G-80DB-21DBM-LM-SFF https://www.pmi-rf.com/product-details/pec2-2g18g-80db-21dbm-lm-sff	2 - 18	10 dB Max	-55 to +10	+21 to +25 Nom	±2.0	2.98" x 0.78" x 0.26" SMA (F)
PEC2-2G18G-2DBM-LM-SFF https://www.pmi-rf.com/product-details/pec2-2g18g-2dbm-lm-sff	2 - 18	10 dB Max	-50 to +30	+2 Nom	±2.0 Max	2.98" x 0.78" x 0.26" SMA (F)
PEC2-2G18G-21DBM-LM-SFF https://www.pmi-rf.com/product-details/pec2-2g18g-21dbm-lm-sff	2 - 18	5 dB Max	-45 to +10	+21 to +25 Nom	±2.0 Max	2.98" x 0.78" x 0.26" SMA (F)
PEC2-3D1G3D5G-60-10DBM-LM-SFF https://www.pmi-rf.com/product-details/pec2-3d1g3d5g-60-10dbm-lm-sff	3.1 - 3.5	8.0 dB Typ	-61 to +30 Min	+8 Min, +11 Max	±1.0 Typ	2.98" x 0.78" x 0.26" SMA (F)

PEC3-40-1D6G2D7G-15LM-SFF
PEC3-40-2G6G-15LM-SFF-HS

PEC2-1G18G-60-9DBM-LM-SFF
PEC2-2G18G-80DB-21DBM-LM-SFF
PEC2-2G18G-2DBM-LM-SFF

PEC2-2G18G-21DBM-LM-SFF
PEC2-3D1G3D5G-60-10DBM-LM-SFF

West Coast Operation:
4921 Robert J. Mathews Pkwy, Suite 1
El Dorado Hills, CA 95762 USA
Tel: 916-542-1401, Fax: 916-265-2597

East Coast Operation:
7311-F Grove Road
Frederick, MD 21704 USA
Tel: 301-662-5019, Fax: 301-662-1731

sales@pmi-rf.com • www.pmi-rf.com

ISO9001-2015 REGISTERED

Microwave Journal

January 2021
Vol. 64 • No. 1
Radar and Antennas
mwjournal.com

CONTENTS

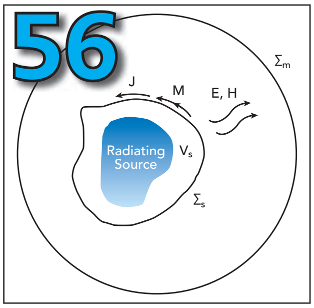

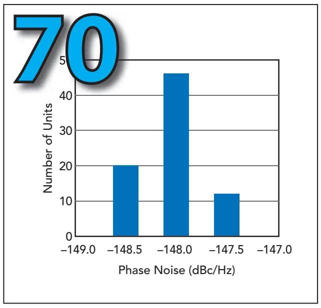

Look for this month's exclusive article online at mwjournal.com

Publisher's Note

Cover Feature

Technical Features

Application Notes

64 YEARS OF PUBLISHING EXCELLENCE

cādence®

Design Smarter with AWR Software

See for yourself how easy and effective it is to streamline your design process, improve end-product performance, and accelerate time to market for MMICs, RF PCBs, microwave modules, antennas, communications systems, radar systems, and more.

Get started at **cadence.com/go/awr/try**.

Microwave Journal

CONTENTS

mwjournal.com

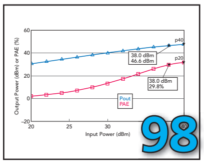

Microwave Journal (USPS 396-250) (ISSN 0192-6225) is published monthly by Horizon House Publications Inc., 685 Canton St., Norwood, MA 02062. Periodicals postage paid at Norwood, MA 02062 and additional mailing offices.

POSTMASTER: Send address corrections to Microwave Journal, PO Box 1028, Lowell, MA 01853 or e-mail mwj@e-circ.net.com. Subscription information: (978) 671-0446. This journal is issued without charge upon written request to qualified persons working in the RF & microwave industry. Other subscriptions are: domestic, $120.00 per year, two-year subscriptions, $185.00; foreign, $200.00 per year, two-year subscriptions, $370.00; back issues (if available) and single copies, $10.00 domestic and $20.00 foreign. Claims for missing issues must be filed within 90 days of date of issue for complimentary replacement.

STAFF

Publisher: Carl Sheffres
Associate Publisher: Michael Hallman
Editor: Patrick Hindle
Technical Editor: Gary Lerude
Managing Editor: Jennifer DiMarco
Associate Technical Editor: Cliff Drubin
Copy Editor: Kelley Roche
Multimedia Staff Editor: Barbara Walsh
Contributing Editor: Janine Love
Electronic Marketing Manager: Chris Stanfa
Senior Digital Content Specialist: Lauren Tully
Digital Content Specialist: Corey Gallagher
Audience Development Manager: Carol Spach
Traffic Manager: Edward Kiessling
Director of Production & Distribution: Robert Bass
Art Director: Janice Levenson
Graphic Designer: Ann Pierce

EUROPE

Office Manager: Nina Plesu

CORPORATE STAFF

CEO: William M. Bazzy
President: Ivar Bazzy
Vice President: Jared Bazzy

EXECUTIVE EDITORIAL OFFICE
685 Canton Street, Norwood, MA 02062
Tel: (781) 769-9750
FAX: (781) 769-5037
e-mail: mwj@mwjournal.com

EUROPEAN EDITORIAL OFFICE
16 Sussex Street, London SW1V 4RW, England
Tel: Editorial: +44 207 596 8730 Sales: +44 207 596 8740
FAX: +44 207 596 8749

SUBSCRIPTION SERVICES
Send subscription inquiries and address changes to:
Tel: (978) 671-0446
e-mail: mwj@e-circ.net

BPA WORLDWIDE

www.mwjournal.com

Printed in the USA

Microwave Journal Online

Visit us @ mwjournal.com

E LEARNING CENTER

How to Efficiently Run Electromagnetic Simulation of Full Circuit Blocks
Sponsored by: Cadence 1/27

Executive Interviews

Kevin Schoenrock, president of the recently formed **OpenRF Association**, discusses the need for interoperability among the myriad of 5G RF front-ends and chipset platforms and how OpenRF aims to facilitate industry-wide interface standards.

Matthias Frei, CEO of **Micram**, discusses the vision that led him to start the custom IC company and his continuing quest to develop the highest speed data converters and signal processing platforms.

FEATURED eBooks

mwjournal.com/ebooks

WHITE PAPERS

cadence — How to Speed Up Large-Scale EM Simulation of ICs Without Comprising Accuracy

Coilcraft — Key Parameters for Selecting RF Inductors

KEYSIGHT TECHNOLOGIES — Application Note: Electronic Warfare Signal Generation Technologies and Methods

ROHDE&SCHWARZ Make ideas real — 5G Evolution – On the Path to 6G

Automated ADAS Test System Trial with Radar Sensors and Electromagnetic Interference

TELEDYNE e2v | Semiconductors Everywhereyoulook — Making History: Advanced System in a Package Technologies Enable Direct RF Conversion

Join Us Online

Follow us
@Pathindle
@MWJGary
@MWJEditor

Join us at the RF and Microwave Community

Become a fan at facebook.com/microwavejournal

Catch *Frequency Matters*, the industry update from *Microwave Journal*,
microwavejournal.com/FrequencyMatters

.COM

Matchmaker

0402DC Series Designer's Kit (C472-2):
20 samples each of 112 inductance values,
including 0.1 nH increments from 2.8 nH to 10 nH

Looking for the perfect high-Q inductor for impedance matching in RF/microwave antenna circuits? This kit has it!

Coilcraft 0402DC Series wirewound chip inductors offer the industry's highest Q factors in an 0402 (1005) size for super low loss in high frequency circuits. And with 112 values from 0.8 to 120 nH, including **0.1 nH increments from 2.8 nH to 10 nH**, you'll have exactly what you need for all your RF and Microwave applications.

The 0402DC also features wirewound construction for extremely high self resonance – up to 28.8 GHz – and offers DCR as low as 25 mΩ, significantly lower than other inductors this size.

Equip your lab with the ultimate impedance matching resource. Our C472-2 Designer's Kit has 20 samples of all 112 values! Purchase one online at **www.coilcraft.com/0402DC.**

Coilcraft®

coilcraftdirect.com
No min order. Next day delivery.

WWW.COILCRAFT.COM

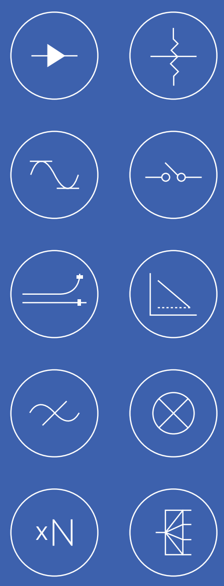
xN

FEBRUARY

MARK YOUR CALENDAR

19-20

VIRTUAL

International Conference on Computing, Communication and Intelligent Systems (ICCCIS-2021) is an international forum which aims to bring together leading academician, researchers and research scholars to exchange and share their experiences and hard-earned technological advancements related to computing, communication and intelligent systems.
www.icccis.in

MARCH & APRIL

6-13

IEEE AEROSPACE CONFERENCE
YELLOWSTONE CONFERENCE CENTER, BIG SKY, MONTANA, MAR 6 - MAR 13, 2021

VIRTUAL

The international IEEE Aerospace Conference is organized to promote an understanding of aerospace systems, their underlying science and technology and their applications to government and commercial endeavors. The plenary sessions feature internationally prominent researchers working on frontiers of science and engineering that may significantly impact the world we live in. Registrants are briefed on cutting edge technologies emerging from and intersecting with their disciplines. Each year, a large number of presentations are given by professionals distinguished in their fields and by high-ranking members of the government and military.
https://aeroconf.org

23-25

VIRTUAL

emv

International exhibition and workshops on electromagnetic compatibility
Stuttgart, 23 – 25 March 2021

If EMC testing, devices, guidelines and certifications are your thing, join us at EMV, the conference and workshops dedicated to electromagnetic compatibility (EMC). The wide range of training options makes day-to-day work in the EMC sector easier for participants. The event covers all aspects of electromagnetic compatibility and provides experts with a dedicated platform to actively work on creating an interference-free future.
https://emv.mesago.com/stuttgart/en.html

3-29/4-1

VIRTUAL

GOMACTech was established primarily to review developments in microcircuit applications for government systems. Established in 1968, the conference has focused on advances in systems being developed by the Department of Defense along with other government agencies and has been used to announce major government microelectronics initiatives, such as VHSIC and MIMIC, and provides a forum for government reviews.
www.gomactech.net

3-31/4-1

Paris, France

The sixth edition of Microwave & RF Show is dedicated to the sectors of radio frequencies, microwaves, wireless, EMC and optical Fiber that will, for two days, provide a 360-degree view of these markets. Highlights of this trade show include eight sessions and conferences covering connected wireless objects; the field of EMC; new methods of measurements or EMC tests; the EMC connectivity, architectures and technologies of microwave functions applied to drones; backhaul to 94 GHz network for 5G; and trends or "point" on the RAN 5G.
www.microwave-rf.com/?lang=EN

FOR DETAILS, VISIT MWJOURNAL.COM/EVENTS

ComingEvents

CALL FOR PAPERS

EuMW 2021
February 26, 2021

IEEE AUTOTESTCON 2021
March 30, 2021

EDI CON China 2021
May 15, 2021

SEMICON West
June 1, 2021

mwjournal.com

JANUARY

IEEE Radio & Wireless Week (RWW)
January 17–20 • Virtual
www.radiowirelessweek.org

96th ARFTG Microwave Measurement Symposium
January 17–20 • Virtual
www.arftg.org

FEBRUARY

International Conference on Computing, Communication and Intelligent Systems (ICCCIS)
February 19–20 • Virtual
www.icccis.in

MARCH

2021 IEEE Aerospace Conference
March 6–13 • Virtual
https://aeroconf.org

EMV
March 23–25 • Virtual
https://emv.mesago.com/stuttgart/en.html

GOMACTech 2021
March 29–April 1 • Virtual
www.gomactech.net

Microwave & RF
March 31–April 1 • Paris, France
www.microwave-rf.com/?lang=EN

APRIL

IEEE WAMICON
April • Clearwater Beach, Fla. & Virtual
www.ieeewamicon.org

DesignCon 2021
April 13–15 • San Jose, Calif.
www.designcon.com/en/home.html

2021 IEEE Conference on Technologies for Sustainability (SusTech)
April 22–24 • Virtual
https://ieee-sustech.org

MAY

IEEE EMC+SIPI 2021
May 3–7 • Raleigh, N.C.
www.emc2021usa.emcss.org

Space Tech Expo USA
May 10–12 • Long Beach, Calif.
www.spacetechexpo.com

PCB East
May 10–12 • Marlborough, Mass.
https://pcbeast.com

CS Mantech
May 24–27 • Orlando, Fla.
www.csmantech.org

JUNE

IEEE MTT-S IMS2021
June 6–11 • Atlanta, Ga.
https://ims-ieee.org/ims2021

IEEE RFIC 2021
June 6–8 • Atlanta, Ga. + Virtual
https://rfic-ieee.org

Military Space USA
June 8–9 • Los Angeles, Calif.
www.smi-online.co.uk/defence/northamerica/milspace-usa

IEEE International Conference on Communications (ICC)
June 14–18 • Montreal, Canada
https://icc2021.ieee-icc.org

MilSatCom USA
June 23–24 • Arlington, Va.
www.smi-online.co.uk/defence/northamerica/MilSatCom-USA

Zooming Ahead to Atlanta

Carl Sheffres
Microwave Journal *Publisher*

I was at the Satellite show with my colleagues last March when the world as we knew it ended. It was day two of the exhibition and late in the afternoon we received word that day three was cancelled, as large gatherings had just been banned. I flew home that night and have not been on an airplane since.

In the ensuing months, nearly all planned industry events, including the venerable IEEE MTT-S International Microwave Symposium, were either cancelled outright or pivoted to a virtual experience. These events varied in their level of success, but one thing proved true—if you deliver valuable information, people will attend. As an example, IMS drew more than 8,000 engineers, students and exhibitors to its virtual event in August. EDI CON Online in October attracted more than 5,300 unique registrants: a 150 percent increase over 2019. We produced a one-day Power Amplifier Design Forum for a client in November that generated more than 1,600 registrants. People are busy, but they still thirst for knowledge.

This year we hope to see a steady movement toward normalcy. The 2020 European Microwave Week event, first postponed and now virtual, takes place this month. It features its typically strong conference sessions and a more dynamic exhibition platform than many of us have experienced. The 2021 event is planned for London on October 10-15 as a live event. You can submit a paper at www.eumw2021.com.

IMS2021 is scheduled for Atlanta on June 6-11. It is planned as a live event, with some virtual components, still to be determined. It will include some new features like the Connected Future Summit showcasing next-generation wireless technologies for mobility, V2X and IoT and the Automotive Pavilion where the latest automotive radar and autonomous driving technology will debut. IMS is typically a networking mecca, so hopefully we can finally gather together again in Atlanta and catch up with one another.

In the meantime, we have many plans to keep you informed and engaged this year. We launched a new virtual panel series last month, with the debut edition titled, "Will Open RAN Work?". This month's panel session is on the "Evolution of the RF Front End" on January 26. Both can be viewed on demand. The editors continue to host their popular Frequency Matters video series and the more recent podcast series, which is both insightful and informative. EDI CON Online moves to every Wednesday in August this year and features tracks on 5G/Wi-Fi/IoT (8/4), PCB/Interconnect (8/11), Signal Integrity/Power Integrity (8/18) and Radar/Automotive/SATCOM (8/25).

This magazine continues to deliver high-quality content in print, digital and mobile formats. You can access it from anywhere and at any time. This month's theme is the always popular "Radar & Antennas" and features a cover story on the "Design of a mmWave MIMO Radar System" authored by Cadence and VTT Technical Research Centre of Finland. January is always a good time to renew your subscription for the year at www.mwjournal.com/subscribe.

After nearly a year, I am more than ready to get back on an airplane and actually see people in person again. I have had enough Zoom and Teams meetings to last a lifetime. See you in Atlanta, if not sooner!

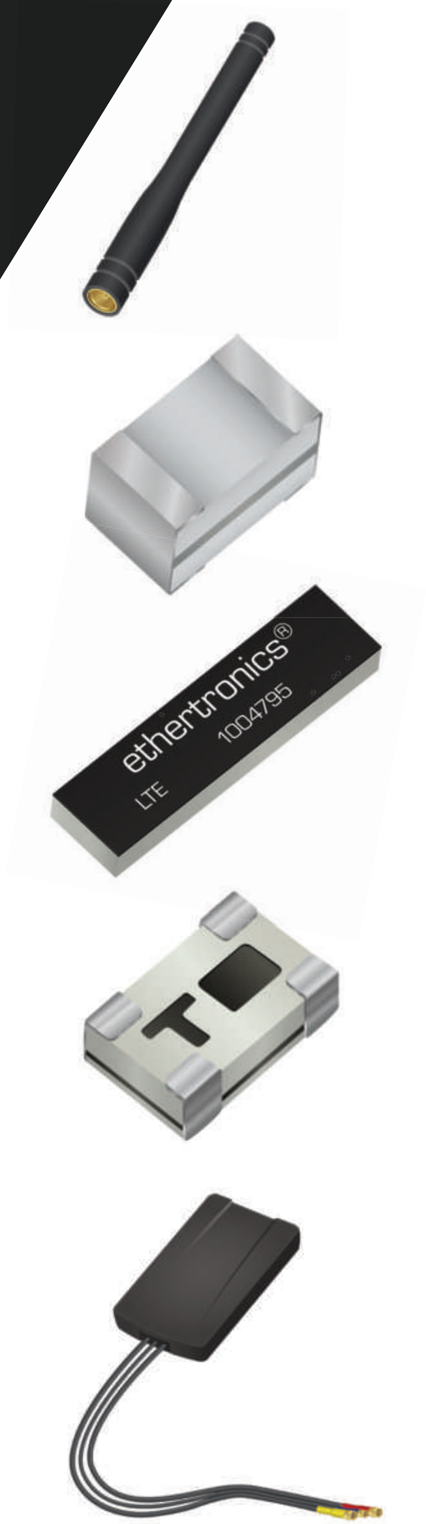
ethertronics®
LTE
1004795

NOW HIRING!

Application Engineers
Design Engineers
Product Engineers
Test Engineers

Waveguide Magic Tees
Offered in waveguide and split-block configurations, low insertion loss, even port balance, and high isolation. Available in full band models across 18 to 110 GHz.

Full Band Attenuators
Waveguide based attenuators of four types: fixed, level setting, direct reading and programmable. These attenuators are offered to cover the frequency range of 18 to 140 GHz.

Tunable Waveguide Shorts
Offered for applications where phase variations are required. The standard offering covers the frequency range of 26.5 to 170 GHz. Higher frequency bands up to 220 GHz are available.

Waveguide to Coax Adapters
Offered in end launch and right angle configurations with numerous environmental accommodations including weather resistant, TVAC, and space applications. Frequency coverage from 8.4 to 130 GHz.

Waveguide Power Dividers
Available in 2N way power dividing configurations up to 32 ways. End launch and right angle versions are available, and models boast low insertion loss and high port isolation. Offered from 18 to 110 GHz.

COVER FEATURE
INVITED PAPER

Design of a mmWave MIMO Radar

Tero Kiuru and Henrik Forstén
VTT Technical Research Centre of Finland Ltd., Espoo, Finland

Radar uses reflected radio waves to determine the range, angle or velocity of objects. These detection systems, which were once the exclusive domain of the aerospace and defense industry, are now gaining popularity in the consumer industry, most notably for automotive radar applications used in adaptive cruise control and autonomous driving assistance systems.[1] The analog and RF hardware in modern frequency modulated continuous wave (FMCW) systems is considerably less complex than that of original pulse-Doppler radar, and commercial adoption is possible, in part, because of high volume semiconductor processes such as SiGe and CMOS technologies, which are enabling cost-effective systems for mass commercial applications.

This article presents a 60 GHz FMCW, frequency-division multiplexing (FDM), MIMO radar system for commercial radar applications.[2] The unique architecture enables the total number of transmit (Tx) and receive (Rx) channels to be scaled by the number of ICs in the system, while still maintaining phase coherence between channels. The approach provides high frame-rate measurement, excellent phase stability and a large field of view (FoV). The radar architecture and ICs are designed so the system can be scaled to much larger radars.

The intended use for the radar system in this article is short-range, high-resolution detection of nearby moving objects when the radar itself might be moving, intended to capture the flow of people, drones and other autonomous systems. In addition, the system can support simultaneous localization and mapping, object detection (e.g., automobiles) and remote multi-target vital sign measurements for medical applications. FDM was determined to be the best choice to address the high-resolution requirements, where code division multiplexing was too complicated and the need for accurate tracking of fast-moving objects made time division multiplexing impractical. In addition, FDM allows accurate phase measurements, which supports medical applications such as remote monitoring of heartbeat and breathing rates from the detection of small movements of the chest.

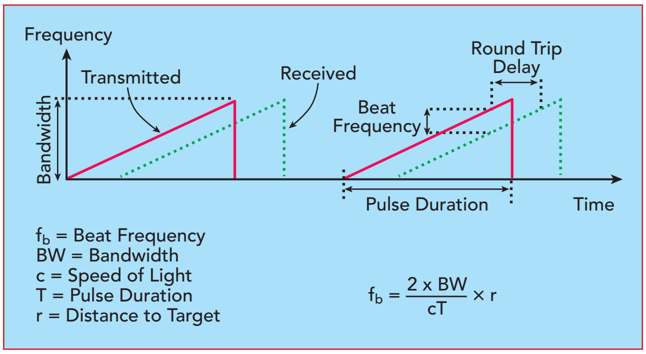

Fig. 1 **FMCW sawtooth waveforms.**

60 GHZ FMCW MIMO RADAR

Requirements for the radar system included fast imaging greater than 200 Hz, range resolution less than 5 cm, multi-target acquisition, moving target capability and high sensitivity to micromotion—all in a small, lightweight, low-cost footprint. The specifications for the system are:

- 1.5-degree angle resolution with 8 Tx – 8 Rx MIMO
- 3 to 5 cm range resolution
- 160-degree horizontal FoV
- 25-degree elevation FoV

The system offers a maximum detection range of 20 to 25 m for stationary human-size objects. Applying background subtraction, this range increases to 60 m for moving targets. The system also supports simultaneous detection of multiple moving objects without physically scanning the antenna. 3D systems with 160 × 160-degree FoV are also available.

While the radar system offers many potential use models, the multi-person vital sign extraction capability is interesting for future applications. For

RF & MICROWAVE FILTERS

RLC has the customized filter solutions you need.

RLC manufactures a complete line of RF and Microwave filters covering nearly every application in the DC to 50 GHz frequency range. We offer different filter types, each covering a specific engineering need.

In addition, our large engineering staff and high volume production facility give RLC the ability to develop and deliver both standard and custom designed filters at competitive costs, within days or a few weeks of order placement.

- Band Pass, Low Pass, High Pass & Band Reject
- Connectorized, Surface Mount, PCB Mount or Cable Filters
- Wave Guide Bandpass and Band Reject
- 4th Order Bessel Filters
- Spurious Free, DC to 50 GHz, Low Loss, High Rejection
- Custom Designs

For more detailed information, or to access ***RLC's exclusive Filter Selection Software****, visit our web site.*

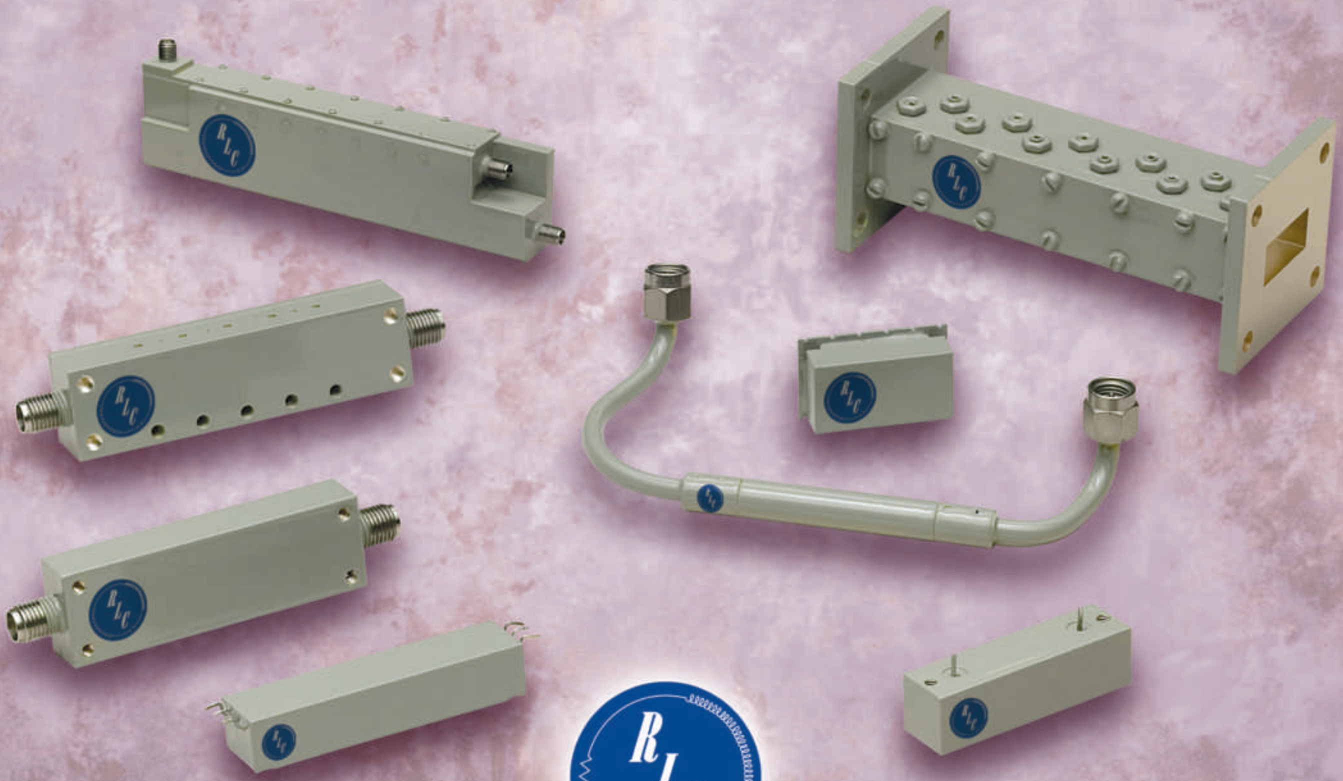

RLC ELECTRONICS, INC.

83 Radio Circle, Mount Kisco, New York 10549 • Tel: 914.241.1334 • Fax: 914.241.1753
E-mail: sales@rlcelectronics.com • www.rlcelectronics.com

ISO 9001:2000 CERTIFIED

RLC is your complete microwave component source...
Switches, Filters, Power Dividers, Terminations, Attenuators, DC Blocks, Bias Tees & Detectors.

data analysis, the speed of the radar technology is key, as it can operate at 200 frames per second (FPS) when not supporting visual graphics and 50 to 100 FPS with visualization.

FMCW OPERATION

A traditional pulsed radar detects the range to a target by emitting a short pulse and observing the time of flight of the returned target echo. This requires the radar to have high instantaneous transmit power and often results in a device with a large, expensive physical structure. FMCW radars achieve similar results using much smaller instantaneous transmit power and size by emitting a continuous microwave signal frequency modulated with a low frequency waveform, such as a sawtooth function with period T, whose duration is much greater than the return time of the echo (see ***Figure 1***).

Unlike pulsed radar, FMCW systems transmit and receive simultaneously, eliminating the blind range that occurs when the receiver in a pulsed radar is turned off during transmission. FMCW systems can detect reflected signals from objects very close to the radar, enabling it to measure distances down to a few centimeters. The system achieves excellent range resolution, which is proportional to the reciprocal of the bandwidth, i.e., $\Delta x = c/(2\Delta f)$, and high signal-to-noise ratio with narrow intermediate frequency (IF) bandwidth.

A simplified diagram of the system implemented in Cadence® AWR Design Environment®, specifically the AWR® Visual System Simulator™ (VSS) system design software, is shown in ***Figure 2***. The signal source is divided between the Tx and Rx sides. Details of the Tx power amplifier (PA) and Rx low noise amplifier (LNA) chains—not shown in the figure—can be developed further. The Tx and Rx signal paths must be well isolated to operate properly, which impacts certain design aspects and limits the Tx power. Otherwise, power from the Tx side will leak into the Rx circuit, potentially saturating the LNA and/or down-conversion mixer.

The simulation diagram illustrates the signal being radiated between the Tx and Rx antennas through a VSS radar target model that includes properties such as the RCS, distance, velocity and ambient conditions. The mixer will down-convert the signal reflected from the target, using the swept frequency from the voltage-controlled oscillator (VCO) as the local oscillator. Taking the difference of these two signals creates a beat signal directly proportional to the distance to the target. This IF is fed to an analog-to-digital converter (ADC) for signal processing, which extracts the target distance using a fast Fourier transform algorithm. Using multiple antennas, the Fourier transform also supports digital beamforming to produce a 2D image of the detected object.

WHY FMCW MIMO?

The developers chose an FDM MIMO architecture to address the technical requirements for fast imaging and high-resolution of multiple targets. Using MIMO, the number of physical elements can

AnaPico Inc.

of Switzerland

We make
the difference

Swiss made RF & MW test and measurement instruments available in the U.S. from Berkeley Nucleonics

ULTRA-AGILE SIGNAL SOURCE FROM 8 KHZ TO 20 GHZ

With Fast Control Port (FCP)

- 8-bit or 16-bit parallel port for fast, time critical operations like frequency hopping and list sweeping
- Switching / settling time 5 µs
- CW and pulse modulated signals
- Low phase noise: -100 dBc/Hz at 20 GHz and 10 kHz offset
- FCP uses an addtional 26 pin connector. TTL signals can be clocked up to 10 MHz
- Single- and multi-channel models in various form factors

MODEL 825-M-20: Available as flange- and rack-mountable module or in a compact desktop enclosure with color touch display and front panel control.

BNC Berkeley Nucleonics

For US Customers:
Call: 800-234-7858
Email: rfsales@berkeleynucleonics.com
Visit: https://tinyurl.com/u9wdx2w

AnaPico of Switzerland

For Non-US Customers:
Email: rfsales@anapico.com
Visit: www.anapico.com

be reduced significantly. For MIMO radar with N_t Tx elements and N_r Rx elements, there are $N_t \times N_r$ distinct propagation channels from the Tx array to the Rx array. Therefore, 64 virtual channels can be synthesized with only eight Rx and eight Tx channels, which greatly reduces system complexity, size and cost.

FDM transmits nonoverlapping frequencies simultaneously from each transmitter so different transmitter signals can be separated at the receiver.[3] For this design, the frequency sweep, or chirp, was generated outside the Tx/Rx channels using a swept 10 GHz, phase-locked loop (PLL) signal generator feeding a 6x frequency multiplier. Direct digital synthesizers generated low frequency, in-phase and quadrature (I/Q) modulation signals with frequency offsets of 1 MHz for each individual Tx channel. External ADCs digitized the IF signals from the down-converted receive signals.

Since the FDM MIMO antennas transmit simultaneously, all Rx channels will receive all Tx channels separated by the constant frequency offset. The demodulator uses the original chirp frequency as a local oscillator (LO) to down-convert the frequency offset signals containing the frequency shift, resulting from the delay of the signals reflected off the targets. The Tx channels are separated at the digital back-end. While this approach can handle moving targets by measuring all the MIMO channels simultaneously, it requires modulators at each Tx for shifting the transmit frequency and faster ADCs, due to the wider IF signal bandwidth. ***Figure 3*** is a conceptual system block diagram showing two

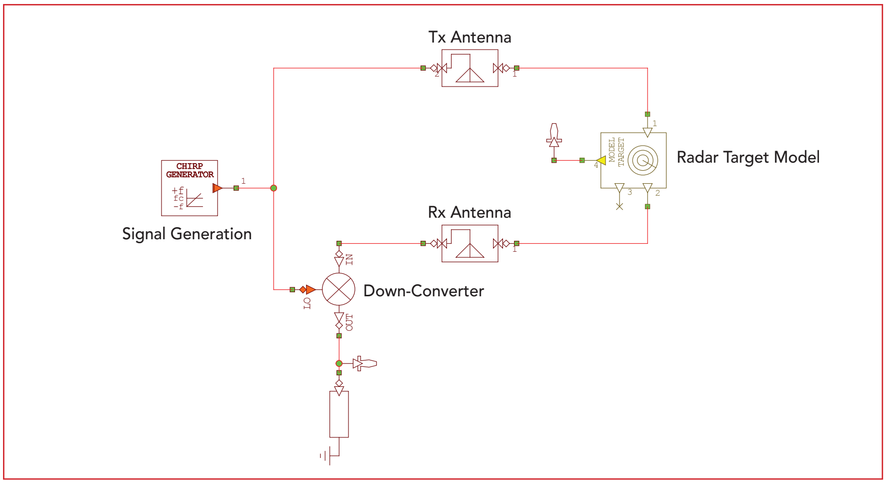

Fig. 2 **Simplified FMCW radar in VSS. PA, LNA and individual MIMO channels not shown.**

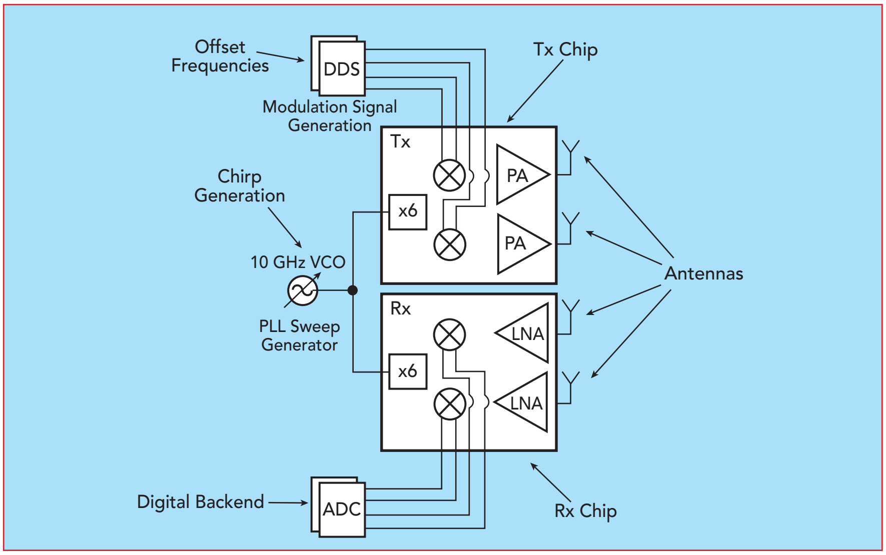

Fig. 3 **Conceptual system with two Rx and two Tx channels.**

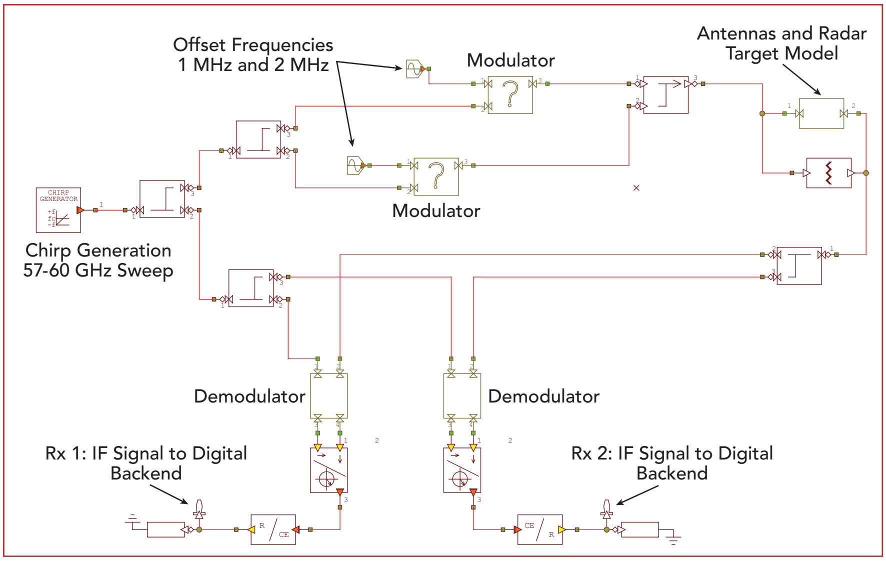

Fig. 4 FMCW MIMO radar block diagram.

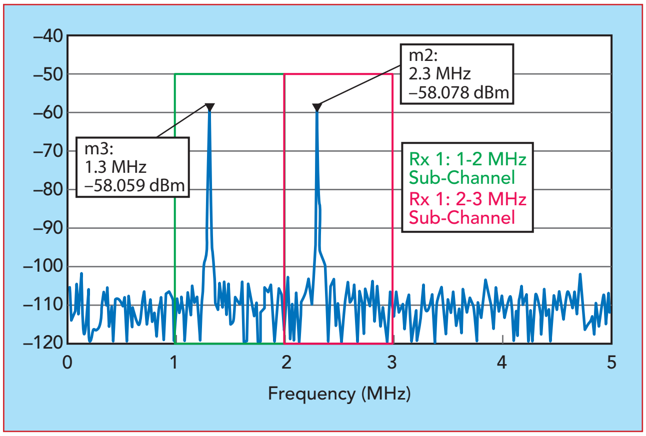

Fig. 5 Simulated down-converted signals.

Rx and two Tx channels.

SYSTEM DESIGN, VERIFICATION

VSS software was used to study the main system-level aspects of the MIMO radar. The software provides a block-level representation of the signal sources, LNAs, mixers, PAs, frequency multipliers, antennas and radar targets (see ***Figure 4***), enabling the designers to tune and optimize the key parameters and incorporate real-world operation of the radar system as more circuit-level details were added. VSS software simulated the IF output at two of the Rx down-converter channels. Using the equation in Figure 1, the beat frequency (f_b) was 300 kHz for a frequency sweep of 3 GHz bandwidth (BW) from 57 to 60 GHz, with a pulse duration (T) of 1 ms and target distance (r) of 15 m. The demodulated signal was the sum of f_b and the offset frequency of each channel. Simulation of the Rx down-converted signal in Tx 1 (the green response in Figure 1) was 1 + 0.3 = 1.3 MHz, and the Rx down-converted signal in Tx 2 (the red response) was 2 + 0.3 = 2.3 MHz (see ***Figure 5***).

RFIC DESIGN AND ANALYSIS

The Tx and Rx RFICs are the core of the radar system. Each contains four channels in a very small area (see ***Figure 6***), and additional ICs can be added to the system to increase the number of channels. It is advantageous for one RFIC to support multiple channels, to reduce assembly complexity and support scaling a system with a large number of channels. Separate Tx and Rx ICs enable independent Tx/Rx scaling, lower the leakage between Tx and Rx and support closer placement to the feed structure to reduce printed circuit board (PCB) losses. A single external VCO and PLL provide the LO signal that is distributed to all RFICs, resulting in excellent phase-noise correlation. A 10 GHz external signal is used for routing on the PCB, since routing a 60 GHz LO would be difficult in a system with

many channels. This 9.75 to 10.25 GHz chirp is multiplied to the operating frequency of the RFICs.

AWR Microwave Office circuit design software was used with the AWR AXIEM® electromagnetic (EM) simulator to design the Tx and Rx ICs from the transistor level, using the IHP SG13S SiGe process design kit (PDK) available for AWR software. The SG13S 130 nm SiGe bipolar CMOS process for mmWave applications has high speed HBTs with f_T = 240 GHz and f_{max} = 330 GHz.

A block diagram of the four-channel Tx RFIC and the actual Tx die are shown in ***Figure 7***. The active balun, 6x harmonic multiplier chain (2x and 3x multipliers cascaded) and one of element's PAs are highlighted to show their locations on the RFIC. Three active power dividers split the signal among four symmetric lines, each feeding a two-stage polyphase filter that generates 90 degree phase shifted I

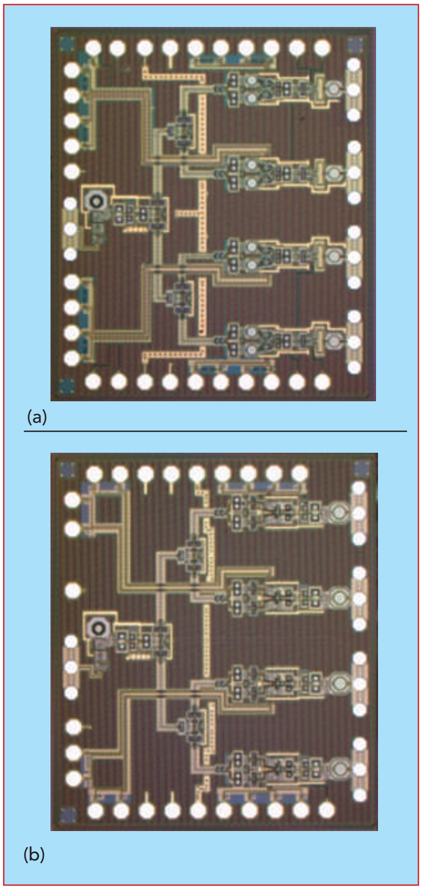

▲ Fig. 6 Tx IC (a) and Rx IC (b), each with four channels.

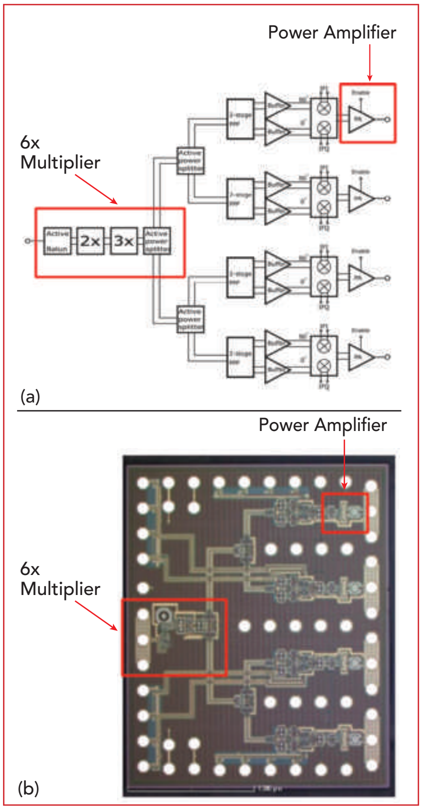

▲ Fig. 7 Four-channel Tx block diagram (a) and IC layout (b).

SHOCKINGLY POWERFUL.

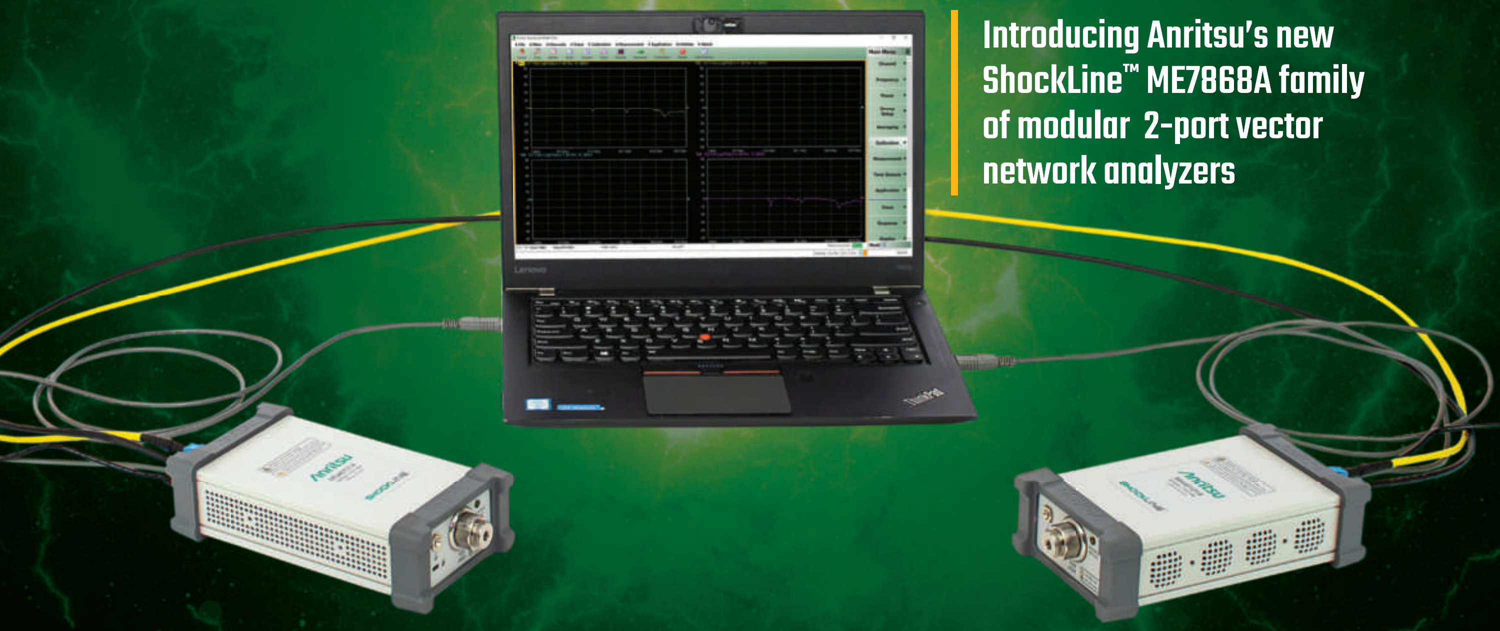

Introducing Anritsu's new ShockLine™ ME7868A family of modular 2-port vector network analyzers

Conduct full vector S-parameter measurements at wide distances of 100 meters or more.

Powered by PhaseLync™ synchronization, the ShockLine ME7868A enables engineers to synchronize two portable ShockLine MS46131As and connect them directly to a DUT to conduct vector transmission measurements over distances of 100 meters or more and at a lower cost. PhaseLync eliminates the need for long test port cable runs, while improving dynamic range and measurement stability of S-parameter measurements.

Be a Leader – Discover how you can get better measurement confidence over distance with Anritsu.

Visit **www.anritsu.com/test-measurement**

KEY FEATURES

- PhaseLync technology eliminates need for long cable runs, improves dynamic range, increases measurement stability of S-parameter
- Lower Cost of Test – Minimizing test times and maximizing throughput
- Simplified VNA Testing – Eliminate the need to utilize conventional benchtop VNAs with long cable runs
- Secure Content - All measurements are stored on a PC rather than the VNA

FOLLOW THE LEADER
220 GHz
ANRITSU

Anritsu

www.anritsu.com

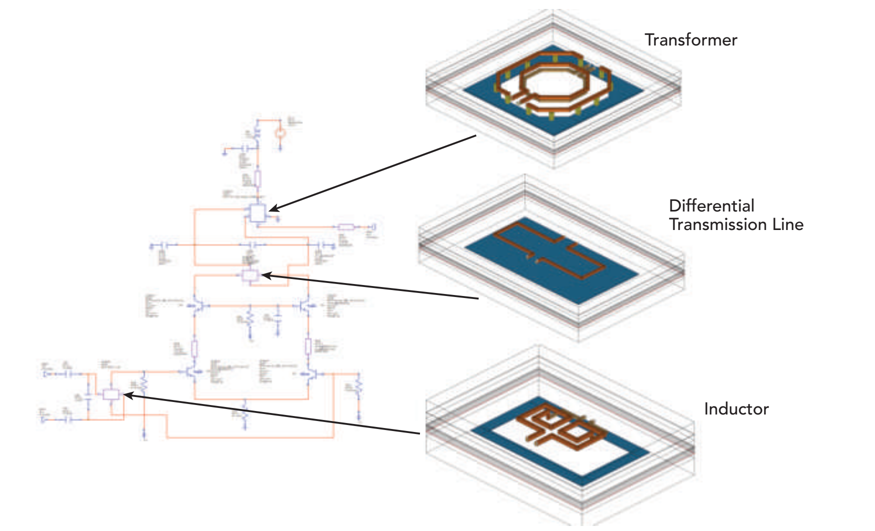

Fig. 8 PA schematic with transformer, differential transmission line and inductor layouts.

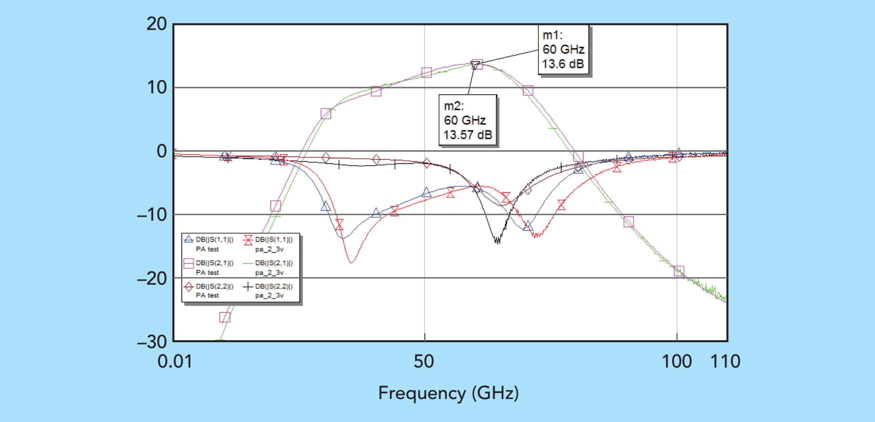

Fig. 9 Simulated vs. measured PA gain, $|S_{11}|$ and $|S_{22}|$.

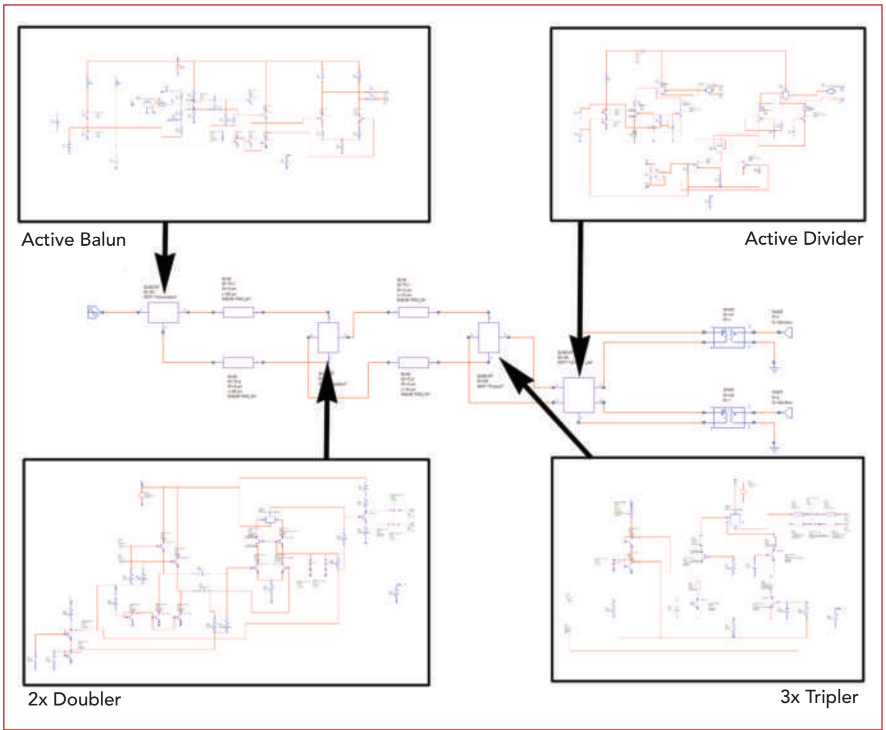

Fig. 10 6x multiplier schematic.

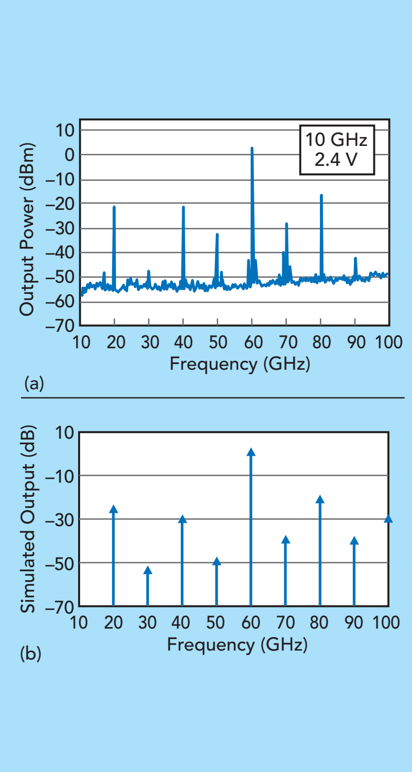

Fig. 11 Measured (a) and simulated (b) output of the 6x multiplier.

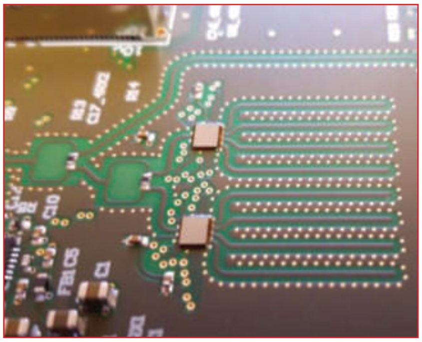

Fig. 12 PCB with eight Rx channels using two Rx ICs.

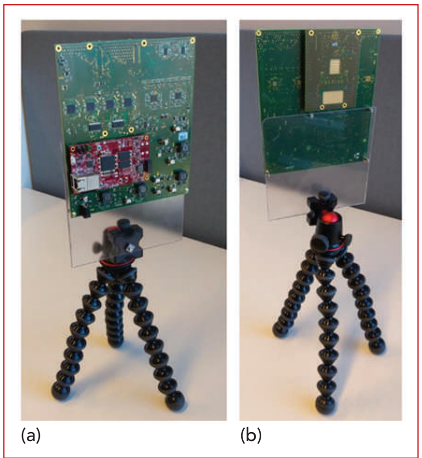

Fig. 13 Back (a) and front (b) views of the radar system PCB.

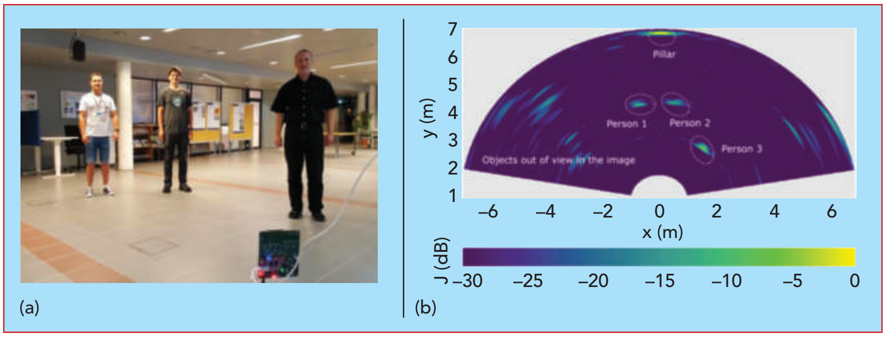

Fig. 14 Three people in the radar field of view (a) and resulting image (b).

and Q LO signals. The power dividers are followed by the buffer amplifier, I/Q modulator and PA stages. A schematic of the PA, developed using components from the foundry PDK for Microwave Office, is shown in ***Figure 8***, highlighting the transformer, differential transmission line and inductor. These passive structures are electrically large compared to the wavelength and required EM analysis and optimization using the AXIEM solver. The EM components were embedded as subcircuits in the schematic for co-simulation with Microwave Office. By including EM analysis combined with the PDK models of the chip-level amplifier yields excellent agreement between the measured performance and the simulation (see ***Figure 9***).

Simulations of the active balun, harmonic multiplier chain and active power divider on the output (see ***Figure 10***) were performed assuming a 10 GHz input and 2.4 V bias. The simulation results shown in ***Figure 11*** provide useful insight into the operation of the multiplier, enabling an understanding of the power levels of the spurious signals being generated. From a radar design perspective, it is beneficial to have this information to suppress these spurious signals, warranting the additional design steps to fine-tune the circuit.

MIMO RADAR MEASUREMENT RESULTS

The RF section of the receiver (see ***Figure 12***) shows eight Rx channels supported by two Rx RF-ICs flip-chip mounted on a PCB. The front and back of the high speed signal processing back-end, mounted on a stand for lab testing, are shown in ***Figure 13***. The phases and amplitudes of the receivers are calibrated with a single-point target measurement. Phase and amplitude correction factors are determined so the point target measurement provides an image of a point target at the correct angle.

"People flow" measurements of the 2D MIMO radar verified it can detect multiple people at the same time with 100 to 200 FPS (see ***Figure 14***). The demonstrated range resolution was 3 to 5 cm, and the angular resolution was 3.5 degrees.


Has Amplifier Performance or
Delivery Stalled Your Program?

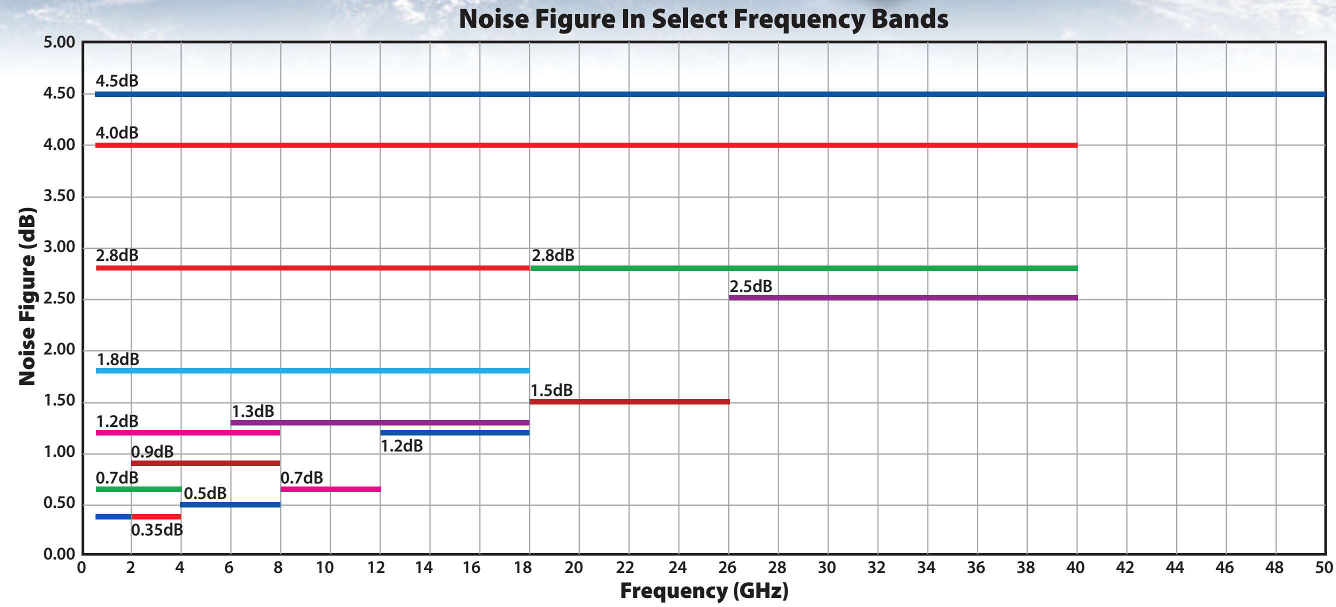
Noise Figure In Select Frequency Bands
Noise Figure (dB)
Frequency (GHz)
5.00
4.50
4.00
3.50
3.00
2.50
2.00
1.50
1.00
0.50
0.00
0
2
4
6
8
10
12
14
16
18
20
22
24
26
28
30
32
34
36
38
40
42
44
46
48
50
4.5dB
4.0dB
2.8dB
2.8dB
2.5dB
1.8dB
1.5dB
1.3dB
1.2dB
1.2dB
0.9dB
0.7dB
0.7dB
0.5dB
0.35dB

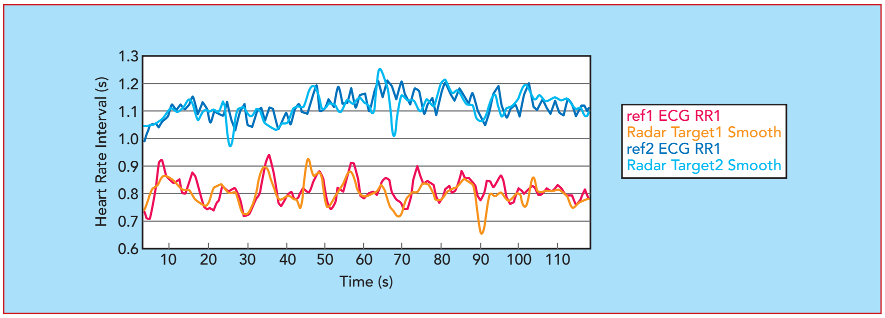

▲ Fig. 15 Results of multi-person HR and HRV extraction.

During image formation, the Hamming windowing function was applied in the range direction and a -25 dB sidelobe level Taylor window was applied in the azimuth direction. The Taylor windowing function slightly degraded the angular resolution but reduced the sidelobe level, enabling the image to be formed with a higher dynamic range. The targets were well separated in the generated image.

Accurate phase measurement is useful when measuring very small movements of a target—using the displacement of the chest to determine the heartbeat and breathing rate of a human, for example. Frequency multiplexing has an advantage over time multiplexing for measuring, since all the channels were measured at the same time. This is seen in the radar multi-person heart rate variability (HRV) extraction, shown in ***Figure 15***. Vital signs such as heart rate, HRV and breathing can be observed from the radar signal.

CONCLUSION

The design of a novel 60 GHz MIMO FMCW FDM radar for commercial applications has been described. The system provides high frame-rate measurement, excellent phase stability and a large FoV. The unique architecture and RFICs were designed so the system can be scaled to much larger radars while maintaining phase coherence among the channels. Both 2D and 3D imaging systems have been demonstrated and, to the best of the authors' knowledge, this is the first 3D imaging, mmWave, frequency-division MIMO system of its kind.■

References

1. J. Hasch, E. Topak, R. Schnabel, T. Zwick, R. Weigel and C. Waldschmidt, "Millimeter-wave Technology for Automotive Radar Sensors in the 77 GHz Frequency Band," *IEEE Transactions Microwave Theory and Techniques*, Vol. 60, No. 3, March 2012, pp. 845–860.
2. H. Forsten, T. Kiuru, M. Hirvonen, M. Varonen and M. Kaynak, "Scalable 60 GHz FMCW Frequency-Division Multiplexing MIMO Radar," *IEEE Transactions Microwave Theory and Techniques*, Vol. 68, No. 7, July 2020, pp. 2845–2855.
3. C. Pfeffer, R. Feger, C. Wagner and A. Stelzer, "FMCW MIMO Radar System for Frequency-Division Multiple TX-Beamforming," *IEEE Transactions Microwave Theory and Techniques*, Vol. 61, No. 12, December 2013, pp. 4262–4274.

RF Amplifiers and Sub-Assemblies for Every Application

Delivery from Stock to 2 Weeks ARO from the catalog or built to your specifications!

- Competitive Pricing & Fast Delivery
- Military Reliability & Qualification
- Various Options: Temperature Compensation, Input Limiter Protection, Detectors/TTL & More
- Unconditionally Stable (100% tested)

ISO 9001:2000 and AS9100B CERTIFIED

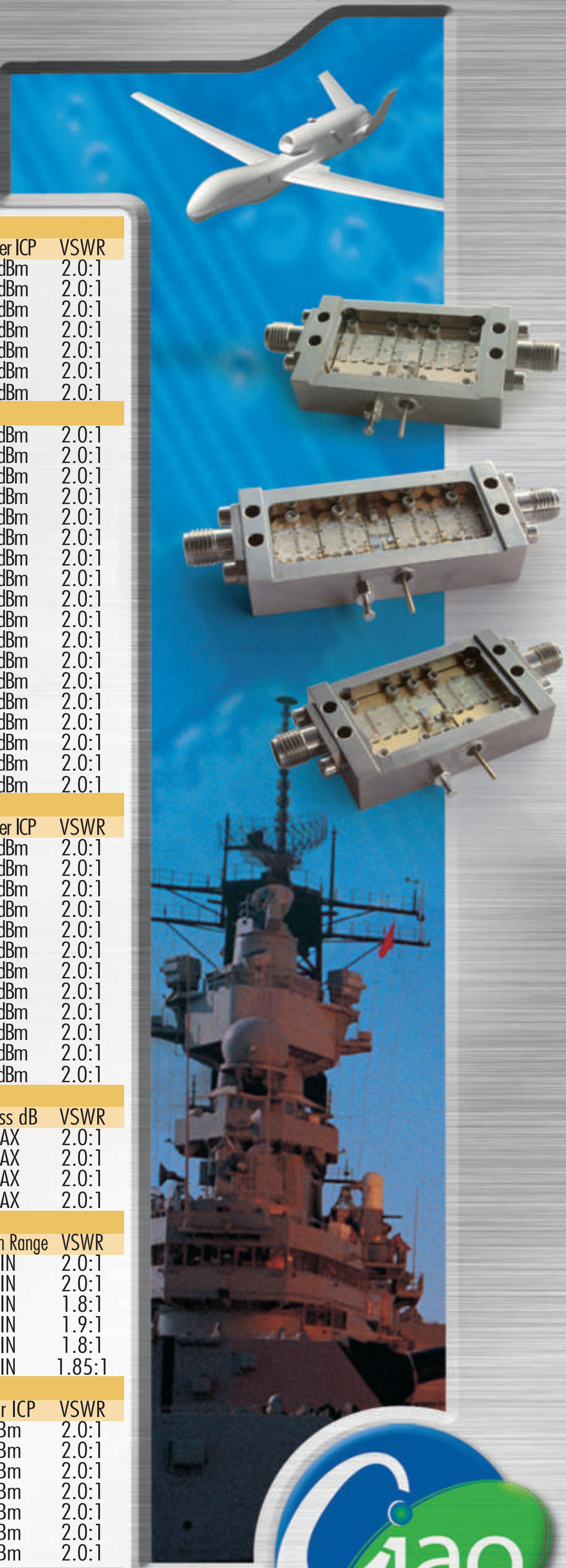

OCTAVE BAND LOW NOISE AMPLIFIERS

Model No.	Freq (GHz)	Gain (dB) MIN	Noise Figure (dB)	Power-out @ P1-dB	3rd Order ICP	VSWR
CA01-2110	0.5-1.0	28	1.0 MAX, 0.7 TYP	+10 MIN	+20 dBm	2.0:1
CA12-2110	1.0-2.0	30	1.0 MAX, 0.7 TYP	+10 MIN	+20 dBm	2.0:1
CA24-2111	2.0-4.0	29	1.1 MAX, 0.95 TYP	+10 MIN	+20 dBm	2.0:1
CA48-2111	4.0-8.0	29	1.3 MAX, 1.0 TYP	+10 MIN	+20 dBm	2.0:1
CA812-3111	8.0-12.0	27	1.6 MAX, 1.4 TYP	+10 MIN	+20 dBm	2.0:1
CA1218-4111	12.0-18.0	25	1.9 MAX, 1.7 TYP	+10 MIN	+20 dBm	2.0:1
CA1826-2110	18.0-26.5	32	3.0 MAX, 2.5 TYP	+10 MIN	+20 dBm	2.0:1

NARROW BAND LOW NOISE AND MEDIUM POWER AMPLIFIERS

Model No.	Freq (GHz)	Gain (dB) MIN	Noise Figure (dB)	Power-out @ P1-dB	3rd Order ICP	VSWR
CA01-2111	0.4 - 0.5	28	0.6 MAX, 0.4 TYP	+10 MIN	+20 dBm	2.0:1
CA01-2113	0.8 - 1.0	28	0.6 MAX, 0.4 TYP	+10 MIN	+20 dBm	2.0:1
CA12-3117	1.2 - 1.6	25	0.6 MAX, 0.4 TYP	+10 MIN	+20 dBm	2.0:1
CA23-3111	2.2 - 2.4	30	0.6 MAX, 0.45 TYP	+10 MIN	+20 dBm	2.0:1
CA23-3116	2.7 - 2.9	29	0.7 MAX, 0.5 TYP	+10 MIN	+20 dBm	2.0:1
CA34-2110	3.7 - 4.2	28	1.0 MAX, 0.5 TYP	+10 MIN	+20 dBm	2.0:1
CA56-3110	5.4 - 5.9	40	1.0 MAX, 0.5 TYP	+10 MIN	+20 dBm	2.0:1
CA78-4110	7.25 - 7.75	32	1.2 MAX, 1.0 TYP	+10 MIN	+20 dBm	2.0:1
CA910-3110	9.0 - 10.6	25	1.4 MAX, 1.2 TYP	+10 MIN	+20 dBm	2.0:1
CA1315-3110	13.75 - 15.4	25	1.6 MAX, 1.4 TYP	+10 MIN	+20 dBm	2.0:1
CA12-3114	1.35 - 1.85	30	4.0 MAX, 3.0 TYP	+33 MIN	+41 dBm	2.0:1
CA34-6116	3.1 - 3.5	40	4.5 MAX, 3.5 TYP	+35 MIN	+43 dBm	2.0:1
CA56-5114	5.9 - 6.4	30	5.0 MAX, 4.0 TYP	+30 MIN	+40 dBm	2.0:1
CA812-6115	8.0 - 12.0	30	4.5 MAX, 3.5 TYP	+30 MIN	+40 dBm	2.0:1
CA812-6116	8.0 - 12.0	30	5.0 MAX, 4.0 TYP	+33 MIN	+41 dBm	2.0:1
CA1213-7110	12.2 - 13.25	28	6.0 MAX, 5.5 TYP	+33 MIN	+42 dBm	2.0:1
CA1415-7110	14.0 - 15.0	30	5.0 MAX, 4.0 TYP	+30 MIN	+40 dBm	2.0:1
CA1722-4110	17.0 - 22.0	25	3.5 MAX, 2.8 TYP	+21 MIN	+31 dBm	2.0:1

ULTRA-BROADBAND & MULTI-OCTAVE BAND AMPLIFIERS

Model No.	Freq (GHz)	Gain (dB) MIN	Noise Figure (dB)	Power-out @ P1-dB	3rd Order ICP	VSWR
CA0102-3111	0.1-2.0	28	1.6 Max, 1.2 TYP	+10 MIN	+20 dBm	2.0:1
CA0106-3111	0.1-6.0	28	1.9 Max, 1.5 TYP	+10 MIN	+20 dBm	2.0:1
CA0108-3110	0.1-8.0	26	2.2 Max, 1.8 TYP	+10 MIN	+20 dBm	2.0:1
CA0108-4112	0.1-8.0	32	3.0 MAX, 1.8 TYP	+22 MIN	+32 dBm	2.0:1
CA02-3112	0.5-2.0	36	4.5 MAX, 2.5 TYP	+30 MIN	+40 dBm	2.0:1
CA26-3110	2.0-6.0	26	2.0 MAX, 1.5 TYP	+10 MIN	+20 dBm	2.0:1
CA26-4114	2.0-6.0	22	5.0 MAX, 3.5 TYP	+30 MIN	+40 dBm	2.0:1
CA618-4112	6.0-18.0	25	5.0 MAX, 3.5 TYP	+23 MIN	+33 dBm	2.0:1
CA618-6114	6.0-18.0	35	5.0 MAX, 3.5 TYP	+30 MIN	+40 dBm	2.0:1
CA218-4116	2.0-18.0	30	3.5 MAX, 2.8 TYP	+10 MIN	+20 dBm	2.0:1
CA218-4110	2.0-18.0	30	5.0 MAX, 3.5 TYP	+20 MIN	+30 dBm	2.0:1
CA218-4112	2.0-18.0	29	5.0 MAX, 3.5 TYP	+24 MIN	+34 dBm	2.0:1

LIMITING AMPLIFIERS

Model No.	Freq (GHz)	Input Dynamic Range	Output Power Range Psat	Power Flatness dB	VSWR
CLA24-4001	2.0 - 4.0	-28 to +10 dBm	+7 to +11 dBm	+/- 1.5 MAX	2.0:1
CLA26-8001	2.0 - 6.0	-50 to +20 dBm	+14 to +18 dBm	+/- 1.5 MAX	2.0:1
CLA712-5001	7.0 - 12.4	-21 to +10 dBm	+14 to +19 dBm	+/- 1.5 MAX	2.0:1
CLA618-1201	6.0 - 18.0	-50 to +20 dBm	+14 to +19 dBm	+/- 1.5 MAX	2.0:1

AMPLIFIERS WITH INTEGRATED GAIN ATTENUATION

Model No.	Freq (GHz)	Gain (dB) MIN	Noise Figure (dB)	Power-out @ P1-dB	Gain Attenuation Range	VSWR
CA001-2511A	0.025-0.150	21	5.0 MAX, 3.5 TYP	+12 MIN	30 dB MIN	2.0:1
CA05-3110A	0.5-5.5	23	2.5 MAX, 1.5 TYP	+18 MIN	20 dB MIN	2.0:1
CA56-3110A	5.85-6.425	28	2.5 MAX, 1.5 TYP	+16 MIN	22 dB MIN	1.8:1
CA612-4110A	6.0-12.0	24	2.5 MAX, 1.5 TYP	+12 MIN	15 dB MIN	1.9:1
CA1315-4110A	13.75-15.4	25	2.2 MAX, 1.6 TYP	+16 MIN	20 dB MIN	1.8:1
CA1518-4110A	15.0-18.0	30	3.0 MAX, 2.0 TYP	+18 MIN	20 dB MIN	1.85:1

LOW FREQUENCY AMPLIFIERS

Model No.	Freq (GHz)	Gain (dB) MIN	Noise Figure dB	Power-out @ P1-dB	3rd Order ICP	VSWR
CA001-2110	0.01-0.10	18	4.0 MAX, 2.2 TYP	+10 MIN	+20 dBm	2.0:1
CA001-2211	0.04-0.15	24	3.5 MAX, 2.2 TYP	+13 MIN	+23 dBm	2.0:1
CA001-2215	0.04-0.15	23	4.0 MAX, 2.2 TYP	+23 MIN	+33 dBm	2.0:1
CA001-3113	0.01-1.0	28	4.0 MAX, 2.8 TYP	+17 MIN	+27 dBm	2.0:1
CA002-3114	0.01-2.0	27	4.0 MAX, 2.8 TYP	+20 MIN	+30 dBm	2.0:1
CA003-3116	0.01-3.0	18	4.0 MAX, 2.8 TYP	+25 MIN	+35 dBm	2.0:1
CA004-3112	0.01-4.0	32	4.0 MAX, 2.8 TYP	+15 MIN	+25 dBm	2.0:1

CIAO Wireless can easily modify any of its standard models to meet your "exact" requirements at the Catalog Pricing.

Visit our web site at **www.ciaowireless.com** for our complete product offering.

Ciao wireless

Ciao Wireless, Inc. 4000 Via Pescador, Camarillo, CA 93012
Tel (805) 389-3224 Fax (805) 389-3629 sales@ciaowireless.com

Aegis Combat System Supports Layered Homeland Defense

The USS JOHN FINN (DDG-113) supported by the U.S. Navy, Missile Defense Agency and Lockheed Martin recently conducted a successful remote engagement (lethal intercept) of an intercontinental ballistic missile (ICBM) target. The flight test maritime (FTM)—44 test marks the first demonstration of an Aegis Baseline engagement of an ICBM-representative target.

This vital test demonstrated the latest Aegis Baseline 9.C2.0 capability against an ICBM class threat and introduces the ability to provide layered Homeland Defense with Aegis. The target was launched from the Reagan Test Site to conduct an Aegis Engage on Remote mission. As designed in the current U.S. command and control architecture, the remote target track and discrimination data was provided by the MDA's Command, Control, Battle Management and Communications (C2BMC) system and forwarded to Aegis for prosecution.

With the successful completion of four Aegis Baseline 9.C2.0 European Phased Adaptive Approach Phase 3 intercepts of intermediate range ballistic missiles, this test demonstrated the ability to provide a globally deployed defensive weapon system. This missile defense system will defend the U.S., its friends and allies from hostile ballistic missiles from all regions, all ranges and during all phases of flight by a single integrated system that is capable of comprehensive layered defense. As C2BMC capability continues to advance, it will help to unlock even more Aegis weapon system capability and lethality.

Working as the Aegis Combat System Engineering Agent, Lockheed Martin engineers updated the Aegis weapon system to integrate the SM-3 IIA weapon and adapted the system to target, identify and intercept the ICBM threat.

Raytheon Intelligence & Space sensors were also part of the historic test from low-Earth orbit. The sensors detected and tracked the target and relayed the data to decision makers in a demonstration of space-based early warning.

(Source: Lockheed Martin)

FCMS, Indra and Thales to Start Designing Sensors that will Contribute to NGWS/FCAS Superiority

Germany, Spain and France, the three driving forces of the NGWS/FCAS program, have entrusted FCMS, Indra and Thales with the development of an innovative suite of sensors that will equip the Future European Combat Air System.

The French Armament General Directorate (DGA), on behalf of the three nations, has signed the contract with Indra as leader of the industrial consortium into incorporate the sensors as part of the Phase 1 contractual framework. The Phase 1 A Concept Study for Sensors will last for one year, a period which may be extended by another six months.

The consortium will work on the design of the concepts required to meet the requirements of 2040 and beyond for the next-generation combat system, involving a connected and distributed architecture of sensors, the design of future sensors architectures and the maturation of the associated sensors technologies.

This distributed sensor architecture will leverage the capabilities provided by the NGWS/FCAS combat cloud, with improved system situational awareness and increased platforms survivability. The Sensors Pillar consortium looks forward to working together with the other NGWS/FCAS pillars (combat cloud, next-generation fighter, remote carriers) to optimize design and integration of the sensors within the system and platforms.

The development of the sensor pillar is essential to ensure consistent architectures that are perfectly integrated into the new generation fighters, unmanned systems, remote operators and the combat cloud. The superiority of the NGWS/FCAS will largely depend on the capacity of its network of sensors to compile more and better information than the adversary.

Joint All-Domain Command, Control Framework for Warfighters

Joint All-Domain Command and Control (JADC2) is the Department of Defense's concept to connect sensors from all military services—Air Force, Army, Marine Corps, Navy and Space Force—into a single network.

The services each have a system looking to tie sensors to shooters. The JADC2 will gather all sensor information and connect all warfighters. A threat could be sensed by an Air Force unmanned aerial vehicle but the best weapon against it could be a Navy missile fired from offshore.

For More Information

Visit mwjournal.com for more defense news.

A call for fire from an infantry battalion could be answered by tube artillery, rocket artillery, naval gunfire, close-air support from any service or something else. Some of this is already happening, and Marine Corps Lt. Gen. Dennis A. Crall (Joint Staff's director of command, control, communications and computers) sees the program growing and evolving. "There are things we can do immediately," he said. "We might onboard some of these things because they're available. You fight with what you have, not with what you want. But eventually, you will fight with what you want. So, the idea of looking at short, medium and long range is very critical. We can't take our eye off the horizon of what we need."

Like every other aspect of the department, JADC2 must contribute to the national defense strategy's lines of effort. "Does it increase lethality?," Crall asked. "The answer should be yes. We're a warfighting organization. That's what this is designed to do."

The framework will strengthen partnerships, another line of effort in the JADC2 strategy, which is currently in the works and being drafted by Crall's staff. Allies and other mission partners are being brought to the program now and not as "a bolt on" after the framework is fielded. He noted that it is very unlikely the U.S. would do anything without allies and partners, and they will have their own sensors and systems that need to be accommodated.

(U. S. Air Force Photo)

The next line of effort is reform and the JADC2 framework is all about changing the paradigm. "It's not a good thing to have everyone run off and develop something on their own. You end up with this idea that if it doesn't work well, at least it's expensive," he said. "We have to spend the money wisely."

Different people look at JADC2 from different perspectives. Some see descriptions of it and only concentrate on the adjectives, he said. Speed, resilient and persistent are just some and they form the "commandments" officials would compare these actions against. Other people look at JADC2 and just see the verbs: sense and act. "There's a lot of sensors on the battlefield," Crall said.

Looking to the future of JADC2, there are exercises and demonstrations, such as Bold Quest, that display capability right now. "If you view this as a puzzle, there are aspects to this capability we can employ today," the general said. "We don't have to wait for five years."

Reactel, Incorporated

Reacting First to All Your Filter Needs.

A Sheer Descent into the Noise

High Performance Notch Filters

- High Q
- Bandwidths as low as 0.5%
- Frequency range up to 20 GHz
- Power levels up to 1000 W

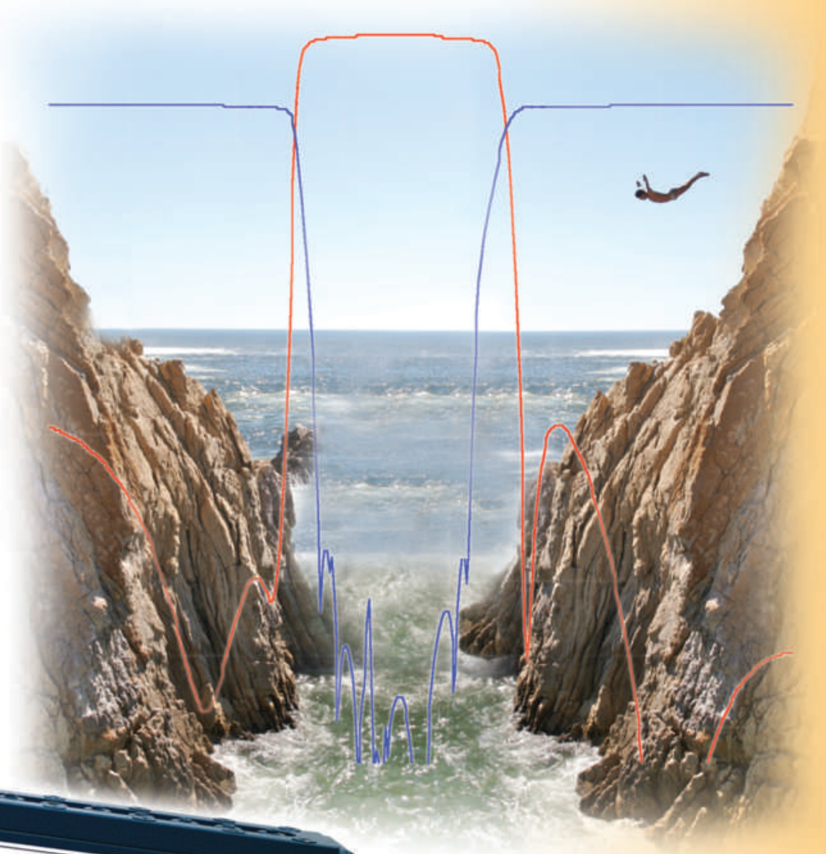

Reactel manufactures a variety of notch filters suitable for most any application.Utilizing Discrete Component, Ceramic, Cavity, Wavegiude or Microstrip technologies, we can create a unit which has extremely low pass band loss, contain up to 16 sections, and can have connectors or surface mount launch options. Contact us with you requirement and let us show you how sharp our notch filters can be.

8031 Cessna Avenue • Gaithersburg, Maryland 20879 • Phone: (301) 519-3660 • Fax: (301) 519-2447
For general inquiries, please email reactel@reactel.com • http://twitter.com/reacteljim • Go online to www.reactel.com to download your Reactel catalog today.

RoHS Compliant 2002/95/EC

@reacteljim

Cliff Drubin, Associate Technical Editor

IoT Leaders Join the Zigbee Alliance's IP Working Group

The Zigbee Alliance recently announced an important movement within the Project Connected Home over IP initiative, forming a team dedicated to the development and promotion of the standard for commercial markets. This move is in alignment with the overall vision for the initiative, which is to develop and promote the adoption of a new, royalty-free connectivity standard, simplifying development for manufacturers and increasing compatibility for customers and consumers.

Offering compelling value across the IoT landscape, the standard is targeting devices in categories such as lighting and electrical, HVAC controls, access control, safety and security, window coverings/shades, TVs, access points, bridges and others; addressing many of the needs of the high-growth commercial buildings category, where the install base of connected devices is expected to grow from 1.7 billion in 2020 to nearly 3 billion by 2025.

"In today's changing world, an IP infrastructure is the necessary backbone for any network to enable companies to leverage a digital architecture and connect their IoT-enabled devices," said Manish Kumar, senior vice president of the Digital Buildings Business, Schneider Electric. "Companies will be able to easily build and add project-based devices to their existing networks in a way that is IT-compliant with the current architecture and management infrastructure."

Promoting IP-Based Convergence for the Commercial Market

To ensure commercial implementers can make the best use of the initiative, to date more than 50 industry leaders around the world with commercial-focused solutions—including Allegion, DSP Group, DSR Corporation, Latch, Legrand, MMB Networks, Nordic Semiconductor, NXP Semiconductors®, OSRAM, Qorvo, Schneider Electric, Signify, Silicon Labs, Somfy and ubisys—have aligned to form the project's Commercial Strategy Group. With a charter to support development and promote the use of the standard within the commercial industry, this team will clarify the commercial use cases that can readily be supported by the project's initial specification, define the new features required for additional commercial use cases, facilitate conversation and collaboration among members to strengthen the use and adoption of IP-based connectivity standards in the commercial market globally and advocate and encourage others to join and contribute to this market-leading effort.

Cellular IoT Device Growth Creating a Connectivity Challenge

Greater than 6 billion IoT devices are connected and active worldwide; 840 million of them use cellular networks, which is just under 8 percent of the total. At the end of 2014, there were 180 million cellular IoT devices active worldwide, and that number increased by over 4.5x in the six intervening years. In another six years' time, there will be a further near-7x growth in cellular IoT devices, bringing the global total to 5.7 billion by 2026, finds ABI Research. This explosive growth means carriers are facing more specific and diverse demands for guarantees from IoT customers, especially when roaming.

"More smart devices are being deployed, and more types of devices are becoming smart," said Jamie Moss, M2M, IoT & IoE research director at ABI Research. "It is clear the ability to connect diverse IoT device types, with different needs, at massive scale and with global coverage is needed now. Next-gen connectivity management platforms (CMPs) and global connectivity coverage solutions are key to accomplishing this task."

Enterprises want a one-stop-shop, more so now than ever. Large multinational corporations that can afford to employ systems integrators to assemble customized systems are few, and while they were some of the earliest IoT adopters, they only represent a portion of the market. Most enterprises do not have the funds or inclination and may not even know what the IoT can do for them. Instead, they value specialist expertise that can deploy and host services for them that "just work," leaving the enterprise itself to focus on what it does best—its existing business. "Next-generation CMPs, such as floLIVE, can provide international connectivity for enterprises by allowing carriers to become International Mobile Virtual Network Operators. The core network of a CMP vendor can collectively manage the routing of IoT traffic across many carrier customers' RANs, allowing them to sell international IoT services with the guarantee of a single price point for data and a consistent QoS," Moss explained.

Private Network Deployments Will Generate Revenues in Excess of US$64 Billion by 2030

With enterprise 5G maturing, the importance of private networks for the enterprise domain will continue to grow. According to ABI Research, the demand for private network deployments will be driven primarily by heavy industry verticals. Industrial manufacturing, energy production (including mining, oil and gas and logistics) alone will generate

For More Information Visit mwjournal.com for more commercial market news.

private network revenues of US$32.38 billion by 2030, representing half of US$64 billion overall private network revenues.

"These findings show the importance of private networks, particularly for automating mission- or even life-critical use cases, that require the highest possible network reliability and availability and are characterized by a high degree of network integrity to prevent data from leaving the enterprise premises," said Leo Gergs, research analyst for 5G Markets at ABI Research. "Enterprises that require network slicing capabilities to separate mission-critical from non-mission-critical use cases within the same physical network will turn to private networks."

Two main factors are causing the surge in private network demand. "The first is a huge rise in demand for automation and enterprise digitization. What has started with Industry 4.0 is now exacerbated by the aftermath of the global COVID-19 outbreak. Enterprises in industrial manufacturing, logistics and oil and gas are now accelerating their digitization plans to reduce their dependency on manual labor availability and increase the resilience of their business operations against sudden disruptions to supply chains. The second is the addition to the demand-side effect. The market for private network deployments will also benefit from a supply-side effect. The freeze of Release 16 gives enterprises the much-needed reassurance of 5G capabilities for enterprise-grade connectivity, which allows chipset and module manufacturers to grow the device ecosystem for compatible hardware. The maturing device ecosystem, in turn, drives down prices per module and therefore makes the deployment of private 5G network more cost-efficient, which will spur additional interest from enterprises," Gergs explained.

> Driven by growth in industrial manufacturing, energy production and logistics

There is a growing number of private network offerings emerging on the market to address this rising opportunity. While private network operators like Ambra, Citymesh or Edzcom are threatening traditional cloud service providers' market share by monetizing managed services other than connectivity, hyperscalers like AWS, IBM and Google are launching their private network offerings in co-creation efforts with telco players. In addition, software companies like Athonet and Quortus benefit from trends toward network virtualization, which allows them to offer a virtualized core network either through system integrators or to enterprises directly.

ERAVANT
FORMERLY **SAGE MILLIMETER**

WAVEGUIDE TRANSITIONS

TAPER | MODE | FLANGE | COMPACT | 8.2 to 260 GHz

SAGE Millimeter is now Eravant, a change that renews our commitment to the millimeterwave industry. Since 2011, we have been delivering quality products and energizing the customer experience to meet the needs of RF engineers working on the technology of the future.

Waveguide Flange Adapters
Flange adapters act as a bridge between different flange patterns with the same waveguide. These adapters are also offered to cover the frequency range from 18 to 170 GHz.

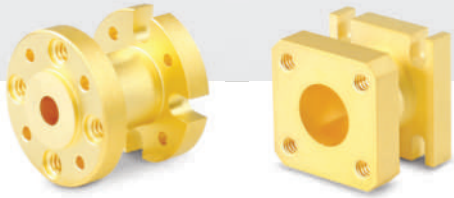

Compact Waveguide Mode Transitions
Compact waveguide mode transitions are manufactured by EDM machining or electro-forming techniques to ensure high accuracy and a quality surface finish. These transitions induce nominal insertion loss and excellent return loss. Available from 12.4 to 140 GHz.

Waveguide Taper Transitions
Taper transitions implemented in the standard models are linear and induces a fraction of a dB insertion loss and a VSWR of 1.05:1 or better when operating in the dominant mode. Available from 8.2 to 260 GHz in adjacent and non-adjacent waveguide sizes.

Waveguide Mode Transitions
Standard models are offered between rectangular waveguides and their correspondencing mid-band circular waveguides. Standard rectangular waveguides to high- and low-band circular waveguides are also available. Offered from 8.2 to 260 GHz.

WWW.ERAVANT.COM

www.eravant.com 501 Amapola Avenue Torrance, CA 90501
T: 424-757-0168

Adapters • Amplifiers • Antenna Feeds • Antennas • Attenuators • Bias Tees • Cable Assemblies • Corner Reflectors • Couplers • DC Blocks • Detectors • Ferrite Devices • Filters • Frequency Converters • Frequency Multipliers • Limiters • Magic Tees • Mixers • Noise Sources • Oscillators • Phase Shifters • Power Dividers • Radar Sensors • Subassemblies • Switches • Termination Loads • Test Equipment • Test Hardware & Accessories • ... Waveguide Sections

Around the **Circuit**

Barbara Walsh, Multimedia Staff Editor

MERGERS & ACQUISITIONS

Nordic Semiconductor announced that it is expanding its in-house wireless technology expertise into Wi-Fi after acquiring the entire Ensigma Wi-Fi development team and associated Ensigma Wi-Fi IP tech assets from industry-leading graphics, vision and AI processing company, **Imagination Technologies**. The acquisition includes a sizable number of Imagination Technologies employees located in the U.K., Sweden, India and Taiwan. Of these, around 15 percent are Bluetooth Low Energy (Bluetooth LE) specialists who will now further strengthen Nordic's existing Bluetooth LE teams as well.

COLLABORATIONS

Electro Rent and **NI** announced a new partnership to rent NI automated test and measurement solutions to customers through Electro Rent's expansive network, starting in North America with a global expansion to follow in later 2021. The collaboration between the two companies will deliver new opportunities for customers to leverage industry-leading solutions on a rental basis, often allowing them to shift investments from a capital (CapEx) to an operational expenditure (OpEx) model, with flexibility on term duration and savings on monthly and annual usage.

Indium Corp. and **Valuetronics International** have formed a strategic partnership to serve customers in the Americas with its cored wire, rework fluxes and bar solder products. The partnership with Valuetronics, a well-known distributor of test and laboratory equipment markets, will help bring Indium Corp.'s proven materials to hand assembly and rework customers. Valuetronics stocks thousands of instruments at their Elgin, Ill., facility with a growing customer base of more than 100,000 global contacts.

ZTE Corp., along with **China Unicom** and **Beijing Jiaotong University**, has introduced the industry's first trusted spectrum sharing solution based on the blockchain technology in the RAN sharing scenario. Meanwhile, the three parties have announced the establishment of "China Unicom-ZTE-BJTU Blockchain Application in RAN Sharing Joint Innovation Lab" and jointly released a white paper on 5G Blockchain Technology. The trusted spectrum sharing solution introduces the blockchain technology into the wireless mobile network. By virtue of the distributed ledger, multi-party consensus and tamper-proof features of the blockchain technology, the operators' key information, such as the spectrum resources and device status, is stored on the blockchain node to achieve fairness, visibility and reliability.

Siklu announced an initiative with **Schréder**, one of the industry's largest manufacturers of outdoor lighting systems, to create the first-ever "Wireless Smart Pole," thanks to a new module available with the Schréder Smart Pole: the famous SHUFFLE. The new module will launch officially in 1Q 2021 under the name "SHUFFLE Wireless Backhaul." This new wireless Smart Pole features all the latest equipment for Smart City services and Gigabit wireless connectivity provided by the Siklu MultiHaul line of radios, all built in into a sleek streetlight unit. The SHUFFLE Smart Pole is constructed of rotatable and interchangeable modules that seamlessly integrate various LED lighting options, security cameras, Wi-Fi Access Points, EV charging sockets, audio speakers and small cells for 4G/5G mobile networks.

Xilinx Inc. announced a collaboration with **Texas Instruments (TI)** to develop scalable and adaptable digital front-end solutions to increase energy efficiency of lower antenna count radios. The solutions leverage Xilinx's adaptable IP to enhance the RF performance and improve the power efficiency of indoor and outdoor radio applications. By combining Xilinx's industry-leading Zynq UltraScale+ MPSoC family and adaptable RF IP with the AFE7769 quad-channel RF transceiver from TI, developers can better address the OpEx and CapEx concerns of large operators and private networks. The next generation of LTE and 5G small cells will need to address many new and evolving requirements.

NEW STARTS

HUBER+SUHNER has announced the expansion of its critical communications portfolio with the full integration of **Kathrein Special Communications**. This development further strengthens the company's ability to provide a host of products and solutions for critical applications. Suitable for use in critical communications networks across the industrial, energy, blue light, defence, government and rail sectors, the portfolio meets the rising demand for versatile, resilient and secure high performance connectivity. In recent years, the security industry has experienced increasing pressure to provide effective and efficient services which ensure the safety of the public, military and emergency mobile field teams.

ACHIEVEMENTS

In a rare show of bipartisanship, the **U.S. House** has unanimously passed a bill that seeks to financially support a domestic 5G equipment market and **Open Radio Access Network (Open RAN)** development with an influx of $750 million in funding over the next 10 years. The bill directs the National Telecommunications and Information Administration to begin issuing competitive grants within 18 months that promote "the use of technology, including software, hardware and microprocessing technology, that will enhance competitiveness in the supply chains of Open RAN 5G networks," and accelerated development and deployment of Open RAN technologies.

Test and measurement specialist **Rohde & Schwarz**, together with connector and cable assembly manu-

For More Information For up-to-date news briefs, visit mwjournal.com

facturer, **Rosenberger** have successfully demonstrated compliance testing for MultiGBASE-T1 supporting 2.5/5/10GBASE-T1 automotive Ethernet speeds, based on the OPEN Alliance TC9 working group test specification. This development enables vehicle manufacturers and component suppliers to have confidence in the performance of future, high speed in-vehicle networks. Automotive applications such as advanced driver-assistance systems are driving in-vehicle network speeds higher, bringing a challenge to car manufacturers and component suppliers to ensure correct performance of the communication channel and avoid EMI issues.

TIM, **Ericsson** and **Qualcomm Technologies Inc.** are leaders once again with a new record for ultrabroadband long distance speed with 5G technology applied to Fixed Wireless Access (FWA). A speed of 1 Gbps on 26 GHz mmWave frequencies, at a distance of 6.5 km from the site (1 Gbps with UDP protocol, 700 Mbps Speedtest Ookla TCP) has been reached on TIM's live network. This record confirms the usability of 5G mmWave spectrum, not only for urban, high speed or high-density-only deployment, but also for wider 5G FWA coverage. It builds on the successes previously achieved with mmWave in September when the TIM network connection stably exceeded a speed of 4 Gbps in downlink on a live 5G network.

Massachusetts Bay Technologies (MBT) announced its ability to process diamond substrates using their proprietary thin film metallization process. Diamond substrates are the preferred material for a wide variety of applications, including high frequency applications, low thermal expansion, excellent dielectric properties, extreme hardness/strength, high thermal conductivity and optical transmission over a wide spectral range. MBT has the knowledge and factory infrastructure to supply any standard or custom diamond thin film design that is used for both commercial and military applications.

Verus® Research, a New Mexico-based team of scientists and engineers specializing in advanced research and technology development, received the honor of the top fast-growing technology firm in New Mexico with more than $10 million in revenue from the *Albuquerque Journal*, the state's largest newspaper. It was also named one of New Mexico's fastest growing companies in the large company category by *Albuquerque Business First*, New Mexico's leading business publication. The *Albuquerque Journal*'s Flying 40 award recognizes the top 40 fast-growing technology firms in New Mexico. The award is broken down into three categories based on revenue.

QuadSAT has successfully completed tests which demonstrated QuadSAT's RF-testing drone's ability to test and validate radar system performance at the site where the radar is deployed. The test course was supported by Terma. The aim of the actual project was to determine whether the QuadSAT solution, originally made for testing satellite antennas, could be used for on-site validation of radar systems.

Sofant Technologies has overcome a significant challenge and achieved world-class cycle reliability, a major technical breakthrough. The Scottish-based company now expects to accelerate its commercial roadmap, bringing volume manufacture to market within the next two years. The benefits of RF MEMS for radio applications have been understood by system designers for decades. However, the technology has historically suffered from reliability problems which caused devices to fail prematurely and prevented widespread adoption of the technology. In its most recent testing period, Sofant's development team achieved 25 billion cycles on production prototypes which were supplied by its volume foundry partner. The devices showed no signs of failure before the test was ended by the Sofant team.

Filtronic plc announced that it has joined the **HAPS Alliance**, a non-profit association dedicated to building a high altitude platform station (HAPS) ecosystem that brings digital connectivity to everyone, everywhere. As a member of the HAPS Alliance, Filtronic will collaborate with world-leading telecommunications, technology, aviation and aerospace companies to accelerate commercial adoption, advocate for safety and regulatory standards and help build a cooperative HAPS ecosystem. This cross-industry collaboration is designed to eliminate the 'Digital Divide,' accelerating the development and adoption of HAPS technology, thus bringing better connectivity to areas globally not served by traditional telecoms infrastructure.

ACHIEVEMENTS

Ranatec, a part of the Qamcom Group AB and supplier of specialized test and measurement equipment for RF and microwave applications, has delivered a 5G testing system to one of the big five (**FAANG**) U.S.-based tech companies. In a significant 2020 product milestone, the Swedish manufacturer wrapped up 2020 deliveries with a substantial order of 500K Swedish kroner, approximately Euro 50K. The supplier of niche test equipment interpreted the influx of orders from the U.S. and Asia last year as an indicator of a market trending towards significant investments in 5G technology.

SMP connectors from **Rosenberger** have been selected for use in the first-ever LTE cellular network on the moon, expected to be operational by the end of 2022. Long-term tested and successfully qualified SMP connectors for aerospace applications will be core components for enabling fast, precise and highly reliable satellite communication across the universe. LTE cellular networks provide the technology required for high speed transmission of huge data rates: necessary for vital command, control functions and remote control of lunar vehicles for scientific research applications; real-time navigation; and streaming of high definition videos from the lunar surface to earth.

CONTRACTS

EM Solutions has recently received a second order to supply its Ka-Band transceivers for the **L3Harris Technologies** Panther II Very Small Aperture Terminals. The new contract, valued at more than $US2M, will deliver over 100 Ka-Band transceivers to L3Harris across the

first half of 2021. The contract award to EM Solutions follows an earlier order to supply 50 transceivers that are already being delivered to L3Harris.

Qorvo® has been selected by the U.S. government to create a state-of-the-art heterogeneous integrated packaging (SHIP) production and prototyping center for RF assemblies, a program valued at up to $75 million. The goal of the SHIP program is to ensure that microelectronics packaging expertise and leadership is available for both U.S. defense contractors and commercial clients requiring design, validation, assembly, test and manufacturing of next-generation RF components. Qorvo's role is to design and deliver the highest levels of heterogeneous packaging integration, which is essential to meet the size, weight, power and cost requirements for next-generation phased array radar systems, unmanned vehicles, electronic warfare platforms and satellite communications.

PEOPLE

SweGaN AB, manufacturer of custom-made GaN-on-SiC epitaxial wafers for components and devices for telecom, satellite, defense and power electronics, announced its Board of Directors Chairman **Mats Andersson** has stepped down, passing the SweGaN torch to Vice Chairman **Agneta Franksson**. Agneta Franksson holds a M.S. in Electrical Engineering. She has extensive experience from several CEO positions and over 25 years experience within R&D, business development and sales focus. Since 2006, she has run her own management consulting company and has served on several boards of directors during the last 14 years. In addition, Franksson is active in providing training at the Swedish Board Academy.

▲ *Agneta Franksson*

▲ *Bill Baumann*

Lectrix announced industry veteran, **Bill Baumann**, has joined them as vice president of Business Development. For over 25 years, Baumann held various executive roles at Penton Media culminating in his position as vice president market leader/group publisher—Design Engineering and Sourcing Group. From 2015 to July 2020, Baumann worked as an industry consultant for several media companies. Most recently, Baumann held the role of VP managing director of EH Media's Robotics Group. With more than 30 years of electronics industry experience, Baumann is well-versed in new product introduction and recognizes that the industry now requires a more strategic marketing solution.

Marki Microwave appointed **Duncan Pilgrim** to serve as vice president of sales and marketing. The former

Around the **Circuit**

▲ *Duncan Pilgrim*

vice president of Integrated Device Technology's radio frequency division brings Marki Microwave over 20 years of experience in the semiconductor space. As vice president of sales and marketing, Pilgrim will be responsible for growing the business, branding and developing thought leadership. Throughout Pilgrim's career, he has successfully held multiple general management and business development positions, as well as design and application engineering roles at various midsize and startup companies.

REP APPOINTMENTS

Keysight Technologies Inc. announced the addition of two new partners, **Batronix** and **Batter Fly**, to the company's expanding European distribution network. The addition of Batronix and Batter Fly will broaden Keysight's distribution channel covering power supplies, oscilloscopes, digital multimeters, waveform function generators, data acquisition and handheld RF products.

PLACES

Mini-Circuits announced the opening of a new warehouse and shipping hub at its facility in Penang, Malaysia. This expansion will allow the company to offer many customers shorter lead times and lower freight costs by shipping orders directly from Penang. It will also add another layer of security to Mini-Circuits' global logistics network by sharing the commitment to prompt, reliable fulfillment with existing corporate shipping locations in the U.S. and Europe, as well as distributor partners around the world. Initially, shipments from the Penang warehouse will support orders for Mini-Circuits' TC-family of surface mount transformers in full-reel quantities with plans to expand stock to MMIC and LTCC product lines in the near future.

Gowanda Components Group announced the completion of a nearly 50 percent expansion at its DYCO Electronics facility in Hornell, N.Y. The 12,000 sq. ft. expansion will help the company address market demand for its products, enhance workflow and improve operational efficiency. DYCO engineers customize solutions for aerospace, military, space, medical and industrial applications, in addition to providing solutions for rail transportation.

AnTrust announced the opening of their new facility location, strategically located in Columbia, Md., of Howard County. AnTrust's core business supports U.S. Government defense and civilian space applications, in addition to selected commercial and ground-based requirements. This new facility expands their capabilities for the design, analysis, fabrication, assembly and testing of these RF/antenna components and spaceflight payloads. A high performance dual-polarization antenna test range will also be commercially available for rental starting in mid-2021, for the testing of antennas, subsystems and payloads within the 1 to 40 GHz frequency spectrum.

Your Preferred Microwave and mmWave modules Supplier, 40-170GHz

Waveguide Active Frequency Multiplier

- ✓ Full U/V/E/W Band
- ✓ High Power up to +25dBm
- ✓ Fast Delivery from Stock

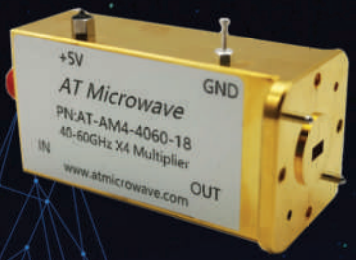

Full Band Active Multiplier:

- ✓ U Band 40-60GHz, X4, Pout=+18dBm
- ✓ V Band 50-75GHz, X4, Pout=+18dBm
- ✓ E Band 60-60GHz, X6, Pout=+13dBm
- ✓ W Band 75-110GHz, X6, Pout=+13dBm
- ✓ F Band 90-140GHz, X8, Pout=0dBm

High Power Active Multiplier:

- ✓ 70-77GHz, X6, Pout=+25dBm
- ✓ 75-86GHz, X6, Pout=+25dBm
- ✓ 90-98GHz, X8, Pout=+20dBm
- ✓ 88-104GHz, X8, Pout=+20dBm

Note:
Higher power is available by adding Power Amplifier
Customized module is available according to request.

Shanghai AT Microwave Limited

Tel: +86-21-6229 1233
Email: sales@atmicrowave.com
www.atmicrowave.com

INVITED PAPER

Toward Augmented OTA Testing: Bringing Full-Wave Numerical Modeling and Antenna Measurements Together

Benoit Derat, Mert Celik and Sebastian Schmitz
Rohde & Schwarz, Munich, Germany

Winfried Simon and Andreas Lauer
IMST GmbH, Kamp-Lintfort, Germany

Evaluating the realistic performance of antennas integrated into complex setups has been a long-term challenge, currently relevant to automotive connectivity, for example. Numerical electromagnetic (EM) modeling offers a cost-effective alternative to device testing but is often limited by an incomplete or inaccurate knowledge of the device under test (DUT). While this shortcoming does not apply to test approaches, the implementation of adequate measurement systems, such as full-vehicle over-the-air (OTA) test setups, requires large investments and, possibly, a significant amount of space. We present a way to converge both worlds in an optimal cost-benefit technique by combining antenna measurements with full-wave simulation.

Three-dimensional EM modeling tools have seen extraordinary technical and commercial development since the early 90s. Now, there is almost no problem involving Maxwell's equations which cannot be solved with the right software and computational resources. Nevertheless, the need for RF measurements continues to grow, and simulations are not foreseen as a substitute for testing soon. The main reason is that full-wave simulation, even performed by an expert, is only as good as the knowledge of the problem modeled. In most circumstances, this knowledge is incomplete, even for the device manufacturer. Taking the example of a mobile phone, some components come from suppliers, material dielectric properties are not fully characterized, manufacturing tolerances and operating uncertainties of the components are not completely accounted for, etc.

Measurements do not suffer from a similar lack of knowledge, as no simplifying assumptions are required about the DUT. However, the complexities of experimental setups, including realistic integration or usage conditions, must be considered. For example, for autonomous driving cars using cellular vehicle-to-everything (C-V2X) technology for data communication, the connectivity in cars is developing to unprecedented levels. Evaluating the accurate performance of all transceivers (i.e., cellular, WLAN, GNSS, etc.) necessitates including the impact of the complete car on all radiated emissions. To address these aspects, the 5GAA organization is currently standardizing the use of full-vehicle OTA testing systems using 10 m or larger anechoic chambers (see **Figure 1**).[1] The corresponding costs are as substantial as the space requirements, and the realizable test scenarios are still limited. A close to real-world test solution would require unreasonable effort, time and cost for measuring the OTA performance of an integrated 5G mmWave antenna module, and no test chamber can assess the effects of various grounds on the measured metrics or an actual link budget


Portable Handheld Field Solutions
Expand your choice of 5G spectrum analysis capabilities
-Coax or Waveguide
24 to 40 GHz
With > 6GHz If Bandwith
M28H2ADC
M28H2ADC-K
26 GHz (24.25 to 27.5 GHz)
28 GHz (27.5 to 28.35 GHz)
38 GHz (37 to 38.6 GHz)
39 GHz (38.6 to 40 GHz)
Innovation in Millimeter Wave Solutions
www.omlinc.com
(408) 779-2698
OML

in a car-to-car transmission.

To overcome the limitations in both antenna simulation and measurement, the best of both numerical and experimental methods can be combined: measure the part of the problem which cannot be accurately modeled and compute the portion which is too costly or complex to measure.

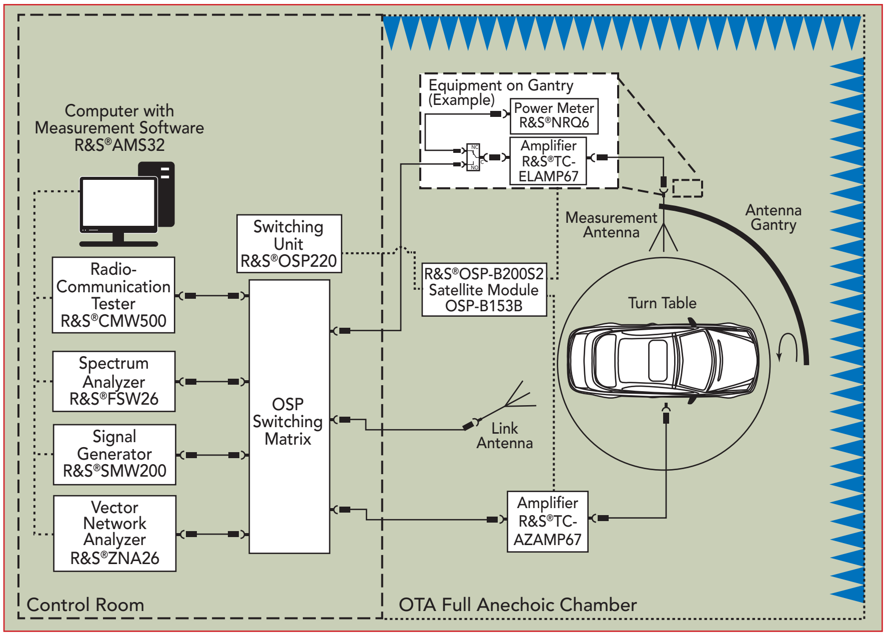

Fig. 1 R&S full-vehicle OTA testing system based on draft 5GAA requirements.

MEASUREMENT + SIMULATION

Combining measurement and simulation is a straightforward outcome of the fundamentals of wave physics. From the Huygens-Fresnel principle or the equivalence theorem, the six components of the electric (E) and magnetic (H) field vectors outside of a volume, V_s, encompassing a radiating source within a surface, Σ_s, can be exactly computed from only two of the EM field components over Σ_s or the associated surface electric and magnetic currents J and M (see ***Figure 2***). Conversely, proven techniques can solve the inverse problem: calculating the currents J and M from two characterized components of E and/or H over a closed surface, Σ_m, containing Σ_s.[2-5]

Imagine that Σ_m is a sphere surrounding an antenna. A test probe scans Σ_m and delivers two voltages at each sampling point, which relate to the local, orthogonal, spherical coordinate phasor components E_θ and E_φ. Knowing the magnitude and phase of these voltages over the sphere is then sufficient to derive a model of the source, equivalent to the antenna under test, in the sense that the model generates the same E and H fields outside of Σ_s. This principle is not limited to a spherical surface; a sphere matches the results where the measurements are obtained using a spherical test range.

Once this new radiating object is created, there is no need to know the details of the DUT to model its operation and integrate it into a more complex environment. The new equivalent source can be imported in an EM simulator. Additional conditions can be introduced, with more quantities computed to

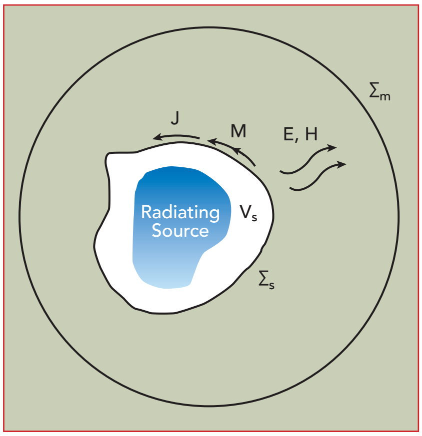

Fig. 2 Equivalent source calculated from complex voltage measurements over a sphere.

simulate the influence of nearby scattering objects on the radiation pattern, the link budget with another antenna, the exposure of a person standing in the near-field and so on (see ***Figure 3***).

Although the three steps of Figure 3 may be implemented in multiple ways,[6] we detail one as an example. In this example, the measurement data are acquired (step 1) with a system comprising an anechoic mobile antenna measurement chamber and a vector network analyzer (VNA). The Rohde & Schwarz anechoic chamber shown in ***Figure 4*** has tip-to-tip dimensions of 0.64 × 1.25 × 0.93 m between the absorbers and contains a distributed-axis positioner with a 360-degree rotating azimuth table to support the DUT. A gantry arm carries the measurement probe and provides elevation from 0 to 165 degrees. The mechanical precision of this spherical scanner is better than 0.03 degrees in both dimensions. The probe is a dual-polarized Vivaldi antenna, suitable for direct far-field and spherical near-field measurements from 12 to 90 GHz. The probe tip retains a separation of 50 cm from the center of the coordinate system, with the center accurately located using built-in lasers. The center of the DUT can be accurately positioned at this point using a crank, which enables fine DUT height adjustment.

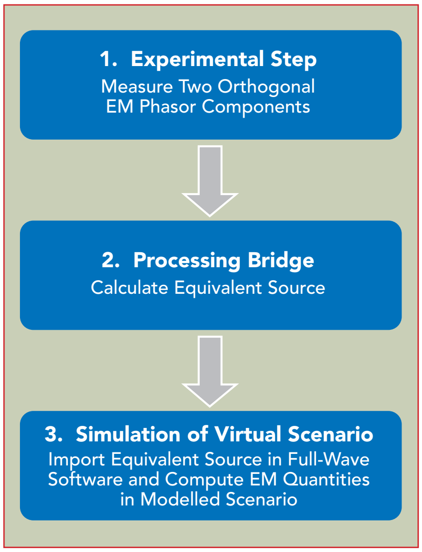

▲ Fig. 3 Steps in the measurement-simulation technique.

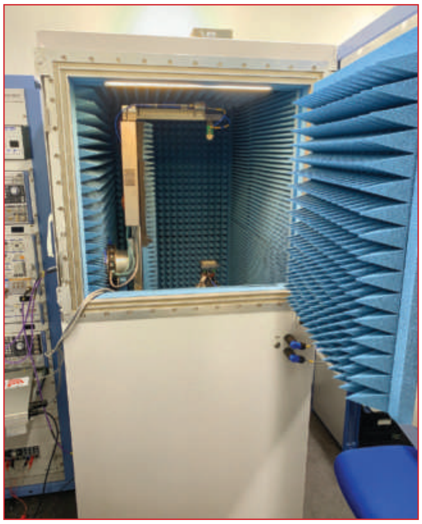

▲ Fig. 4 Anechoic chamber with spherical scanner, measurement probe supported by the elevation arm, and DUT positioned at the azimuth pole.

In this test setup, three ports of the VNA are used: Port 1 feeds the RF signal to the DUT via a cable through the azimuth pole. Ports 2 and 3 collect the received signals simultaneously, connecting to a feedthrough at the chamber side and two cables running to the two polarization ports of the probe. To avoid cable movement, rotary joints for both azimuth and elevation are integrated into the chamber. A full measurement obtains S21 and S31 (i.e., magnitude and phase) for all desired angular positions.

Step 2 is performed using the Fast Irregular Antenna Field Transformation Algorithm (FIAFTA).[2] The FIAFTA, which was developed at the Technical University of Munich, implements a generalized minimal residual equation solver for reconstructing the equivalent currents over a triangular mesh covering Σ_s from the measured S-parameters. The reference complex far-field of the test probe is injected in the algorithm to include a full probe correction. The resolution of the inverse problem is dependent on the applied domain boundary conditions. This study applies the "Huygens radiator" option, which assumes a fixed free-space impedance boundary condition at Σ_s. This approach is computationally efficient at delivering solutions for the emissions, predominantly radiating toward the outside of Σ_s. Subsequently, Σ_s was chosen to be a rectangular box

EXODUS ADVANCED COMMUNICATIONS
OUTPUT
INPUT
ONLINE
TABLE
ALC
FAULT
FAULT
POWER
OFF
ON

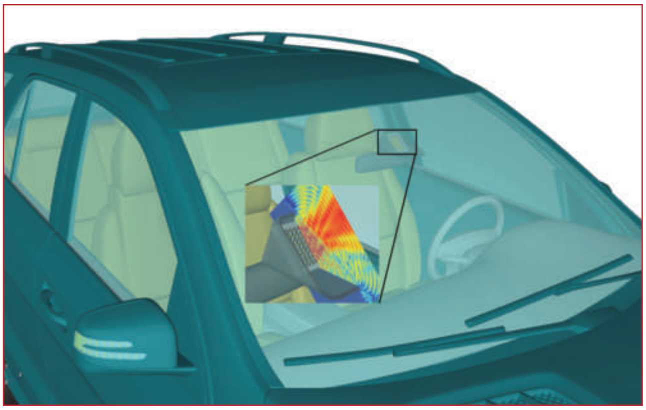

Fig. 5 mmWave antenna array integrated in the rear-view mirror.

closely encompassing the DUT.

In step 3, the box of equivalent currents is used as an EM source in the finite difference time domain (FDTD) software EMPIRE XPU by IMST GmbH.[7] To correctly import the data, equivalent currents are interpolated so the triangular mesh is converted into a cube. The original triangulation must be fine enough to ensure the stability conditions of the FDTD are fulfilled. A sampling of λ/15, where λ is the free-space wavelength, meets this requirement.

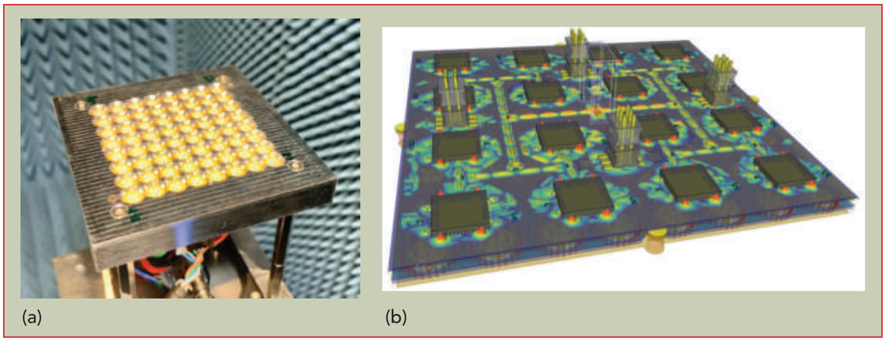

Fig. 6 Antenna side of the 8 x 8 phased array (a). Simulation of the IC side of the array, showing the E-fields at the IC and antenna feeds (b).

FULL-VEHICLE APPLICATION

Considering the full-vehicle OTA case, the measurement system shown in Figure 1 can be used to evaluate the performance of a 5G mmWave module integrated into a car; however, it is costly and time-consuming. First, the cost of a large positioning system with a mechanical accuracy meeting the requirements of near-field testing at this frequency range are exorbitant. Second, the car is unlikely to be positioned on the turntable with the antenna module at the center of the coordinate system. With an offset and the small wavelength, the probe would have to scan the upper hemisphere—at least a large portion of it—with angular resolution of less than 1 degree. The test time would be extremely long, as distributed-axis positioners of this size have typical speeds of 6 to 12 degrees/s in azimuth and 1 to 2 degrees/s in elevation, respectively. On the other hand, only performing a full-wave simulation of the antenna integrated within the car is not completely suitable, as the simplifying assumptions would not guarantee a suitable model of the real-world installation.

To show the utility of combining measurement and simulation, we study a 5G mmWave transceiver integrated in the rear-view mirror behind the windshield of a car (see ***Figure 5***). Measurements of the antenna module are used as an input to a full-wave computation, where the module is virtually integrated into a numerical model of the car. The approach uses the Rohde & Schwarz anechoic chamber measurement system with FIAFTA and EMPIRE XPU processing, previously described.

The DUT is an 8 × 8 antenna array with a mmWave front-end module operating at Ka-Band (see ***Figure 6***).[8] The array uses a 1:8 divider to distribute the signal from one waveguide interface to 16 beamforming ICs. Each IC feeds four, dual-port circular patch antennas, providing

Enabling wideband frequency agility

GaN and GaAs Solid-State Power Amplifiers for Multi-Function, Radar and EW System Design

Whether your application is narrowband, wideband or ultra-wideband, operating in pulsed or CW mode, CTT's power amplifiers are an especially attractive choice for new multi-function frequency-agile systems that effectively conserve weight, space and power consumption.

The characteristics of the portion of the electromagnetic spectrum selected for any of these particular system designs are undoubtably the most important to the end user, as it has the greatest impact on the type of information required and received.

Engineered specifically to meet the stringent requirements imposed by many modern system designs, CTT's family of GaN and GaAs-based solid-state power amplifiers excel in a wide range of applications.

CTT has delivered production quantities of amplifiers with power levels from 10 through 600 Watts – and higher – for a variety of multi-function, radar and EW applications.

- **AMDR** • **Shipboard Radar** • **SAR** • **AESA Radar** • **TCDL**
- **VLO/FLO Threats** • **New Land Radar** • **EW** • **UAVs**

More than 37years ago CTT, Inc. made a strong commitment to serve the defense electronics market with a simple goal: **quality**, **performance**, **reliability**, **service** and **on-time delivery** of our products.

Give us a call to find out how our commitment can support your success.

It's that simple.

Microwave Technology Leadership

- **Power Amplifiers**
  - **NEW GaN and GaAs Models**
  - Radar Bands up to 1kW
  - EW Bands up to 400W
  - Pulse and CW
  - Solid-State Microwave Power Modules
  - Rack-Mount Configurations
- **Low-Noise Amplifiers**
- **Up and Downconverters**
- **Subsystems**
- **SWaP Optimization**
- **Custom Engineered Options**

nsai
IS9100C
ISO 9001:2008

USA-based thin-film microwave production facility

CTT INC.

5870 Hellyer Avenue • Suite 70 • San Jose • California 95138 • Phone: 408-541-0596 • Fax: 408-541-0794
www.cttinc.com • E-mail: sales@cttinc.com

individual phase and amplitude control of every antenna element. Both physical and full numerical versions of the array were used. The numerical model, including all accessible knowledge of its architecture and key parameters, was used to design the array.

During the measurement step, the complete sphere around the DUT was scanned with 2 degree angular steps in both azimuth and elevation. To verify the results, two methods were used to compute directivity. With the first method, the acquired near-field data was processed using FIAFTA. The algorithm created the equivalent current box, which was then imported into EMPIRE XPU, where the fields were propagated via FDTD through the complete computational domain. With the second method, a far-field multilevel, fast multipole method translation, also supported in FIAFTA, was used to directly compute the far-field radiation pattern from the measurement data.[9] The results of the two methods, compared in ***Figure 7***, agree across the complete angular region. Observations of additional near-field distributions at various locations show complete consistency between the fields for Σ_S obtained only with FIAFTA and the combination with EMPIRE XPU.

In the next stage, the FDTD software was used to simulate the antenna integrated in the windshield of the car, shown in Figure 5. The computations were performed using two approaches: 100 percent numerical, where both the antenna and the vehicle were modeled, and hybrid, where the combination technique was employed, with the array represented in the EM simulation by its measurement-based equivalent source. ***Figure 8*** compares the two, showing the near-field E-field magnitudes in a defined plane at 29 GHz. The field distributions agree with some differences, especially in the region between the array and the windshield. ***Figure 9*** compares the far-field directivity patterns, showing reasonably consistent results when φ = 0 degrees and more

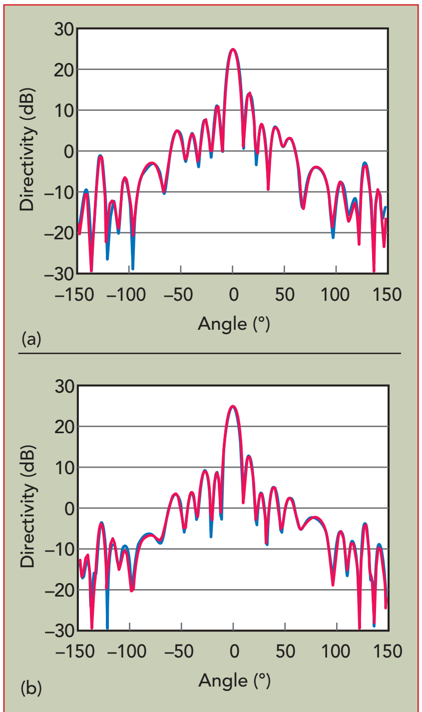

▲ Fig. 7 29 GHz azimuth patterns comparing the near-field to far-field processed results (red) with the pattern reconstructed using the combination technique (blue). φ = 0° plane (a); φ = 90° plane (b).

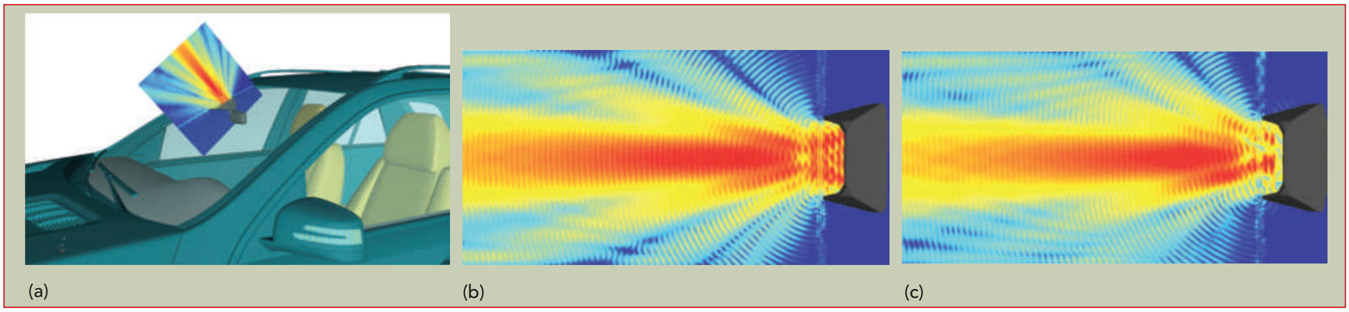

Fig. 8 Near E-fields at 29 GHz using a 40 dB scale: cut-plane orientation with respect to computed model (a), FDTD-only calculations (b) and combination technique (c).

deviations, especially in the sides lobes, when φ = 90 degrees.

These differences are expected. The FDTD model of the array does not account for production tolerances or tolerances in the operation of the electronics. Other error contributors include DUT modeling errors (e.g., imperfect knowledge of dielectric properties), measurement uncertainty and boundary conditions applied at Σ_s for deducing the radiating currents. A more systematic uncertainty evaluation is required, which will be the subject of future investigation.

At this point, neither of the two computational approaches delivers better results, i.e., closer to the real-world implementation. The hybrid or combined approach yields much

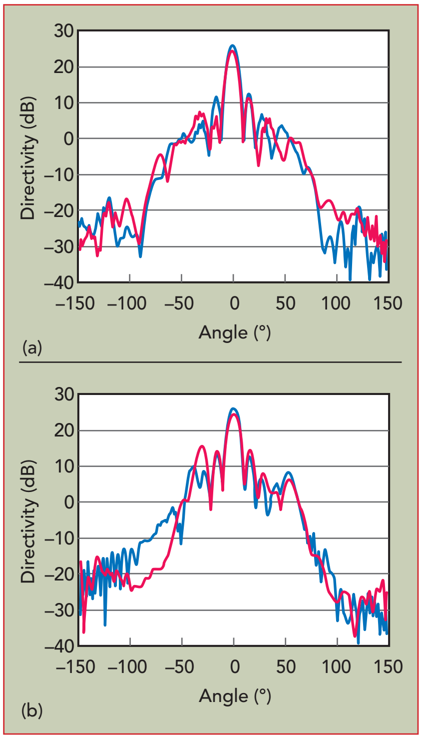

Fig. 9 29 GHz azimuth patterns comparing full-wave computation only (blue) with measurement–simulation (red). φ = 0° plane (a); φ = 90° plane (b).

higher computational efficiency than the 100 percent numerical analysis. Simulating the full EM model of the array is challenging due to the fine details in the multi-layer structure of the 5G module and the computational complexity of the scenario. Simulating the full model with 3600 million FDTD cells requires a computational time of 180 minutes and RAM usage of 108 GB. As these fine details disappear in the hybrid model, the simulation complexity drops to 320 million FDTD cells for the same calculation volume, requiring a calculation time of only 15 minutes and 10 GB of memory.

CONCLUSION

As the need to improve antenna design and performance in real-world applications is constantly growing, as is the complexity of the scenarios, converging measurements with the power of numerical computation seems an unavoidable way forward. This article presented an augmented measurement or augmented simulation technique, exploring this approach and revealing multiple advantages. Numerical computation can be made more realistic, as no a priori and in-depth knowledge of the DUT, including manufacturing tolerances, is required. Calculations are also more efficient—by 12× in speed and 10× in memory in the example described—as much of the complexity in modeling the radiating source is removed. Measurements can be more cost and time effective. In the example, an expensive, full-vehicle OTA facility can be replaced by a 1.3 m^2 spherical scanning anechoic chamber, used just to measure the array module. Integration of the module in the car is obtained by processing. Future articles will demonstrate such techniques for other applications, involving measurements of active devices transmitting modulated signals and including more systematic evaluation of uncertainty contributors.■

References:

1. *5G Automotive Association,* Web: 5gaa.org.
2. T. Eibert et al., "Electromagnetic Field Transformations for Measurements and Simulations (invited paper)," *Progress In Electromagnetics Research*, Vol. 151, Dec. 2015, pp. 127–1250.
3. R. A. M. Mauermayer, Y. Weitsch and T. F. Eibert, "Electromagnetic Field Synthesis by Hierarchical Plane Wave-based Field Transformation," *IEEE Transactions on Antennas and Propagation*, Vol. 63, No. 12, Dec. 2015, pp. 5561–5572.
4. O. Neitz, R. A. M. Mauermayer, Y. Weitsch and T. F. Eibert, "A Propagating Plane-Wave based Near-field Transmission Equation for Antenna Gain Determination from Irregular Measurement Samples," *IEEE Transactions on Antennas and Propagation*, Vol. 65, No. 8, June 2017, pp. 4230–4238.
5. T. F. Eibert, "A Diagonalized Multilevel Fast Multipole Method with Spherical Harmonics Expansion of the k-space Integrals," *IEEE Transactions on Antennas and Propagation*, Vol. 5, No. 2, Feb. 2005, pp. 814–817.
6. A. Cozza, B. Derat, N. Ribiere-Tharaud, "A Near SAR Assessment Procedure for Homogeneous and Heterogeneous Flat-phantoms Based on Near-field Free-space Measurements," *Annual Symposium Antenna Measurement Tech Assoc. (AMTA)*, Nov. 2007.
7. A. Lauer, W. Simon, A. Wien, "XPU Technology for Fast and Efficient FDTD Simulations using Modern CPUs Cache Memory Bandwidth," *European Conference on Antennas and Propagation*, Vol. 13, No. 15, Mar. 2015, pp. 2584–2589.
8. W. Simon et al., "Highly Integrated Ka-Band Frontend Module for SATCOM and 5G," *Asia Pacific Microwave Conference*, Dec. 2019.
9. A. Tzoulis, T. F. Eibert, "Fast Computation of Electromagnetic Near-fields with the Multipole Method Combining Near-field and Far-field Translations," *Advances in Radio Science.*, Vol. 4, Sept. 2006, pp.111–115.

INVITED PAPER

Characterization of Additive Phase Noise in Microwave Amplifiers

Lily Geller
Tufts University, Medford, Mass.
Paul Blount and Charles Trantanella
Qorvo, Inc., Chelmsford, Mass.

High-power signals with minimal phase noise are crucial for radar and communication systems, for phase noise is directly related to receiver sensitivity. At the heart of each system is an oscillator, which can be configured to have very low phase noise. However, oscillators tend to have low output power, so they often must be boosted by amplifiers. The addition of amplifiers presents other issues, most notably the addition of phase noise to signals passing through the system. This additive phase noise can mask a target or otherwise interfere with signal integrity and transmission.

One serious issue faced by systems designers is quantifying the level of additive phase noise, since this parameter is challenging to measure. In this article, we discuss additive phase noise and the reasons why reducing an amplifier's contribution to phase noise is important to a system's performance. We also demonstrate the techniques needed to improve additive phase noise measurements across frequencies for reliable product classification. We further investigate the impact of amplifier type and compression level on additive phase noise and explore how the optimization of these characteristics can improve phase noise performance dramatically. Finally, we verify our findings through production testing and convey the ramifications for engineering design.

ADDITIVE PHASE NOISE

Phase noise refers to the stability of a signal's frequency over time.[1–3] Ideally, an oscillator produces a perfect sinusoid at a singular frequency—which we call the carrier or desired signal—that has zero phase noise. However, the presence of noise causes all oscillators to behave in a non-ideal fashion. The two main sources of phase noise are background noise and the up-conversion of near DC (1/f) flicker noise (see ***Figure 1***).

As the figure shows, background noise is constant over time and dominates the high frequency spectrum away from the source frequency. The power of the background noise, P_N, is defined as

$$P_N = kTB \tag{1}$$

where k is Boltzmann's constant, B the frequency bandwidth and T the temperature of the system. The background noise is, therefore, related to operating conditions in addition to the oscillator itself.

The other type of phase noise, the up-conversion of flicker noise, manifests as a skirt around the desired frequency, rather than a single tone in the frequency domain. As shown in Figure 1, flicker noise decreases linearly on the logarithmic scale until it reaches the corner frequency, which is where the spectrum becomes dominated by the high frequency background noise. Since this second source of phase noise is produced close to the carrier, it causes significant signal interference.

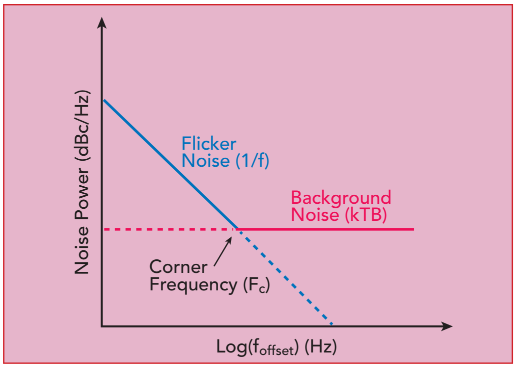

Fig. 1 Phase noise contributors in oscillators.

In a system requiring high sensitivity, an oscillator with low absolute phase noise is an ideal signal generator. However, many applications require higher power levels than a standard signal generator can produce, so amplification must be introduced into the transmit chain. Rather than solely amplifying the oscillator's carrier signal and associated phase noise skirt, though, the amplifier adds phase noise of its own (see ***Figure 2***). As shown in this figure, the width and height of the output skirt increases due to the additive phase noise of the amplifier. If an amplifier's phase noise is too high, it can overpower the noise associated with the oscillator, eliminating the benefits of a low noise oscillator. As a result, properly characterizing and measuring the phase noise of amplifiers and other components is important to ensure the successful performance of RF systems.

ADDITIVE PHASE NOISE MEASUREMENT

Additive phase noise can be notoriously difficult to measure because it is often 30 to 40 dB lower than the absolute phase noise of the reference signal.[3,4] Therefore, phase cancellation is used to perform the measurement. This method has been examined by Breitbarth and Koebel[5] and implemented in commercially available phase noise analyzers, such as the Holzworth Instrumentation HA7701A used in this study. A block diagram of the measurement setup is shown in ***Figure 3***, including the internal components of the analyzer. The block diagram shows how the phase cancellation measurement system isolates the amplifier additive phase noise.

The reference signal provides the source power for the system and is split to power the local oscillator (LO) and RF paths separately. The RF path passes through the device under test and includes attenuators to set the appropriate drive level. The attenuators before the amplifier control input power and compression level, since high power can overdrive the amplifier. The attenuators after the amplifier protect the internal mixer; they impact the phase noise readings by approximately

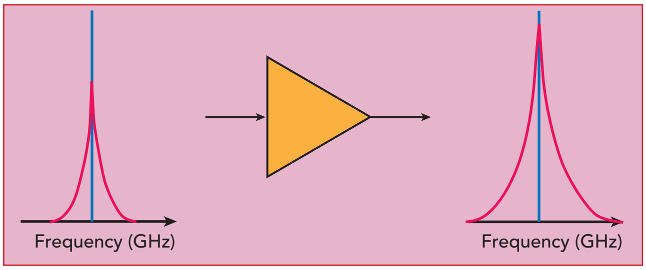

Fig. 2 An amplifier's effect on phase noise.

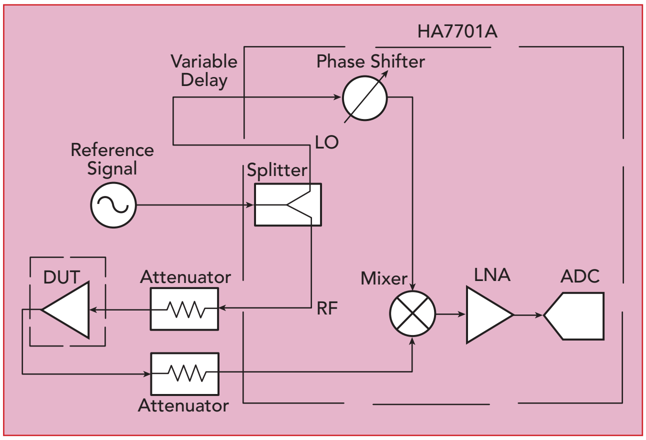

Fig. 3 Phase noise measurement setup.

1 dB, depending on the amount of attenuation. If the output power from the amplifier is very low, minimizing the RF drive attenuation is beneficial to ensure the phase noise analyzer can detect the input signal.

The LO path includes a variable delay line and a 90-degree phase shifter to maintain quadrature between the LO and RF paths. Phase cancellation is highly dependent on LO and RF phase matching, so the variable delay is important to overcome inherent errors in the phase shifter. By performing manual adjustments to the LO path, we have seen measurements improve up to 4 dB. Short cables and low loss paths are needed on the LO

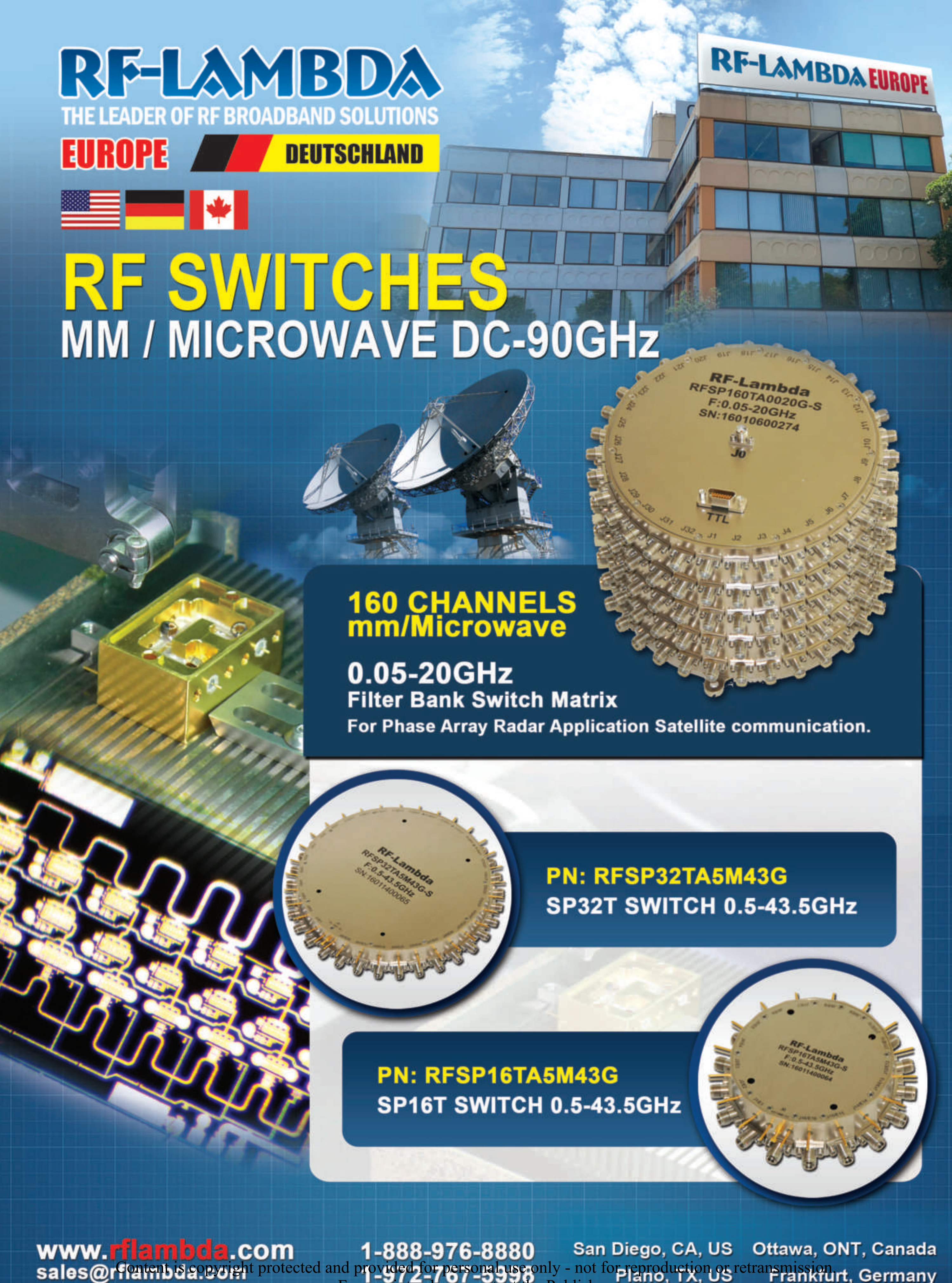
RF-LAMBDA
THE LEADER OF RF BROADBAND SOLUTIONS
EUROPE
DEUTSCHLAND
RF-LAMBDA EUROPE
RF SWITCHES
MM / MICROWAVE DC-90GHz
RF-Lambda
RFSP160TA0020G-S
F:0.05-20GHz
SN:16010600274
J0
TTL
160 CHANNELS
mm/Microwave
0.05-20GHz
Filter Bank Switch Matrix
For Phase Array Radar Application Satellite communication.
PN: RFSP32TA5M43G
SP32T SWITCH 0.5-43.5GHz
PN: RFSP16TA5M43G
SP16T SWITCH 0.5-43.5GHz
www.rflambda.com
1-888-976-8880
1-972-767-5998
San Diego, CA, US
Ottawa, ONT, Canada
Plano, TX, US
Frankfurt, Germany

TABLE 1

AMPLIFIER PHASE NOISE COMPARISON

Product	Process	Frequency (GHz)	Saturated Output Power (dBm)	Phase Noise (dBc/Hz @10 kHz offset)
CMD315	PHEMT	4–10	21	-154
CMD316	PHEMT	6–20	18.5	-149
CMD317	PHEMT	1–24	24	-160
CMD274	HBT	2–20	22	-165

side to ensure sufficient input power to the mixer, helping compensate for the output power limitations of standard signal sources, especially at higher frequencies. High LO drive of 15 to 18 dBm reduces the amplitude modulation (AM) noise in the phase detector, which lowers the system measurement floor. After the mixer cancels out the reference signal, the signal that remains represents the additive phase noise associated with the amplifier. The phase noise analyzer amplifies this using an internal low noise amplifier (LNA) and the voltage signal is applied to an analog-to-digital converter. The resulting trace provides a sweep of the single sideband phase noise by offset frequency.

Using this measurement technique, we measured amplifiers from Qorvo's standard products line, testing different power levels and frequencies. ***Table 1*** summarizes the median phase noise for four amplifiers. Compared to the reference signal's phase noise of about -120 dBc/Hz, the low phase noise values measured show the effectiveness of the test system's noise cancellation.

AMPLIFIER TRENDS

As shown in the table, the phase noise of the four amplifiers—low noise, driver and wideband distributed amplifiers—varies from approximately -150 to -165 dBc/Hz. To explain the differences, we compared amplifier topologies, but found it is not a defining factor. Rather, the differences are largely determined by device technology.

Figure 4 compares the phase noise of a PHEMT amplifier (CMD316) to one using HBTs (CMD274). The phase noise measurement of the HBT amplifier is 10 to 15 dB lower than the PHEMT amplifier when operated in saturation and at the same frequency. Although PHEMT amplifiers have higher output power and frequency capabilities than HBT amplifiers, they typically have worse phase noise. Compared to PHEMTs, HBTs have lower electron mobility, leading to less fluctuations in charge and electron movement within the device channels.[6] Less variation contributes to fewer up-conversions in HBT amplifiers, so they have considerably lower phase noise than PHEMT amplifiers.[7]

A second trend investigated for PHEMT and HBT amplifiers was the relationship between phase noise and amplifier compression, concentrating on the three main regions of an amplifier's transfer characteristic: linear, saturated and 1 dB compression. In an amplifier's linear region, the output power is directly proportional to input power. At saturation (P_{sat}), an amplifier produces no additional output power as input power increases. At 1 dB compression (P_{1dB}), the gain of the amplifier is reduced by 1 dB from its linear level, an intermediate region between linear and saturated operation. To compare the phase noise of these three states, we used attenuation to regulate the amplifier's input power to consistently measure performance and see the trends.

Figure 5 shows phase noise measurements of a PHEMT amplifier (CMD315) driven at different levels of compression. The phase noise is a minimum at P_{1dB}, achieving -156.3 dBc/Hz at 10 kHz offset, a significant phase noise improvement versus be-

Custom RF Testing from JFW...
• Transceiver Test Systems
(For Ad Hoc & Mesh Network Testing)
• Handover Test Systems
(For Cellular & WiFi Testing)
• Variable Attenuator Banks
(For Flexible Network Emulation)
• RF Matrix Switches
(Blocking, Non-Blocking, Super Non-Blocking, & More)
• RF Power Distribution Systems
(Divider / Combiner Networks)
jfw
JFW Industries, Inc.
5134 Commerce Square Drive
Indianapolis, Indiana 46237
USA
jfwindustries.com
1 (317) 887-1340
1-877-8874539

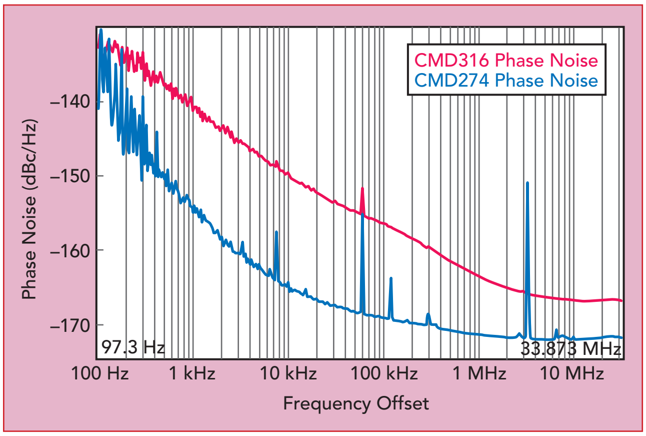

▲ Fig. 4 **HBT (CMD274) vs. PHEMT (CMD316) amplifier phase noise, both in saturation at 6 GHz.**

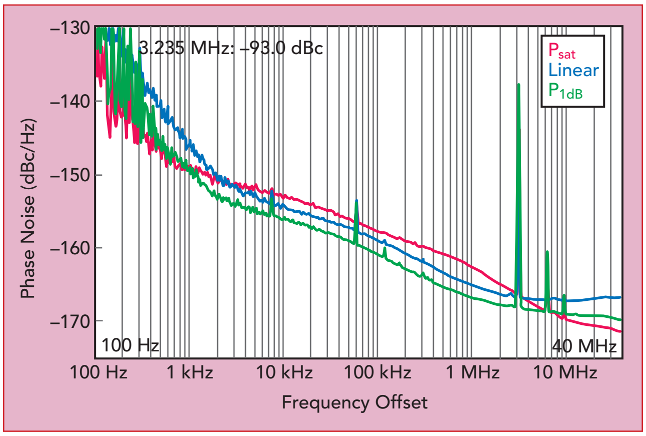

▲ Fig. 5 **CMD315 PHEMT amplifier phase noise vs. signal level at 6 GHz.**

ing operated at either linear or P_{sat}. At frequencies close to the carrier, many other amplifiers show the same trend in phase noise versus compression, i.e., the phase noise is typically minimized at P_{1dB}, followed closely by the linear drive region. Saturated operation generally leads to the highest phase noise, often 3 to 4 dB higher when compared to P_{1dB}.

We believe the optimal result at P_{1dB} can be explained considering the distortion in amplifiers caused by amplitude-to-amplitude (AM-AM) and amplitude-to-phase (AM-PM) modulation. AM-AM refers to the change in an amplifier's output amplitude depending on the input power level, while AM-PM refers to the change in the output phase of a signal depending on changes in the input amplitude. Each type of modulation contributes to the additive phase noise of an amplifier, so minimizing these distortions will minimize the overall noise.

The AM-AM and AM-PM distortions on the CMD315 PHEMT amplifier are shown in ***Figure 6***. Note that the AM-AM and AM-PM trends appear to correlate closely to amplifier saturation levels. One explanation may be the following: In the linear region (less than 0 dBm input power), both the AM-AM and AM-PM distortions are minimized. Any AM noise at the input will appear primarily as amplified, undistorted AM noise at the output and will cause minimal additional phase noise. As the amplifier enters compression around 2 dBm input power, its gain roll-off attenuates the AM-AM noise and lessens its impact on phase deviation at the output. At the same time, however, the AM-PM phase distortion begins to grow. The AM-PM distortion increases as the amplifier reaches deep saturation, while the impact from the AM-AM noise is lessened further. Therefore, it appears the contribution to an amplifier's additive phase noise is maximized in the linear region by AM-AM noise and maximized in the saturated region by AM-PM distortion. However, as shown in Figure 5, the lowest phase noise of the CMD315 amplifier is at P_{1dB}. This region represents a near ideal situation where the AM-AM distortion is partially suppressed, while the AM-PM distortion is still small, less than 2 degrees at 2 dBm of input power (see Figure 6). Operating the amplifier at P_{1dB} yields the minimum overall noise of the device and, therefore, the lowest additive phase noise. Many GaAs PHEMT and HBT amplifiers follow this trend; however, it may not be

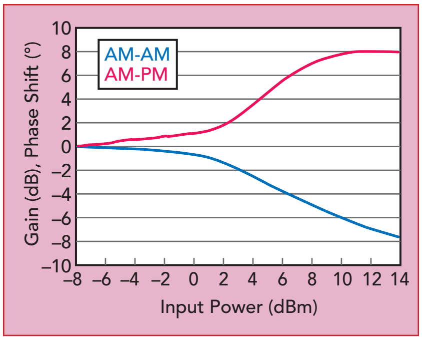

Fig. 6 AM-AM and AM-PM distortion of the CMD315 PHEMT amplifier at 6 GHz.

universal across all amplifiers, especially where the AM-PM distortion is greater at lower input power.

Finally, note a curious phenomenon in Figure 5, where the trends in phase noise change for frequency offsets of 2 MHz or greater. At these higher offset frequencies, P_{sat} becomes the preferred cooperating level to achieve the lowest phase noise.[8] This relationship is governed by

$$L = -177 - (P_{in}) + NF \qquad (2)$$

where L is the phase noise after the spectrum levels out, -177 is the power of the thermal noise floor at room temperature, P_{in} is the input power to the amplifier and NF is the amplifier's noise figure. As an amplifier enters saturation, its input power increases at a much faster rate than its output noise, resulting in decreasing phase noise at high offset frequencies. As we were more concerned about the impact of phase noise at lower offsets, e.g., <100 kHz, we did not investigate this trend further.

PHASE NOISE VARIABILITY

As phase noise will certainly vary from part-to-part and between lots, it is important for system engineers to know the bounds of this variation. We tested phase noise on production lots of the CMD264, a standard product LNA, to confirm the relationships between phase noise and power were consistent for all units in a lot. The packaged parts were manually tested using an expanded phase noise analysis setup, which included a manual production test fixture and longer cables. Since the apparatus re-

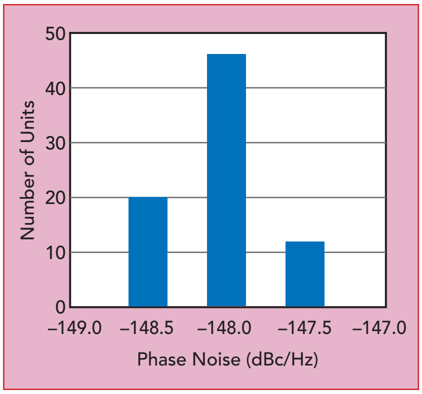

Fig. 7 CMD264 phase noise distribution at 10 kHz offset from an 8 GHz carrier at 1 dB compression.

duced connectivity and drive power levels, the average phase noise measured across the lot increased slightly compared to the initial baseline.

Figure 7 shows the phase noise distribution at 10 kHz offset for 78 units within a single lot at P_{1dB}. The phase noise variation fits a normal distribution about the mean for all units tested. Phase noise values have a range of about 1.3 dB and a standard deviation of 0.3 dB, a rela-

Our Re-Flex™ Cables Really Have the Competition Bent Out of Shape...

...Because It's Cool to Be RE-FLEXible

IW's Re-Flex Cables were designed to offer a highly flexible alternative to standard semi-rigid & conformable cables. IW's unique laminate dielectric, combined with a tin/alloy plated outer braid provide a double shielded, low loss, re-formable cable that eliminates the failure mode of traditional semi-rigid & conformable cables. Industry standard line sizes provide a range of interconnect options including SMA, TNC, N-type, 3.5mm, 2.92mm, 1.85mm, GPO™ & GPPO™, with standard length SMA male/male assemblies available from 2", in stock.

Impedance:	50 Ω	**RF leakage:**	Equivalent to semi-rigid cable
Time delay:	1.4 ns/ft	**Temp range:**	-55°C to 165°C
Cut off frequency:	62 GHz for RF 085 34 GHz for RF 141	**Bend radius:**	1/16 inch for RF 085 1/8 inch for RF 141

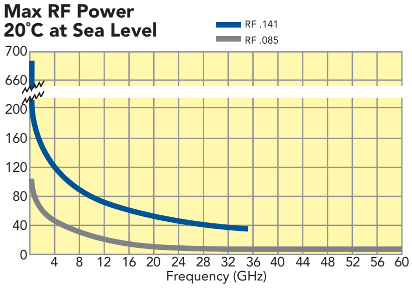

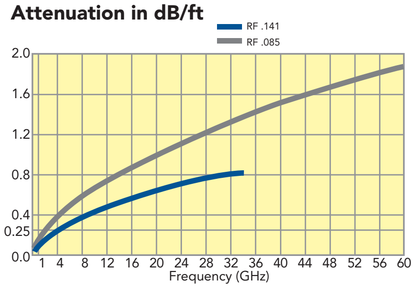

Call us today with your project specs and we'll show you the most reliable way to ***get connected*** in the industry.

AS9100 Rev. D and ISO9001:2015 certified.

Standard length SMA/SMA Re-Flex assemblies now in stock at our distribution partners!

NORTH AMERICA:
Hasco Inc., Moorpark, CA
www.hascoinc.com

Microwave Components, Inc.,Stuart, FL
www.microwavecomponents.com

UK & EUROPE:
Castle Microwave Ltd. Newbury, Berks, UK
www.castlemicrowave.com

INSULATED WIRE, INC.
203.791.1999
www.iw-microwave.com
sales@iw-microwave.com

Scan code to find out how you can ***get connected***

We're how the microwave industry ***gets connected!***

tively tight distribution for the part. The similarities indicate that phase noise is related more to the semiconductor process used for an amplifier, rather than manufacturing deviations among the units. Also, this margin of error is small enough that the relationship between compression and phase noise cannot be discounted as a measurement error.

CONCLUSION

In this article, we examined the use of a phase cancellation technique for making accurate additive phase noise measurements. We also identified methods for improving the system noise floor performance and optimizing the phase detector to enhance measurement capabilities. Using these techniques, we explored phase noise trends considering the amplifier's semiconductor process and compression level. We also validated these trends by testing amplifiers in a single lot to demonstrate phase noise consistency.

To minimize additive phase noise, we recommend selecting an HBT amplifier. To optimize the phase noise of PHEMT amplifiers, we recommend operating at P_{1dB} to minimize both AM-AM and AM-PM distortion. If operation at P_{1dB} is not feasible, then the linear region provides the next lowest phase noise. Overall, we strongly recommend considering phase noise capabilities when choosing an amplifier for sensitive RF systems.■

ACKNOWLEDGMENTS

The authors acknowledge the following colleagues for their contributions to this work: Joe Koebel and Aaron Potosky of Holzworth Instrumentation, for information about the functionality of the phase noise analyzer; R&S, for allowing access to the FSWP phase noise analyzer and the SMA signal generator to validate our findings; Keysight, for confirming our measurements during a virtual demo; Bob Festa, Paul Jackson and Pete Rutigliano of Qorvo, for their technical assistance in the lab and Helen Leung, for creating the block diagram of the phase noise measurement setup.

References

1. Custom MMIC, "Addressing Phase Noise Challenges in Radar and Communication Systems."
2. E. Rubiola and R. Boudot, "Phase Noise in RF and Microwave Amplifiers," *2010 IEEE International Frequency Control Symposium*, 2010, pp. 109–111.
3. "Mastering Phase Noise Measurements" *Rohde & Schwarz*, Oct. 2016.
4. D. Owen, "Good Practice Guide to Phase Noise Measurement," *National Physical Laboratory*, May 2004.
5. J. Breitbarth and J. Koebel, "Additive (Residual) Phase Noise Measurement of Amplifiers, Frequency Dividers and Frequency Multipliers," *Microwave Journal*, Vol. 51, No. 6, June 2008, pp. 66–72.
6. A. Dasgupta, S. Khandelwal and Y. S. Chauhan, "Compact Modeling of Flicker Noise in HEMTs," *IEEE Journal of the Electron Devices Society*, Vol. 2, No. 6, Nov. 2014, pp. 174–178.
7. P. J. Garner, M. J. Howes and C. M. Snowden, "Ka-band and MMIC pHEMT-based VCO's with Low Phase-noise Properties," *IEEE Transactions on Microwave Theory and Techniques*, Vol. 46, No. 10, Oct. 1998, pp. 1531–1536.
8. N. Garmendia and J. Portilla, "Study of PM Noise and Noise Figure in Low Noise Amplifiers Working under Small and Large Signal Conditions," *2007 IEEE/MTT-S International Microwave Symposium*, 2007, pp. 2095–2098.

Metal-flange

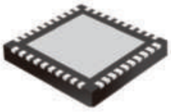

QFN

Die

ASX
AGN family
AGT

5G GaN 20 W

Internally Matched MMIC

5G

AGN0542D/M/Q	4.4~5.6 GHz	20 W

VSAT

AGN0642M	5~7 GHz	15 W
ASX0837HG	7.5~8.5 GHz	4 W
AGN1440M	12.5~14.5 GHz	10 W
ASX1436	13.5~14.5 GHz	3 W
ASX1437	13.5~14.5 GHz	5 W
ASX2934Q	27~30 GHz	2.5 W

SDR, Mobile

AGT0510	30~2700 MHz	10 W
AGT0515	30~2700 MHz	15 W

Radar

ABX0618Q	6~18 GHz	1 W
ASX1037HG	8.5~10.5 GHz	4 W
ASX1037	8.5~10.5 GHz	5 W
AGN0942D/Q	7.7~10.7 GHz	12 W
AGN0944D/M/Q	8.5~10 GHz	25 W

ISO 9001
ISO 14001
IATF 16949
www.asb.co.kr

ASB

INVITED PAPER

Applications & Considerations for Double-Ridge Guide Horn Antennas

Kevin Hietpas
Fairview Microwave, Lewisville, Texas

A general trend in telecommunications, radar and other sensing applications is higher operating frequencies, into the mmWave bands. Though the bandwidth/throughput, spectrum congestion and resolution are attractive at mmWave frequencies, mainstream applications at these higher frequencies can interfere with critical military, government, weather sensing, satellite sensing, satellite communications and other scientific research. Ensuring minimum interference for critical applications in the mmWave spectrum will be a burden on the electromagnetic compliance (EMC) certification and electromagnetic interference (EMI) authorities, as well as anyone working in applications vulnerable to unintended—or intentional—interference.

A key antenna technology for testing and EMI/RFI monitoring/surveillance is the double-ridge guide horn (DRGH) antenna. This article explores the trends influencing the utility of DRGH antennas, their performance and technology developments.

DRGH ANTENNAS

Pyramidal horn antennas are widely used, classic aperture antenna configurations, where a rectangular waveguide is gradually transitioned into a horn, which provides an impedance-matched path from the waveguide to free space. These linearly polarized waveguide antennas have been a popular choice for many high gain, point-to-point radio links at mmWave frequencies. Closed-form equations enable a designer to closely match the antenna's gain to its dimensions, and the radiation pattern can be closely approximated. However, these antennas typically perform over a relatively narrow bandwidth, which limits their use for certain testing scenarios. With EMI testing, for example, the immunity and emissions tests typically measure noise containing frequency components spanning a much wider bandwidth.

DRGH antennas introduce ridges—internal ridged arches attached to the edges of the pyramid on the E-plane—adding capacitance effects that lower the cut-off frequency of the dominant TE10 propagation mode, which extends the single-mode bandwidth. This eliminates the need for additional antennas to cover the required bandwidth, with their respective connections and potential paths for additional EMI.

The main DRGH antenna radiation pattern occurs on the main axis, i.e., at 0 degrees. At high frequencies, the main beam becomes narrower, and the side lobes increase in power. At high frequencies, i.e., >12 GHz, the main lobe splits into four off-axis lobes, where the amplitudes of these four lobes eventually surpass the power of the on-axis lobe.[1]

The components of a conventional DRGH involve the coax-to-waveguide feed, a standard pyramidal horn structure and two cen-

tral ridges (i.e., top and bottom), as shown in ***Figure 1***. Classic iterations of the DRGH antenna use dielectric sidewalls instead of the standard flared aperture found in horn antennas. The ridges are tapered to vary the impedance from the 50 Ω feed point to the impedance of free space at the aperture of the horn antenna, i.e., 377 Ω. The shielding ground of the coaxial feed is connected to the first ridge, the second ridge is connected to the center pin through an extension of the coaxial inner conductor. The cavity at the base of the structure is connected to the flared walls of the horn through a secondary metallic box, which creates a shorting plate that reduces the return loss in the waveguide transition.

DESIGN IMPROVEMENTS

Several design modifications have attempted to overcome the deteriorating radiation pattern at high frequencies.[2–4] These include:

- Adjusting the ridges to reduce edge diffraction
- Modifying the side flares with a metallic grid, dielectric sidewalls or removing them entirely

Each of these approaches improves the bandwidth of the antenna by increasing the frequency where the characteristic deterioration of the radiation pattern occurs, extending it to Ka-Band.

In some DRGH antenna designs, the ridges have a "fast" opening or rapid transition from the waveguide to free space. The downside is particularly severe at the aperture: higher mismatch and unwanted loss. The sharp edges within the ridges can also cause diffraction affecting the radiation pattern at higher frequencies. To optimize this impedance transition, various ridge designs have been used: linear, exponential, circular or other mathematical functions—even sinusoidal. Some impedance tapers use a combination of linear (near the feed), exponential (in the middle) and circular (near the aperture) to improve the antenna's performance.[3]

Modifying the side plates within the pyramidal horn structure includes completely removing the H-plane flares; adding dielectric H-plane flares; or adding thin metallic strips to form a bridge between the E-plane plates, which improves the structural integrity of the antenna (see ***Figure 2***). The conventional DRGH has one ridge positively charged, the other negatively charged, which support an E-field between the ridges that propagates toward the aperture of the horn. With this design, a high E-field occurs between the ridges and a relatively low E-field between the ridges and the flares orthogonal to them, i.e., the flares that do not have ridges. This property makes these H-plane flares extraneous. They can be removed to reduce weight, with the additional benefit of increasing the half-power beamwidth at high frequencies.[3]

Using a dielectric sidewall causes the degrading gain reduction to occur on-axis at the upper frequency limit of the DRGH, likely due to higher-order modes (e.g., TE_{20}, TE_{30}). However, removing the sidewalls entirely degrades the low frequency performance: the on-axis beamwidth increases and the gain decreases.[2] For this reason, a metallic grid is often used; it has a less severe gain dip at the upper frequencies without degrading the low frequency performance of the antenna.

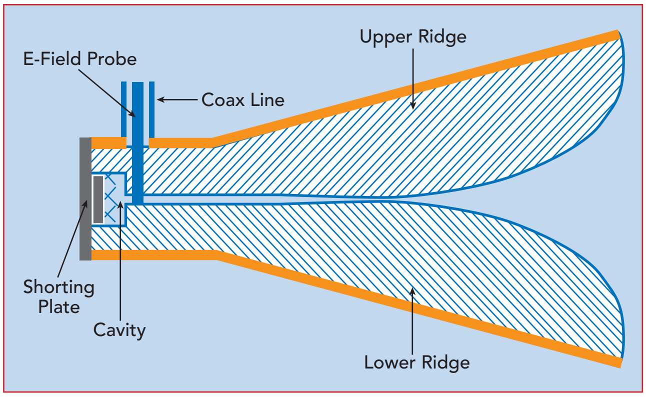

Fig. 1 **Side view of a DRGH antenna.**

Fig. 2 **DRGH antenna with metal straps for the H-plane flares.**

EMC MEASUREMENT METHODS

Electromagnetic (EM) emissions emanate from many sources, including pulse generators, oscillators, digital logic circuits, switching power supplies, motors and converters—typical components found in electronic equipment. For standards and testing, the EMI from these components is typically classified in two categories: conducted and radiated emissions. Radiated testing involves emissions testing of near-field and far-field radiation, as well as immunity testing, i.e., determining the susceptibility of a device to emissions from surrounding devices. Conducted emissions are related to the EM signals from nearby or interconnected circuits. Standards for EMC testing include:

- CISPR 16-1-4
- EN 55022/55011
- ANSI-C 63.2/63.4/63.7
- DEF STAN 59-41
- MIL-STD-461F

Typically, EMI tests occur within an open-area test site (OATS), test cell or screened room (i.e., a reverberating or anechoic chamber). Test setups use a table, where the antenna is placed at a specified distance above the ground, e.g., 0.8 m, and a determined distance from the equipment under test (EUT), typically from 3 to 30 m. The height of the antenna varies between 1 and 6 m and the EUT is rotated until the maximum emissions are observed. The tests are conducted in both horizontal and vertical polarizations, using various approaches to speed testing: an automated test setup with the EUT on a turntable, antenna on a mechanical mast, software-controlled measurement equipment and broadband antennas.

Several types of antennas are used for EMI testing (see ***Table 1***).

TABLE 1

ANTENNAS SPECIFIED FOR CONDUCTED AND RADIATED EMISSIONS TESTING

Standard	Test Type	Frequency Range	Antenna Type
MIL-STD-461	Magnetic Field Emission	30 Hz to 30 kHz	Loop
	Electric Field Emission	14 kHz to 25 MHz	Rod (Monopole)
	Emission and Susceptibility	20 MHz to 200 MHz	Biconical
		200 MHz to 1 GHz	Conical Logarithmic Spiral
		1 GHz to 10 GHz	Conical Logarithmic Spiral
	Harmonic Spurious and Output	200 MHz to 1 GHz	Cavity-Backed Spiral
		1 GHz to 12 GHz	Cavity-Backed Spiral
		12 GHz to 40 GHz	Horn
ANSI C63.4	Magnetic Field Emission	9 kHz to 30 MHz	Loop
	Electric Field Emission	9 kHz to 30 MHz	Rod (Monopole)
		30 MHz to 1 GHz	Log-Periodic Dipole Array or Calibrated Linearly Polarized
		1 GHz to 40 GHz	Linearly Polarized with a Smaller Main Lobe Than Antennas <1 GHz (e.g., DRGH)

Typically, active antennas—antennas that include components such as integral amplifiers, preamplifiers and other active devices to amplify the signal—are effective for low frequency measurements, such as active loop and active rod (monopole) antennas. E-field measurements typically use monopole antennas, while low frequency H-field measurements use loop antennas. Broadband antennas, such as the biconical antenna, can be used for the 30 to 300 MHz range, with a log-periodic antenna for 300 MHz to 1 GHz and broadband horn antenna from 1 to 40 GHz.

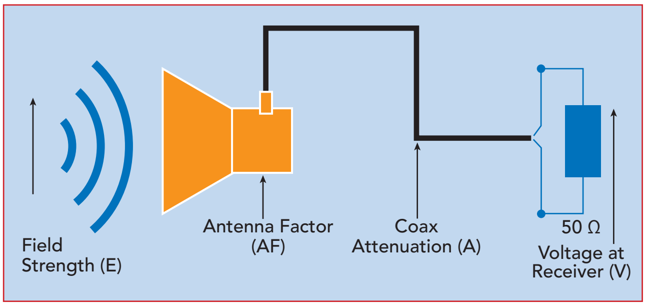

Fig. 3 Calibrating an antenna's field strength for EMS measurements.

TEST ACCURACY

For most EMC standards, the antenna is the primary measurement transducer coupling the measured variable in the antenna's radiated EM field into the measuring receiver, so understanding its behavior in the test environment is critical. The E-field strength is specified in units of V/m at a specified distance from the EUT, while the test receiver is calibrated in voltage across a 50 Ω impedance. The antenna is calibrated to the voltage at the 50 Ω input of the receiver for a given electric field strength (V/m) at a given frequency. This calibration is known as the antenna factor (AF), the incident E-field divided by the voltage measured at the receiver and specified in dB/m. While the typical parameters for measuring antenna performance are gain, VSWR and directivity, these are not as important for EMC emissions measurements as the AF. The AF gives a more accurate assessment of the antenna's

ERAVANT

FORMERLY **SAGE MILLIMETER**

POWER **AMPLIFIERS**

GaN | GaAs | COMPACT | BROADBAND | BENCHTOP | DC to 170 GHz

SAGE Millimeter is now Eravant, a change that renews our commitment to the millimeterwave industry. Since 2011, we have been delivering quality products and energizing the customer experience to meet the needs of RF engineers working on the technology of the future.

Bench Top Amplifiers
Standard and sturdy equipment grade benchtop amplifier for gain and power boosting. Both low noise and power.

Compact Lab Amplifiers
Direct power from test bench or wall outlet. Low noise and power with gain from 15 to 40 GHz. Flexible and easy to use.

Uni-Guide™ Based Amplifiers
Offered in both low-noise and power models. Various port configurations and orientations. Three frequency bands available (Ka, Q, and U-Band) from 26.5 to 60 GHz.

Standard Modular Amplifiers
Covering the frequency range of 18 to 170 GHz with gain 10 to 50 dB. Waveguide and coaxial interfaces.

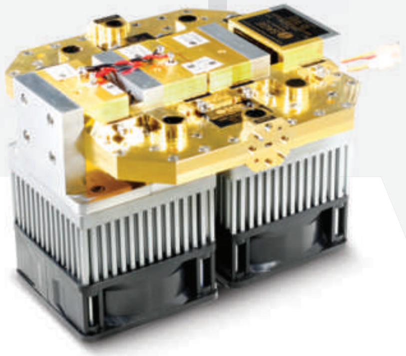

High Power Amplifiers
GaAs and GaN technology based. Power up to 10 Watts CW in the frequency range of 18 to 94 GHz.

WWW.ERAVANT.COM

www.eravant.com 501 Amapola Avenue Torrance, CA 90501
T: 424-757-0168

Adapters • Amplifiers • Antenna Feeds • Antennas • Attenuators • Bias Tees • Cable Assemblies • Corner Reflectors • Couplers • DC Blocks • Detectors • Ferrite Devices • Filters • Frequency Converters • Frequency Multipliers • Limiters • Magic Tees • Mixers • Noise Sources • Oscillators • Phase Shifters • Power Dividers • Radar Sensors • Subassemblies • Switches •

performance, ensuring the antenna is oriented for maximum response. For a typical test setup (see ***Figure 3***), the field strength at the antenna (μV/m in dB) is equal to the sum of the AF, the attenuation of the interconnecting cable (in dB/m) and the voltage at the receiver (μV in dB):[5]

$$E(\mu V/m \text{ in dB}) = AF(dB/m) + A(dB) + V(\mu V \text{ in dB}) \quad (1)$$

The AF must be known to adequately measure test site parameters such as the site VSWR and normalized site attenuation (NSA). Determining the NSA involves measuring the insertion loss between the terminals of the transmit and receive antennas and including the AF of each antenna:

$$NSA = V_{DIRECT} - V_{SITE} - AF_R - AF_T \quad (2)$$

where V_{DIRECT} is the voltage measured at the terminal of the transmit antenna, V_{SITE} is the voltage at the receive antenna and AF_R and AF_T are the AFs for the receive and transmit antennas, respectively.

The NSA of the test site is compared to the loss of an ideal site, based on a list of theoretical values over frequency, with the differences known to be deviations caused by test site imperfections. The CISPR standard for a test environment requires the site be within ±1 dB of the ideal test site, which requires a test environment to have very tight tolerances. As the calibration accuracy depends upon the site, these tolerances are necessary for measurement accuracy. Two forms of calibrations are typically performed: a tuned dipole in an OATS and the standard site method. Using a tuned dipole as a reference antenna requires retuning at each frequency and depends on the integrity of the antenna and test site. The standard site method bypasses these conditions, instead using three uncalibrated antennas that are calibrated using three measurements between pairs of antennas. However, this approach also requires a high-quality test site.

DRGH BENEFITS FOR EMC TESTING

EMC testing requires a balance between the main lobe beamwidth and gain of an antenna. The broader the beamwidth, the more energy can be collected by an antenna over an area; on the other hand, the higher the gain, the better the system noise performance. Highly directive antennas offer less sensitivity to off-axis reflections, making the imperfections of the test site less relevant. However, less area is covered at a distance, so larger objects cannot be tested. In this case, EUTs are measured in consecutive sweeps with the antenna aimed at different parts. Broader beamwidth often correlates with lower gain, so more power is required. In this case, a balun is often used at the antenna's feed to prevent damage to the antenna, particularly for biconical and log-periodic antennas, where power can accumulate in the core and windings of the antenna structure. The addition of a balun

limits the input power that can be applied, which subsequently increases the VSWR and reduces the total power being radiated and the overall efficiency of the test system.

Practically, waveguide generally dissipates excess heat from high transient powers efficiently because of the large metallic surface area of the guide. For this reason, they are often used in the antenna feeds for high frequency radars, where high-power handling is required.

The DRGH antenna has inherently higher frequency performance and higher power handling—to hundreds of Watts—compared to other broadband antennas used for EMC emissions testing, so a balun is typically not necessary when using DRGH antennas.

In an EMC test environment, the DRGH aperture dimensions are specified by many standards, defined by the distance between the antenna and the EUT. For instance, the ANSI standards require the aperture dimension of a horn antenna to be small enough so the measurement distance is equal to, or greater than, the far-field distance.[6] The far-field distance, also known as the Rayleigh distance (R_m), is given by:

$$R_m = \frac{2D^2}{\lambda} \tag{3}$$

where D is the largest dimension of the antenna aperture and λ the free space wavelength.

CONCLUSION

The DRGH antenna design modifies the classic pyramidal horn antenna to extend the bandwidth. While this leads to design challenges associated with the DRGH's radiation pattern at higher frequencies, structural adjustments can address them, such as tailoring the ridges and replacing the H-plane flares with a grid-type metallic structure. Also, the high frequency operation of the DRGH antenna can be extended without compromising its low frequency performance. The DRGH is specified in EMC emissions testing standards because of its broadband performance and coverage above 1 GHz. It is a desirable alternative to the log-periodic and biconical antennas for EMC applications.■

References

1. C. Bruns, P. Leuchtmann and R. Vahldieck, "Analysis and Simulation of a 1-18-GHz Broadband Double-ridged Horn Antenna," *IEEE Transactions on Electromagnetic Compatibility*, Vol. 45, No. 1, Feb. 2003, pp. 55–60.
2. B. Jacobs, J. W. Odendaal and J. Joubert, "An Improved Design for a 1–18 GHz Double-Ridged Guide Horn Antenna," *IEEE Transactions on Antennas and Propagation*, Vol. 60, No. 9, Sept. 2012, pp. 4110–4118.
3. M. Abbas-Azimi, F. Arazm and J. Rashed-Mohassel, "Design of a New Broadband EMC Double Ridged Guide Horn Antenna," *2006 First European Conference on Antennas and Propagation*, Nice, 2006, pp. 1–5.
4. M. Botello-Perez, H. Jardon-Aguilar and I. G. Ruiz, "Design and Simulation of a 1 to 14 GHz Broadband Electromagnetic Compatibility DRGH Antenna," *2005 2nd International Conference on Electrical and Electronics Engineering*, 2005, pp. 118–121.
5. T. Williams, "EMC for Product Designers," *Newnes*, 2017.
6. "American National Standard for Electromagnetic Compatibility–Radiated Emission Measurements in Electromagnetic Interference (EMI) Control–Calibration and Qualification of Antennas (9 kHz to 40 GHz)," *ANSI C63.5-2017 (Revision of ANSI C63.5-2005)*, May 2017, pp.1–114.

PRECISION PASSIVE COMPONENTS & ELECTRONIC PACKAGES

PROVEN RELIABILITY. TRUSTED PERFORMANCE.

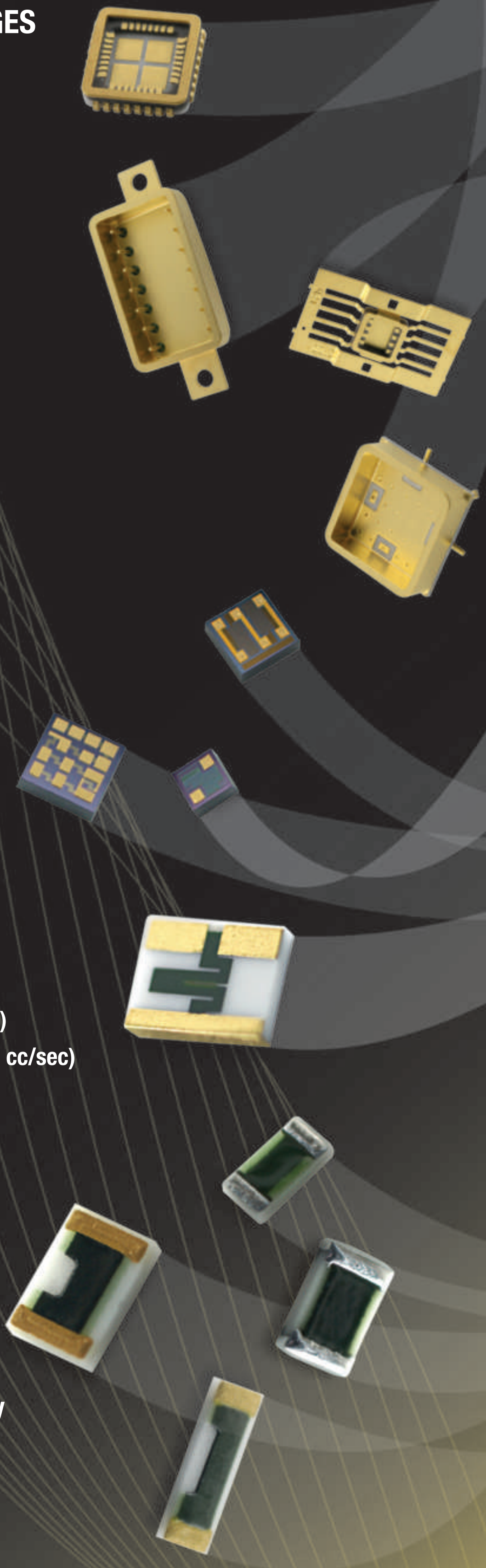

Thick & Thin Film Resistor Products

- Faithful scheduled deliveries under 2 weeks
- Values from 0.1 Ohm to 100G Ohm
- Abs. tolerance to ±0.005%, matching to ±0.0025%
- TCR's to ±2ppm/°C, tracking to ±1ppm/°C
- Operating frequencies to 40GHz
- High performance at cryogenic temperatures
- Case sizes to 0101
- Space level QPL's, F.R.-"S", per MIL-PRF-55342
- Zero failures with over 200 million life test hours
- ISO 9001:2000 certified
- Full line of RoHS compliant products
- 24-hour quote turnaround

Electronic Package Products

- Hi Reliability Hermetic Packages:
  - Lightweight glass sidewall flatpacks, SO-8, and SO-14 packages
  - Surface mount and plug-in packages
  - Metal flatpacks, leadless chip carriers (LCC), ceramic quad flatpacks (CQFP)
- Hermeticity per MIL-STD-883, Method 1014, Condition A4 (less than 10^{-10} atm cc/sec)
- Plating per MIL-DTL-45204 and QQ-N-290 for standard packages (unless otherwise specified)
- Custom design available
- RoHS and DFARS compliant

When it comes to today's military, aerospace, and medical applications, the reliability and performance requirements of electronic components have never been so demanding. By delivering superior-quality products for over forty five years, it's easy to see why Mini-Systems is a supplier of choice among design engineers.

CELEBRATING 1968–2018 50 MSI Mini-Systems, Inc.

MSI MINI-SYSTEMS, INC. SINCE 1968

508-695-0203
mini-systemsinc.com
info@mini-systemsinc.com
20 David Road, North Attleboro MA 02761-0069

Three Digitally-Controlled Tunable Filters for VHF to 18 GHz Applications

Analog Devices, Inc.
Wilmington, Mass.

Tunable filters have played an essential role in many RF/microwave signal chains, whether employed in a system front-end or as harmonic rejection for local oscillators. The new digitally-controlled tunable filter IC product offering from Analog Devices (ADI) provides leading performance with enhanced digital functionality to address many of these applications.

In today's multi-channel, wideband, multi-octave tuning systems, it is necessary to filter out unwanted blockers to preserve the signals of interest. Common ways of implementing a filter in many systems is to either use discrete switched filter banks or analog tunable filters. Discrete switched filter banks often increase board real estate, filter development time and cost—opposite the goals of lowering size, weight, power and cost. Analog tunable filters, while small and compact, have their own compromises: tuning voltage generation, phase noise and switching speed. These solutions are often designed for a specific application, requiring significant system engineering development time.

To address these compromises and reduce development time, ADI has developed three digitally tunable filter products that combine an enhanced semiconductor process with common industry packages. This results in compact filters, highly configurable by standard serial-to-parallel interface (SPI) communication and with fast RF switching speeds. ADI has incorporated a 128 state lookup table within each IC to quickly change filter states for fast frequency hopping systems. The latest products introduced by ADI are the:

- ADMV8818, with four highpass and four lowpass filters, operating from 2 to 18 GHz
- ADMV8913, with a highpass and lowpass filter, operating at X-Band
- ADMV8052, with three bandpass filters, operating at UHF and VHF frequencies

Making the difference

Sivers Semiconductors drive some of the world's most extraordinary technological achievements and we're justifiably proud of our reputation for quality, reliability, and speed.

By providing the most robust connection in any solution – our proven, cutting edge technology empowers you to dream bigger, helping you to build the future – today.

Launching a remarkable piece of engineering optimized for Fixed Wireless Access

Sivers Semiconductors presents a new, innovative RF Module covering the full 14 GHz of bandwidth (57 - 71 GHz) with 2D beam steering (steering in both azimuth and elevation). This module enables you to differentiate and meet the requirements of large-scale manufacturing of your 60 GHz Fixed Wireless Access (FWA) products without sacrificing competitive performance.

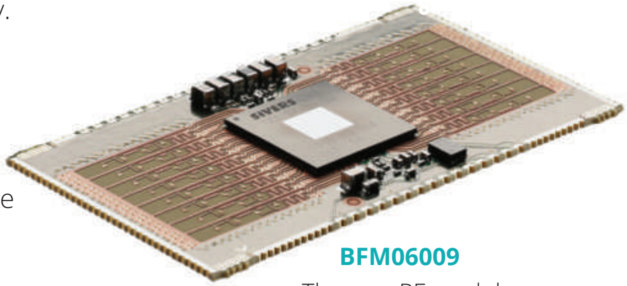

BFM06009
The new RF module
from Sivers Semiconductors

Key features

- 57-71 GHz
- Optimized and prepared for unlincensed 5G spectrum (802.11ad and 5G NR-U, TDD)
- Beam steering:
  - Azimuth ± 54 degrees
  - Elevation ± 25 degrees
- +40 dBm TX EIRP
- Autonomous calibration

For more information, please visit:
www.sivers-semiconductors.com/rf-modules/

Sivers Wireless now look for future colleagues to our upcoming US office!

We look for people that share our passion for perfection and exceeding customers' expectations. Are you the one we are looking for?

Please contact us at: **career@sivers-wireless.com**

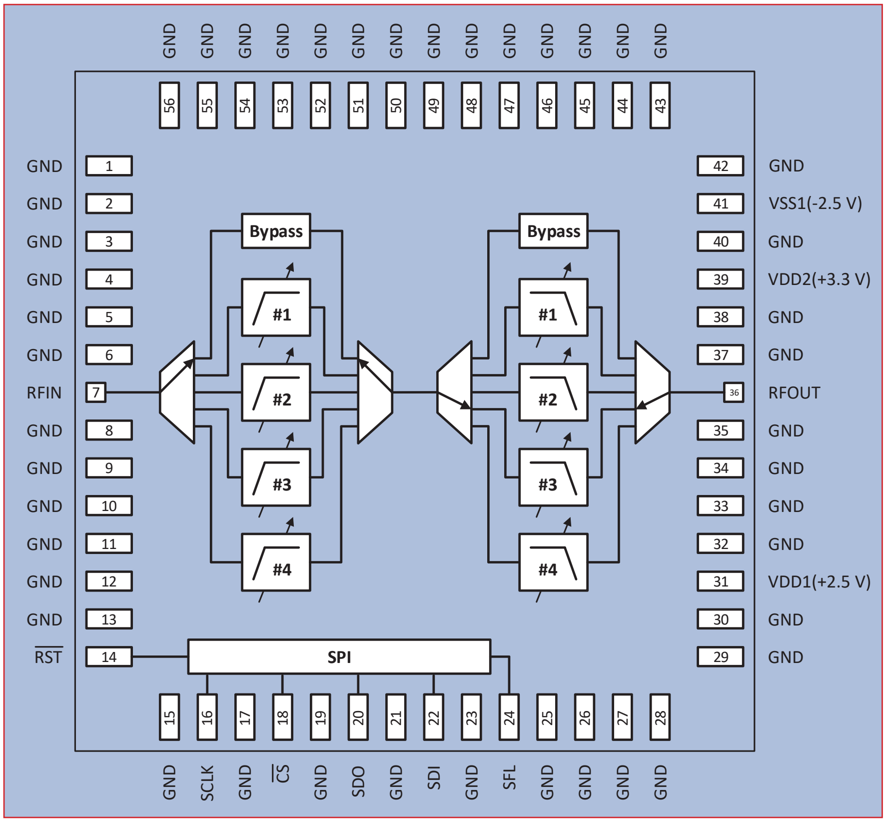

▲ Fig. 1 ADMV8818 functional block diagram.

ADMV8818

The ADMV8818 is a flexible filter that provides tunable bandpass, highpass, lowpass, bypass or all-reject responses between 2 and 18 GHz. The IC comprises two sections: input and output (see ***Figure 1***). The input has four highpass filters and an optional bypass, selected by the two RFIN switches. Similarly, the output section has four lowpass filters and an optional bypass, selected by the two RFOUT switches. Each highpass and lowpass filter is tunable with 16 states (four-bit control word) to adjust the 3 dB frequency (f_{3dB}). This flexible architecture provides full frequency coverage without any dead zones.

Any wideband defense or instrumentation application where high speed data converters are used is an application for the ADMV8818. Electronic warfare (EW) is one important application, as the filter provides rapid reconfigurability and a small form factor. This enables multi-channel systems to scan the full 2 to 18 GHz spectrum, selecting a frequency of interest to be digitized. The flexibility of the filter expands the design possibilities for future EW systems.

ADMV8913

The ADMV8913 a combination highpass and lowpass filter designed for X-Band applications (see ***Figure 2***). It has low insertion loss of 5 dB. The highpass and lowpass filters are also tunable with 16 states (four-bit control word) to adjust f_{3dB}. The ADMV8913 also has a parallel logic interface for setting the filter states without using the SPI interface. A parallel interface is advantageous for systems requiring fast filter response time because it eliminates the delay of the SPI transaction.

X-Band radar systems, whether mechanically steered or high channel-count phased arrays, often require filtering solutions that must be compact, easily configurable and have low insertion loss. The ADMV8913 is well suited for this, with low insertion loss, a small form factor and either SPI or parallel digital interface options. These features enable it to be placed close to the front of the systems to optimize performance and reduce integration complexity.

ADMV8052

The ADMV8052 integrates three bandpass filters that span bands from 30 to 520 MHz, with a typical 3 dB bandwidth of 9 percent and insertion loss of 4 dB (see ***Figure 3***). The bandwidth can be adjusted by ±2 percent, and the insertion loss will vary by ±1 dB. Depending on the location of the filter in a system, the bandwidth and insertion loss can be traded. The ADMV8052 uses a patent-pending interpolation technique enabling a simple method to adjust the filter states with an eight-

Exceptional Phase Noise

Dielectric Resonator Oscillator

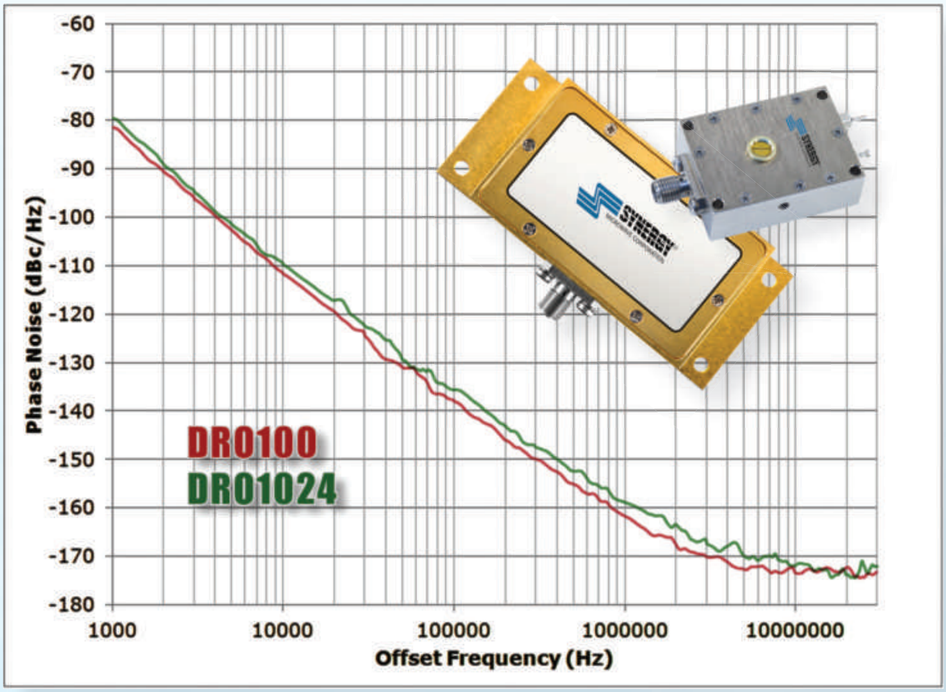

Available In Surface Mount.

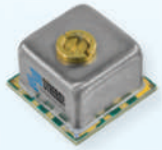

SDRO Series
0.75" x 0.75 x 0.53"

RoHS ***Patented Technology***

Model	Frequency (GHz)	Tuning Voltage (VDC)	DC Bias (VDC)	Typical Phase Noise @ 10 kHz (dBc/Hz)
Surface Mount Models				
SDRO800-8	8.000	1 - 10	+8.0 @ 25 mA	**-110**
SDRO900-8	9.000	1 - 10	+8.0 @ 25 mA	**-112**
SDRO1000-8	10.000	1 - 15	+8.0 @ 25 mA	**-107**
SDRO1024-8	10.240	1 - 15	+8.0 @ 25 mA	**-105**
SDRO1118-7	11.180	1 - 12	+5.5 - +7.5 @ 25 mA	**-104**
SDRO1121-7	11.217	1 - 12	+5.5 - +7.5 @ 25 mA	**-106**
SDRO1130-7	11.303	1 - 12	+5.5 - +7.5 @ 25 mA	**-106**
SDRO1134-7	11.340	1 - 12	+5.5 - +7.5 @ 25 mA	**-107**
SDRO1250-8	12.500	1 - 15	+8.0 @ 25 mA	**-104**
Connectorized Models				
DRO80	8.000	1 - 15	+7.0 - +10 @ 70 mA	**-114**
DRO8R95	8.950	1 - 10	+7.0 - +10 @ 38 mA	**-109**
DRO100	10.000	1 - 15	+7.0 - +10 @ 70 mA	**-111**
DRO1024	10.240	1 - 15	+7.0 - +10 @ 70 mA	**-109**
DRO1024H	10.240	1 - 15	+7.0 - +10 @ 70 mA	**-115**
KDRO145-15-411M	14.500	*	+7.5 @ 60 mA	**-100**

* Mechanical tuning only ±4 MHz

Talk To Us About Your Custom Requirements.

SYNERGY® MICROWAVE CORPORATION

Phone: (973) 881-8800 | Fax: (973) 881-8361
E-mail: sales@synergymwave.com | Web: www.synergymwave.com
Mail: 201 McLean Boulevard, Paterson, NJ 07504

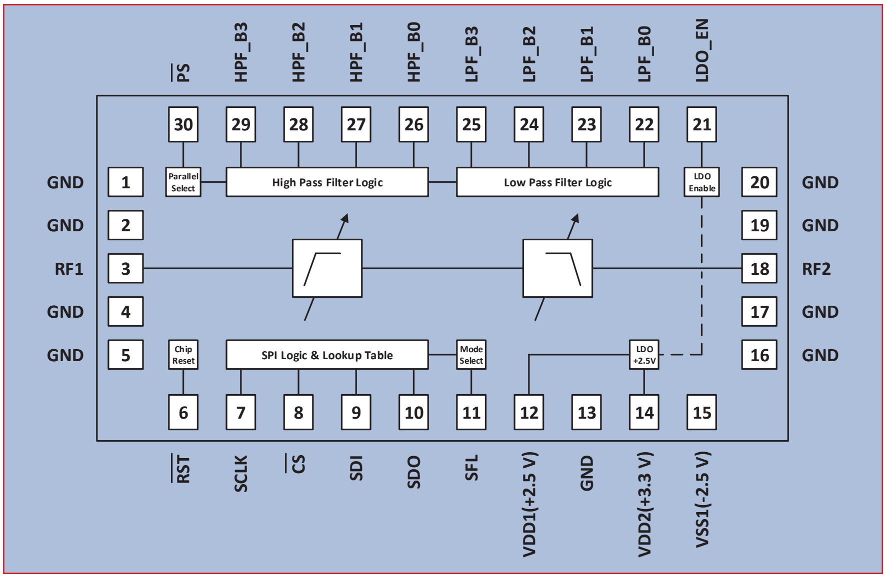

Fig. 2 ADMV8913 functional block diagram.

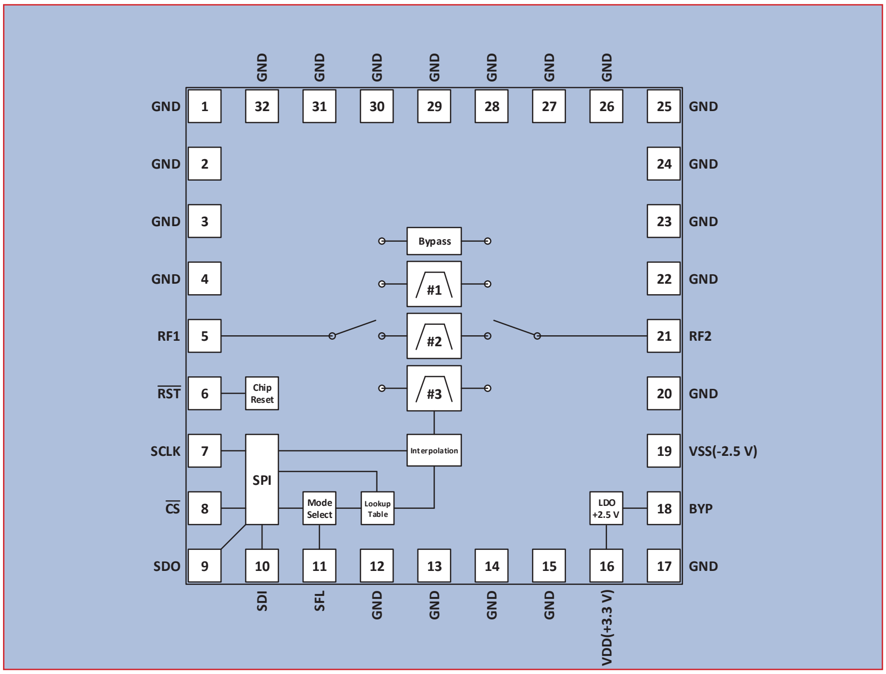

Fig. 3 ADMV8052 functional block diagram.

bit value (i.e., 256 states). Using this, each filter has approximately 0.5 percent resolution in setting the center frequency. The ADMV8052 includes a mode where the filters can be bypassed.

The VHF and UHF coverage of the ADMV8052 is tailored to next-generation radios in military and civilian communication systems—manpack, handheld and public safety—where undesired signals must be filtered. Its low insertion loss, bandpass filtering performance and digital reconfigurability simplify transceiver design.

In summary, the new digitally-controlled tunable filter IC product offerings from ADI provide leading performance with enhanced digital functionality, offering advantages for many applications. These three products are the first in ADI's digitally tunable filter portfolio.

VENDORVIEW

Analog Devices, Inc.
Wilmington, Mass.
www.analog.com

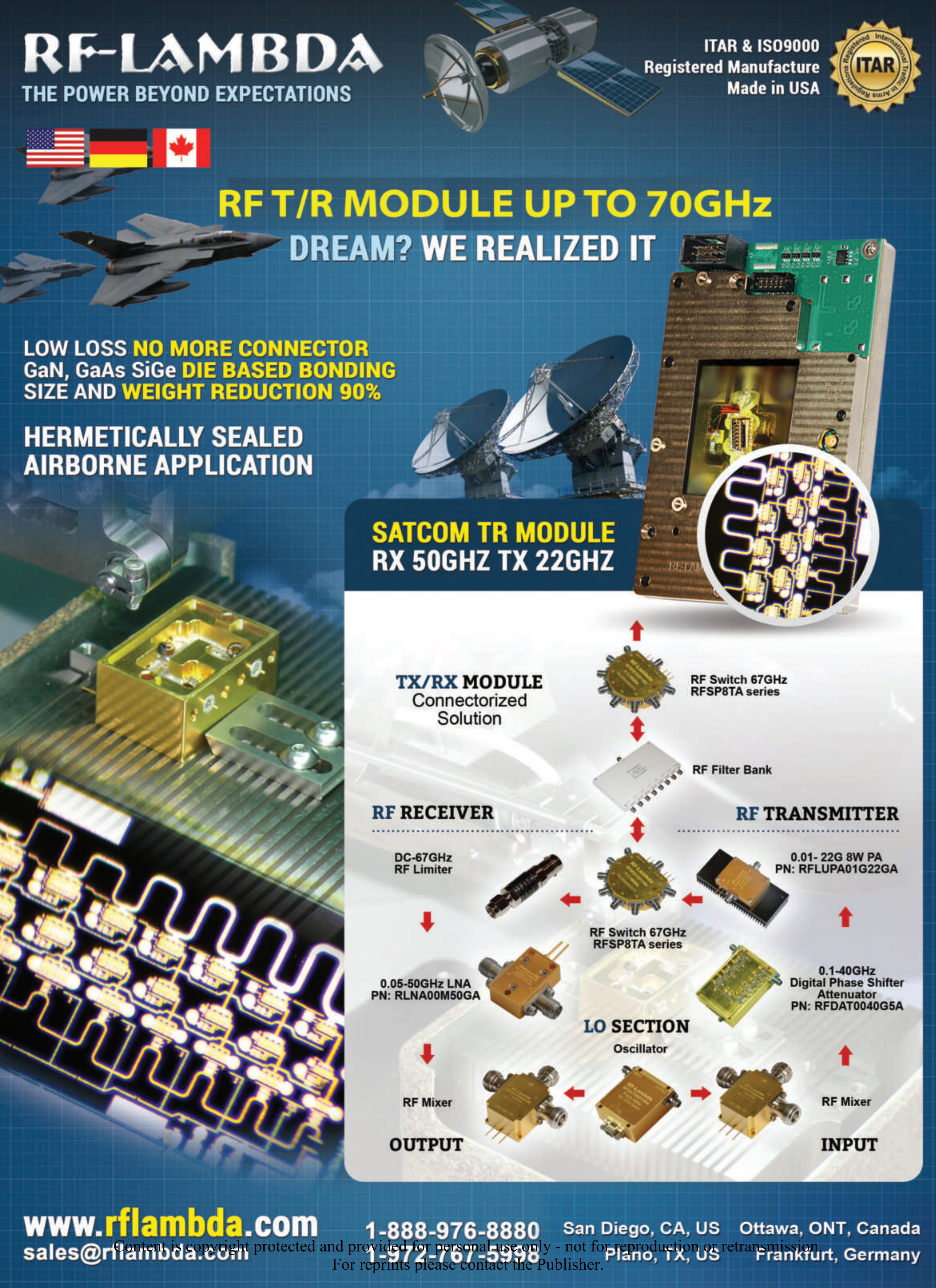
RF-LAMBDA
THE POWER BEYOND EXPECTATIONS
ITAR & ISO9000
Registered Manufacture
Made in USA
ITAR
Registered International Traffic in Arms Regulations
RF T/R MODULE UP TO 70GHz
DREAM? WE REALIZED IT
LOW LOSS NO MORE CONNECTOR
GaN, GaAs SiGe DIE BASED BONDING
SIZE AND WEIGHT REDUCTION 90%
HERMETICALLY SEALED
AIRBORNE APPLICATION
SATCOM TR MODULE
RX 50GHZ TX 22GHZ
TX/RX MODULE
Connectorized
Solution
RF Switch 67GHz
RFSP8TA series
RF Filter Bank
RF RECEIVER
RF TRANSMITTER
DC-67GHz
RF Limiter
0.01- 22G 8W PA
PN: RFLUPA01G22GA
RF Switch 67GHz
RFSP8TA series
0.05-50GHz LNA
PN: RLNA00M50GA
0.1-40GHz
Digital Phase Shifter
Attenuator
PN: RFDAT0040G5A
LO SECTION
Oscillator
RF Mixer
RF Mixer
OUTPUT
INPUT
www.rflambda.com
sales@rflambda.com
1-888-976-8880
1-972-767-5998
San Diego, CA, US
Plano, TX, US
Ottawa, ONT, Canada
Frankfurt, Germany

Wideband Power Amplifier Design: 50 Ω Operation is a Curse

Werlatone Inc.
Patterson, N.Y.

High-power transistors are formed from a group of smaller transistor cells, paralleled on a single die or in a package, to achieve the highest output power possible. As packaging and testing dominate manufacturing cost, power is "squeezed" into the package for highest cost-effectiveness. This gives the most "bang per buck," typically measured in dollars per watt. However, while increasing the power in a single package reduces device cost per watt, it lowers system efficiency through many subtle effects:

- Densely packed power transistor cells do not play well together: collocating the smaller power cells reduces thermal performance and efficiency.
- The layout of the cells must be optimized for all cells to contribute equally to the output power. The inner transistor cells run hotter, creating undesirable hot spots that reduce the cell's power.
- The optimum load impedance decreases monotonically as the transistor gets larger, becoming difficult to match into the typical 50 Ω system over a broad bandwidth. The associated low impedance bias tee becomes large and lossy and can significantly affect the output matching.
- Often, on-chip impedance matching is used to increase the optimum external load impedance to more practical levels, easing the design task for the board designer. However, the in-package matching has as much loss as doing the transformation externally.

THE SYSTEM VIEW

From a system perspective, the bang—the output power performance—is measured at the system output, not at the device. The buck—the total cost—includes cooling and the total DC power consumption. What is optimum for the device is not necessarily optimum for the system. A different bang per buck perspective for power amplifier (PA) design prioritizes increasing system efficiency and eliminating heat as the drivers determining the buck, where device bang is reduced to a "bong" by the combining efficiency. This is illustrated by the following 240 W PA example, where the conventional combiner design results in 600 W total dissipation, while the Werlatone combiner design results in only 400 W total.

CURSE OF THE 50 Ω INTERFACE

A 60 W LDMOS power transistor is selected for the design of a 240 W PA at 500 MHz. To achieve the highest output power

TABLE 1

MRF9060 OPTIMUM SOURCE AND LOAD MATCH V_{DD} = 26 V, I_{DQ} = 450 mA, P_{OUT} = 60 W Peak Envelope Power

Frequency (MHz)	Z_{source} (Ω)	Z_{load} (Ω)
930	0.80–j0.10	2.08–j0.65
945	0.80–j0.05	2.07–j0.38
960	0.81–j0.10	2.04–j0.37

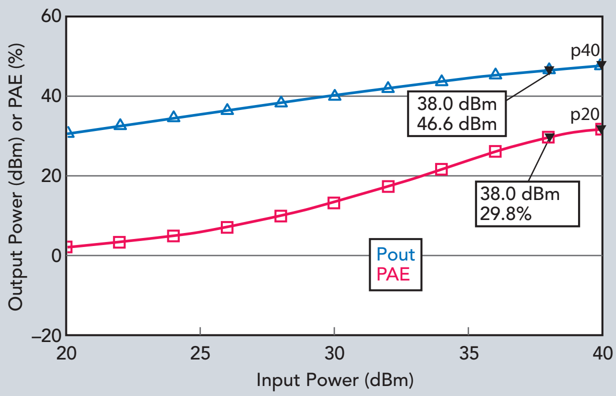

Fig. 1 Output power and PAE vs. input power at 500 MHz, with the device output matched using three N-squared transformer stages.

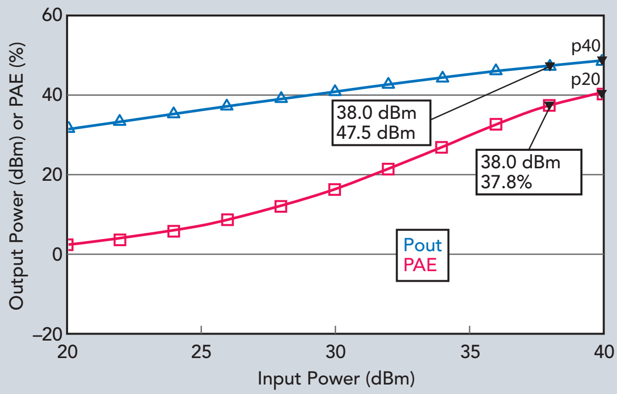

Fig. 2 Output power and PAE vs. input power at 500 MHz, with the device output matched to a 12.5 Ω four-way combiner using a single non-N-squared transformer stage.

TABLE 2

Werlatone Wideband Combiners

Model	Frequency Band (MHz)	Typical Insertion Loss/Return Loss (dB)
QH8849	80-1000	0.6 / 20
QH8922	200-2000	0.6 / 20
QH7622	500-3000	0.6 / 20
QH10541	700-6000	0.5 / 20

and power-added efficiency (PAE), the optimum source impedance and output load for the NXP MRF9060 transistor are shown in ***Table 1***. The real parts of the source and load match are 0.8 and 2 Ω, respectively. Consider the following two approaches to matching the output:

Conventional Design—Each 60 W device will be matched to 50 Ω using N-squared transformers, then combined with a four-way 50 Ω combiner to achieve a nominal 240 W. This approach requires three stages of N-squared transformers to transform from 2 to 50 Ω, which incurs 1.2 dB of insertion loss, assuming a typical insertion loss of 0.4 dB per stage. This impedance transformation reduces the output power of each MRF9060 to 46.6 dBm (45 W) from the specified 47.8 dBm (60 W) and the PAE is reduced to 29.8 percent from the specified 40 percent. The four-way 50 Ω combiner adds 0.8 dB insertion loss, making the total output power of the PA 51.8 dBm (151 W) at 25.2 percent efficiency, with a thermal dissipation of 449 W. The resulting power and PAE performance are shown in ***Figure 1***.

Alternative Design—Using a Werlatone 12.5 Ω combiner, the transistor is matched to 12.5 Ω, rather than 50 Ω. As the sum port on the combiner is at 50 Ω, combining four of the 60 W amplifiers is straightforward. With this architecture, only a single stage of a non-N-squared transformer is needed, which adds 0.3 dB insertion loss and reduces the output power of the MRF9060 to 47.5 dBm (56 W) from its specified 47.8 dBm (60 W). The PAE decreases to 37.8 percent from the specified 40 percent. The four-way 12.5 Ω combiner adds 0.5 dB insertion loss, further reducing the output power to 53 dBm (200 W) at 33.3 percent efficiency, with a thermal dissipation of 400 W. The power and PAE of the 240 W PA design using this approach are shown in ***Figure 2***.

With the conventional design, achieving 200 W output power would result in 600 W thermal dissipation. The alternative design approach reduces the loss by using impedance transforming combiners, which have less loss than four-port 50 Ω combiners. This has inspired Werlatone to design a family of input power combiners with interface impedances of 8 or 12 Ω and an output sum port of 50 Ω. ***Table 2*** shows a partial list of these combiners, illustrating the bandwidth capability Werlatone can provide. Various customized versions, with the port impedances set to customer requirements, can readily be designed, up to input-sum port impedance ratios as high as 4:1 referenced to 50 Ω over bandwidth ratios of 10:1.

SUMMARY

Werlatone's product line of transforming impedance combiners—12.5 Ω input and 50 Ω output featured in this article, but customizable to other impedances—greatly improves PA PAE by reducing transformer and combiner losses. Should more power be needed, additional transforming combiners can be used to quadruple the power with little additional combiner loss. Where an unusual impedance transformation is needed, no compromise is necessary with Werlatone's non-N-squared transformer techniques.

Werlatone Inc.
Patterson, N.Y.
www.werlatone.com
(845) 278-2220

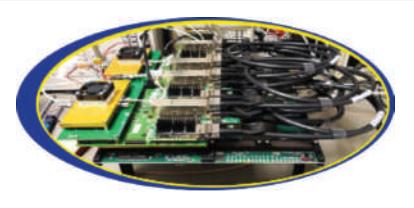

Modular, High Speed Prototyping Platform

The Micram USPA Platform is a modular, real-time signal processing platform offering speed, bandwidth and scalability to support rapid prototyping projects. Seamless integration of Micram VEGA UltraFastSiGe™ DAC and ADC signal converters, with proFPGA systems from PRO DESIGN, creates a high performance, fully programmable, real-time platform for developing and testing new signal processing algorithms; ultrafast data generation; acquisition, ASIC and SoC development applications.

The speed of Micram's established line of VEGA signal converters, combined with a current selection of over 25 high speed Xilinx and Intel® FPGAs, in single or multiple proFPGA configurations from PRO DESIGN, enables a powerful development environment. The USPA platform supports fast and capable module configurations, such as a 64 Gbaud transceiver verification system (shown above).

Unlike custom prototyping systems, investment in the Micram USPA Platform can be staged, starting with a basic configuration and scaling up as development progresses. The fully modular USPA architecture supports rapid specification and platform changes, reducing the risks often associated with leading edge or speculative design projects. USPA modules are reusable and can be quickly reconfigured to support future projects or projects running in parallel.

Micram and PRO DESIGN plan to expand the USPA platform with a series of product releases delivering faster, more complex USPA modules, incorporating the latest FPGAs, while maintaining full backward module compatibility and providing investment protection not available with custom prototyping systems.

For over a decade, Micram VEGA signal converters have been the standard for speed and bandwidth. Micram is a leader in UltraFastSiGe technology, creating record-breaking silicon devices. Micram VEGA signal converters power a line of ultrafast test and measurement products, including arbitrary waveform generators and rapid prototyping systems.

Micram
Bochum, Germany
www.micram.com

V-Band Balanced Mixer Offers Full Band Coverage

HASCO's V-Band double balanced mixer offers full waveguide band coverage, with the RF and LO frequency ranges from 50 to 75 GHz and IF from 1 to 10 GHz. The HWMX15-SFV mixer can be used either as an up-converter or down-converter and only needs 13 dBm LO drive to achieve 10 dB conversion loss, which reduces intermodulation distortion. LO to RF isolation is typically 20 dB.

The HWMX15-SFV achieves excellent performance across the extended frequency range by using zero bias, beam lead, GaAs Schottky diodes to achieve the lowest capacitance. The RF and LO ports, oriented at right angles, were designed for full WR15 coverage. The IF port, opposite the RF port, interfaces with an SMA coaxial connector, making the overall size of the mixer compact for integration in the next level of assembly.

Complementing the V-Band design, HASCO offers broadband mixers for E- and W-Band. The HWMX12-SFE covers E-Band, from 60 to 90 GHz, with WR12 waveguide RF and LO ports. The IF frequency range is 0.1 to 10 GHz. Typical conversion loss is 9 dB with +13 dBm LO drive and 20 dB LO to RF isolation. The HWMX10-SFW covers W-Band, from 75 to 110 GHz, with an IF from 0.1 to 10 GHz. The RF and LO ports mate with WR10 waveguide. With +13 dBm LO drive, the conversion loss is typically 9.5 dB, and the typical LO to RF isolation is also 20 dB.

Certified to AS9120:B and ISO 9001:2015, HASCO is a global distributor of quality RF/microwave components, specializing in a large selection of high performance connectors, adapters, attenuators, cable assemblies, terminations, filters and mixers—all available in stock for next-day delivery.

VENDORVIEW

HASCO, Inc.
Moorpark, Calif.
www.hasco-inc.com/amplifiers

E LEARNING CENTER

Presented by: Microwave Journal

Webinars

NOW 1/27

How to Efficiently Run Electromagnetic Simulation of Full Circuit Blocks

Sponsored by: cadence®

www.microwavejournal.com/events/2025

Now On Demand

RF/Microwave Design in the Era of Connected Cars

Sponsored by: cadence®

www.microwavejournal.com/events/2021

Now On Demand

RF to Millimeter-wave Front-end Component Design for 5G NR

Sponsored by: cadence®

www.microwavejournal.com/events/2020

Now On Demand

Enabling Next Generation RF System-in-Package Through Flip Chip

Sponsored by: COBHAM ADVANCED ELECTRONIC SOLUTIONS

www.microwavejournal.com/events/2009

Register to attend at mwjournal.com/webinars

FEATURED

e→Books

mwjournal.com/ebooks

MAKING WAVES

Amplifier Search Feature

Check out Agile Microwave's new parametric amplifier search feature! Find the best match for your custom specification by frequency band, gain, power, NF or model number.

Agile Microwave
www.agilemwt.com

Introducing APITV

Want to learn why quantum computing installations require coaxial attenuators? Then watch APITV! APITV delivers short, engaging videos that reveal APITech's leadership in critical components and high-reliability technologies for the most essential industries.

APITech
https://apitech.pub/3goTyiX

Software Release

The latest V15.02 release of Cadence® AWR Design Environment® software, is now available for customer download. Version 15.02 of the software contains over 50 updates and improvements.

Cadence
www.cadence.com

New Website Goes Live

Comtech PST has announced the first update of the company's website. The new format is user and mobile friendly and has information about all their products; high-power amplifiers and control components. Additionally, you can now request a virtual meeting to be setup with someone from their sales department.

Comtech PST
www.comtechpst.com

Celebrating 50 Years of Filtering Solutions

Celebrating 50 years, K&L Microwave is one of the largest suppliers of RF and microwave filters and related assemblies in the industry.

K&L Microwave
www.klmicrowave.com

SOL/SOLT Calibration Kits

In this video, Senior Product Line Manager for Interconnects with Fairview Microwave, Steve Ellis, gives you a look inside Fairview's high-quality SOL/SOLT Calibration Kits. These high precision VNA calibration kits are offered in seven connector series and are available to ship same day.

www.fairviewmicrowave.com

New 2021 RF Product Guide

Pasternack's new 2021 RF Product Guide is now available. The 374-page catalog contains thousands of in-stock products including RF cable assemblies, amplifiers, waveguide components and more!

Pasternack
www.pasternack.com

The Accidental Engineer

Reactel's new blog covering their line of filter products and topics of interest with Jim Assurian debuted this past April. Sometimes informative, sometimes funny, always interesting.

Reactel
https://reactel.com/category/blog/

Accidental Engineer

WaveFarer Radar Simulation Software Update

The new features in Remcom's WaveFarer Radar Simulation Software provide a more accurate representation of conditions that vehicles encounter in the real world. The updates include diffuse scattering from rough surfaces and transmission through materials like glass, walls, composites and more!

Remcom
www.remcom.com

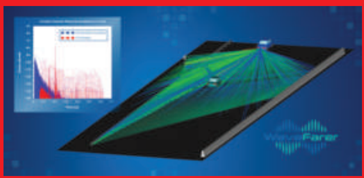

New Website Tool

Samtec recently released a tool for finding interconnect solutions faster on their website, using pictures. Products searchable include cable assemblies, cable connectors, board connectors and original solutions.

Samtec
samtec.com/picturesearch/RF

Front-End Module for 3G, 4G and 5G Applications

SKY58085-11 mid- and high-band FEM is designed to support 3G/4G/5G mobile devices and meets stringent 5G NR and LTE advanced requirements. Watch the demo today!

Skyworks
www.youtube.com/watch?v=ReBbmXNx06U

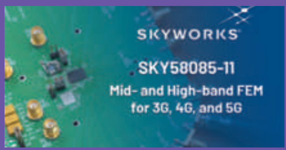

thinkRF Catalog: Real-Time Spectrum Analyzers

Deploy a WSN in the field, in-building, on vehicles for monitoring, management, surveillance of transmitters. Capture short duration, low-powered or sporadic signals of interest.

thinkRF
http://thinkrf.com/rtsa-demo-request-mwj-cu

NEW PRODUCTS

FOR MORE NEW PRODUCTS, VISIT WWW.MWJOURNAL.COM/BUYERSGUIDE
FEATURING VENDORVIEW STOREFRONTS

COMPONENTS

TTL-Controlled Bi-Phase Modulators

VENDORVIEW

Fairview Microwave Inc. has just released a new line of bi-phase modulators covering broad octave frequency bands from 0.5 to 40 GHz. These models use TTL logic to phase modulate data onto an RF carrier signal using two-phase shift keying. Useful applications include military and commercial communications systems, microwave radio, radar, high-data-rate test and measurement, serial data transmission and wireless base station infrastructure.

Fairview Microwave Inc.
www.fairviewmicrowave.com

High-Power, 300 W CW, 30 dB Coupler

Model D30H005060 is a 0.5 to 6 GHz ultra-wide band high-power 300 W CW, 3 KW peak power 30 dB directional coupler. It has DC pass function, can handle 300 W CW and 3 KW peak power. Over the very wide 0.5 to 6 GHz frequency range, it has 30 ±0.7 dB maximum coupling, 0.6 dB maximum insertion loss, ±1.0 dB coupling flatness, 1.3:1 maximum VSWR and 16 dB minimum directivity. The main line connectors are N type female. Coupling port connector is SMA female. Component size is 174.8 x 30 x 43.4 mm, operating temperature is -54° to +85°C.

Fujian MIcable Electronic Technology Group Co. Ltd.
www.micable.cn

Directional Coupler

VENDORVIEW

KRYTAR Inc. announced a new directional coupler operating in the frequency range of 0.5 to 8.0 GHz offering nominal coupling of 30 dB in a compact package. KRYTAR's new directional coupler, Model 158030, is uniquely designed for systems applications where external leveling, precise monitoring, signal mixing or swept transmission and reflection measurements are required. The new directional coupler also lends itself to wireless designs and many test and measurement applications from UHF through C-Band.

KRYTAR Inc.
www.krytar.com

3 dB Hybrid Combiner/Dividers

VENDORVIEW

High-power, 3 dB hybrid couplers useful in public safety applications for combining two transmitters to share one antenna or high-power splitting. Covering 350 to 570 MHz UHF unique air-line construction provides lowest possible insertion loss while delivering high isolation (27 dB typ), exceptional VSWR (1.15:1 typ) and superior phase balance (3 degrees maximum). Rated for 500 W average and available with 7/16 DIN and type N interfaces. Made is U.S. with 36-month warranty.

MECA Electronics Inc.
www.e-MECA.com

Direct Reading Digital Display Waveguide Attenuator

Millimeter Wave Products (Mi-Wave) has released a new 515 series, highly accurate direct reading digital waveguide attenuator. Based on the industry standard 510 series direct reading attenuator, the new model 515 boasts resolutions down to 0.01 dB, 0 to 20 dB and 0.1 dB from 20 to 60 dB. Attenuation accuracies rival vector network analyzer performance. Waveguide bands WR-112 to WR-03 are available. The attenuator operates from a standard USB C that charges the internal battery, up to 40 hours of usage and powers the unit.

Millimeter Wave Products Inc.
www.MIWV.com

Fixed Attenuators Designer's Kit

VENDORVIEW

Mini-Circuits' model K1-QAT+ fixed attenuators designer's kit contains five of each of 15 different-value fixed attenuators, or 75 total attenuators, each with bandwidth of DC to 50 GHz. The kit supplies miniature fixed attenuators with values of 0, 1, 2, 3, 4, 5, 6, 7, 8, 9, 10, 12, 15, 20 and 30 dB. Typical VSWR for the 0 dB attenuator is 1.05:1 from DC to 5 GHz and 1.39:1 from 40 to 50 GHz.

Mini-Circuits
www.minicircuits.com

High Performance RF Circulators/ Isolators

VENDORVIEW

Pasternack has just expanded its line of high performance circulators/isolators that are ideal for 5G telecommunication, automotive radars, satellite communication, point-to-point radios and aerospace applications. Pasternack's extended selection of RF circulators/isolators includes 75 models with a maximum power rating of up to 100 W. They cover operating frequency ranges up to 42.5 GHz and are available with same-day shipping with no minimum order quantity.

Pasternack
www.pasternack.com

PIN Diode Attenuator

VENDORVIEW

PMI Model PDVAT-100M20G-30-8B is an eight-bit programmable 30 dB PIN diode attenuator with a step resolution as low as 0.25 dB over the frequency range of 100 MHz to 20 GHz. This model offers excellent attenuation accuracy and flatness over the entire 100 MHz to 20 GHz frequency range. At 30 dB the measured attenuation accuracy is ±0.09 dB and flatness of ±0.87 dB. Operates on a single +12 VDC to +15 VDC supply at 150 mA maximum/measured at 64 mA.

Planar Monolithics Industries Inc.
www.pmi-rf.com

High-Power 18 GHz SPDT Switch

RLC Electronics announced the addition of a high-power 18 GHz SPDT switch with N connectors to its product capabilities. The switch can handle 1,000 W at 100 MHz, 200 W at 4 GHz and 125 W at 18 GHz and provides high reliability, long life and excellent electrical performance characteristics over the frequency range (including high isolation). Options on the switch include operating mode (failsafe or latching) and coil voltage (12 or 28 VDC), as well as indicator circuitry and a TTL Driver.

RLC Electronics
www.rlcelectronics.com

Vehicular Power Conditioner

thinkRF™ P120 vehicular power conditioner powers in-vehicle equipment through a standard vehicle power supply while protecting equipment from vehicular power transients. The P120 is a must have for mobile spectrum analysis applications. The P120 is designed to give a single regulated output of +12 VDC under different input voltages ranging from +8 V to +32 V. The P120 is compact, lightweight and portable for easy use in vehicles, vans, boats or UAVs. Protect your equipment today.

thinkRF™
www.thinkrf.com

CABLES & CONNECTORS

PHASEFLEX Microwave/RF Test Assemblies

GORE PHASEFLEX microwave/RF test assemblies by W. L. Gore & Associates are considered the Gold Standard for aircraft testing. Military aircraft applications such as radar, EW and C5ISR suites demand reliable testing. For test applications that require precise, repeatable measurements, microwave/RF test assemblies from Gore provide excellent phase and amplitude stability with flexure. Gore's rugged, lightweight assemblies deliver reliable performance with longer service life and reduced equipment downtime resulting in lower costs for testing in laboratory, production and field test environments.

W. L. Gore & Associates
www.gore.com

AMPLIFIERS

2 to 26.5 GHz Bypassable Amplifier

VENDORVIEW

The AM1101 is a broadband bypassable amplifier covering the 2 to 26.5 GHz frequency range. The device provides low noise figure and flat gain across the entire frequency range while drawing only 100 mW of power. Packaged in a 3 mm QFN with an integrated amplifier bypass path and internal 50 Ω matching, the AM1101 represents a dramatic size reduction over a discrete implementation of a bypassable amplifier.

Atlanta Micro Inc.
www.atlantamicro.com

"U" Series Amplifiers

VENDORVIEW

AR RF/Microwave Instrumentation has added two amplifiers to its "U" (Universal) Series. The new models, 150U1000 (150 W) and 250U1000A (250 W), both cover the 10 kHz to 1,000 MHz bandwidth, adding even more options to a series of amplifiers with universal applications. These Class A amplifiers replace the need for multiple amplifiers to cover the same bandwidth and eliminate dual-band operation. They are fully mismatched tolerant. Ideal for EMC testing, medical/physics research and many other applications.

AR RF/Microwave Instrumentation
www.arworld.us

Solid State Power Amplifier Module

COMTECH PST introduced its latest development for the TWT Replacement market covering the full 2000 MHz to 6000 MHz band providing 75 W linear power in a small, compact, lightweight, ruggedized form factor, ideally suited for UAV, fixed wing, rotary wing applications. This SSPA features built in protection and monitoring circuits, low voltage prime power input, high efficiency and reliable solid-state technology. Unit will self-protect under fault conditions and automatically return to normal operation when fault conditions are removed.

COMTECH PST
www.comtechpst.com

S-Band Magnetron Driver 2.9 to 3.5 GHz

VENDORVIEW

Empower RF's model 2239 produces a minimum 1 KW peak pulsed power with pulse widths up to 500 μsec. Duty cycles up to 20 percent and 400 KHz PRF's are noteworthy. A fast TTL gate input is standard and its use optional when complete shutoff of the output stage is desired between pulses. The 2239 is an intelligent amplifier in a compact 3U rack compatible footprint with features ideal for integrating into Magnetron, IoT, Klystron and TWT systems.

Empower RF
www.EmpowerRF.com

D-Band Low Noise Amplifier

SBL-1141741365-0606-E1 is a D-Band low noise amplifier with a typical small signal gain of 13 dB and a nominal noise figure of 6.5 dB across the frequency range of 110 to 170 GHz. The DC power requirement for the amplifier is +8 VDC/40 mA. The input and output port configuration offers an inline structure with WR-06 waveguides and UG-387/U-M anti-cocking flanges. Other port configurations are available under different model numbers.

Eravant
www.eravant.com

Wideband HPA

VENDORVIEW

ERZIA Technologies has announced the release of a new, compact, wideband high-power amplifier (WHPA) that operates from 2 to 20 GHz (S-Band through K-Band) while providing 37 dBm of output power and 36 dB of gain. This extremely linear wideband amplifier is being used in some of the industry's most sophisticated military, aerospace and SATCOM applications and is being discovered for other uses in microwave radio and telecom, industrial, laboratory and even deep space applications.

ERZIA Technologies
www.erzia.com

Low Noise Amplifier

VENDORVIEW

Exodus Advanced Communications offers a low noise amplifier covering 2 to 18 GHz. The LNA1019A produces 24 dBm power with a minimum power gain of 60 dB. The unit is a compact Class A linear design for optimum reliability and ruggedness for all applications. The unit has nominal dimensions of 53.4 × 25.5 × 9.7 mm with SMA female connectors.

Exodus Advanced Communications
www.exoduscomm.com

New**Products**

Dual Channel DVGA

VENDOR**VIEW**

RFMW announced design and sales support for a digital variable gain amplifier (DVGA) from Renesas. The F0443, dual DVGA is a highly integrated 0.6 to 2.7 GHz device designed for use in diversity/MIMO receivers. Two independent receiver paths deliver 29.5 dB typical maximum gain and 3.2 dB NF at 2.5 GHz. For each path, gain control is split into four separate digital step attenuators: DSA0 provides 6 dB of attenuation in a single step.

RFMW
www.rfmw.com

Bi-directional SSPA

Triad RF Systems has announced the development of a dual, bi-directional amplifier that supports 2 × 2 MIMO radio applications. Model TTRM2005D is a solid-state-power amplifier (SSPA) that operates at a frequency of 2,200 to 2,500 MHz. It is designed for military and commercial use and supports a variety of signal types, from simple CW/FM signals to complex, highly modulated carriers such as 64 and 256QAM.

Triad RF Systems
www.triadrf.com

SOURCES

Front-End Module (FEM)

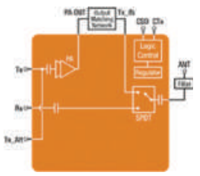

Skyworks introduced the SKY66121-11, a high efficiency, high performance transmit/receive FEM that provides greater than 4x range extension. The device features low power consumption and enables fast switch timing in a compact 4 x 4 mm package. The SKY66121-11 is ideal for IoT applications including smart metering, connected home, smart city sensors and industrial, scientific and medical.

Skyworks Solutions Inc.
www.skyworksinc.com

High Performance Low Noise Fixed PLO

VENDOR**VIEW**

Z-Communications Inc. announced a new RoHS compliant fixed frequency phase locked loop model that is sure to enhance any application needing premium performance while operating in the X-Band region. The SFS13500H-LF is a simple to use plug and play PLO allowing for quick and simple integration into any system design. It is specified to produce a fixed signal at 13.5 GHz while locked to an external 100 MHz reference oscillator source.

Z-Communications Inc.
www.zcomm.com

SOFTWARE

Multiphysics® Version 5.6

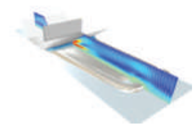

COMSOL has released version 5.6 of the COMSOL Multiphysics® software. The new version features faster and more memory-lean solvers for multicore and cluster computations, more efficient CAD assembly handling and application layout templates. A range of new graphics features—including clip planes, realistic material rendering and partial transparency—offer enhanced visualization for simulation results. Four new products expand the capabilities of COMSOL Multiphysics for modeling fuel cells and electrolyzers, polymer flow, control systems and high accuracy fluid models.

COMSOL
www.comsol.com

COMPLETE+3D Library™ v20.8

VENDOR**VIEW**

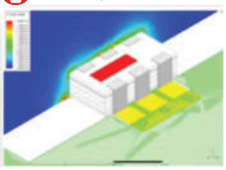

Modelithics announced the release of version 20.8 of the COMPLETE+3D Library for use with Ansys HFSS. The library contains over 325 highly scalable Microwave Global Models™ for capacitor, inductor and resistor families from many popular vendors, plus a collection of nearly 300 Modelithics' 3D geometry models for inductors, capacitors, filters, packages and connectors. This library now represents a total of 22,000 individual components with circuit and/or 3D EM models. Version 20.8 adds nine new part value, pad and substrate scalable models.

Modelithics
www.modelithics.com

Radar Simulation Enhancements in WaveFarer

VENDOR**VIEW**

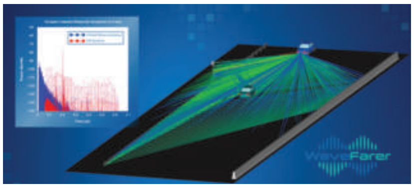

Remcom announced diffuse scattering from rough surfaces and transmission through materials in the latest release of WaveFarer®, its high fidelity radar simulation software for drive scenario modeling and indoor detection applications. New features reveal backscatter from road surfaces and vehicle interiors, elevating realism of simulations by providing a more accurate representation of conditions in the real world. In addition, several new tools increase accuracy for target detection, including scripts for setting up simulations with chirp waveforms and post-processing utilities for predicting Doppler velocity and generating range-Doppler plots.

Remcom
www.remcom.com

ANTENNAS

Dual-Band GNSS/BT Embedded Antenna

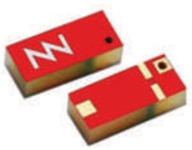

Richardson RFPD Inc. announced the availability and full design support capabilities for the DUO mXTEND™ dual-band embedded antenna from Fractus Antennas S.A. The DUO mXTEND antenna booster is part of a new generation of antenna solutions based on Fractus Antennas' Virtual Antenna™ technology. This technology enables replacing conventional and custom antenna solutions with a new class of antenna boosters, including miniature and off-the-shelf chip antenna components.

Richardson RFPD Inc.
www.richardsonrfpd.com

ONLINE PANEL SERIES

Evolution of the RF Front End

January 26

The smartphone RF Front End has dramatically evolved over the last decade moving from a discrete amplifier and controller module to a complex module with duplexers/filters, switches, controllers and amplifiers that have to consider more than 1,000 frequency band combinations which will grow to more than 10,000 with 5G. This panel will discuss the evolution of the RF Front End from 4G to 5G; the best current technologies for acoustic filters, switches, amplifiers and power management; will OpenRF work to reduce costs and improve performance; and what future mobile device RF Front Ends are expected to look like.

Sponsored by:

Qualcomm | TELEDYNE e2v | Semiconductors Everywhereyoulook | GLOBALFOUNDRIES | RichardsonRFPD An Arrow Company

Will Open RAN Work?

Now On Demand

Open RAN promises to lower network costs and barriers to entry to create competition through the standardization of hardware and software. But will this reduce the innovation in hardware and software design by dumbing down the systems? Will it increase security risks? Will it decrease economies of scale that the larger companies have developed? How would this effect RF component design and integration with system providers? What are the test challenges and can standard testing be implemented? This panel discusses and debates the pros and cons of Open Radio Access Networks from a components and sub-systems point of view along with testing challenges and solutions. The session will be moderated by Joe Madden of Mobile Experts.

Sponsored by:

Qualcomm | KEYSIGHT TECHNOLOGIES | ANALOG DEVICES AHEAD OF WHAT'S POSSIBLE™ | VIAVI Solutions | XILINX

Organized by: Microwave Journal

Register Now at mwjournal.com/onlinepanels

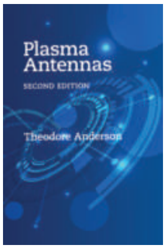

Plasma Antennas, Second Edition

Theodore Anderson

"Amongst the most prominent antenna engineers of the last 150 years, Dr. Anderson deserves a place. History will treat him well. My advice is to enjoy the book, then keep it as it will increase in value every day you have it on the bookshelf."

—Kevin O. Shoemaker,
Senior Systems Scientist, Specialized Arrays, Inc.,
Antenna and Radar Engineer, Melbourne, Fla.

This updated edition of an Artech House classic contains steering, focusing and spreading of antenna beams using the physics of refraction of electromagnetic waves through a plasma. Pulsing circuitry for ionizing plasma antennas with low-power requirements are covered. New and improved smart plasma antenna and applications to Wi-Fi and the applications of plasma antennas are discussed. Experimental work on plasma antenna noise and new progress on ruggedization and custom-made plasma tubes are also presented.

This unique resource provides readers with a solid understanding of the efficient design and prototype development of plasma antennas to meet the challenge of reducing the power required to ionize the gas at various plasma densities. Thorough coverage of the technical underpinnings of plasma antennas, as well as important discussions on current markets and applications are discussed. Additionally, the book presents experimental work in this cutting-edge area and reveals the latest developments in the field.

To order this book, contact:

Artech House
www.artechhouse.com
Email: artech@artechhouse.com
US 800-225-9977
UK +44 (0)20 70596 8750

ISBN: 978-1-63081-750-3
350 pages
$169 £147

Use code PA25 to receive 25% discount on this title! (expires 01/31/2021)

IEEE Boston Section

Advancing Technology for Humanity

Professional Development & Education for Advancing Your Career

Upcoming WEBINARS

Artificial Intelligence Series—What's in it for me?

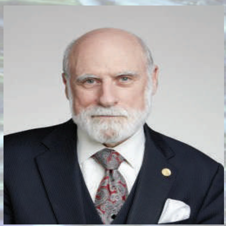

Vinton G. Cerf
Google

Steve Wozniack
Apple Computer

Helen Greiner
iRobot

REGISTRATION OPEN!

http://ieeeboston.org/artificial-intelligence-webinar-series/

Python Applications for Digital Design & Signal Processing on February 4, 2021 with Dan Boschen, Principal Engineer, Microchip

Register Now at http://ieeeboston.org/python-for-signal-processing/

Registration for our Self-Paced On-Demand Courses available ieeeboston.org

Plus Free IEEE Webinar Technical Talks!

One Centre Street, Suite 203, Wakefield, MA | Tel 781-245-5405 | Email: ieeebostonsection@gmail.com

IEEEBOSTON.ORG

AdvertisingIndex

Sales Representatives

Microwave Journal

Eastern and Central Time Zones
Michael Hallman
Associate Publisher
(NJ, Mid-Atlantic, Southeast, Midwest, TX)
4 Valley View Court
Middletown, MD 21769
Tel: (301) 371-8830
FAX: (301) 371-8832
mhallman@mwjournal.com

Shannon Alo-Mendosa
Northeastern Reg. Sales Mgr.
(New England, New York, Eastern Canada)
685 Canton Street
Norwood, MA 02062
Tel: (781) 619-1942
FAX: (781) 769-5037
salomendosa@horizonhouse.com

Pacific and Mountain Time Zones
Brian Landy
Western Reg. Sales Mgr.
(CA, AZ, OR, WA, ID, NV, UT, NM, CO, WY, MT, ND, SD, NE & Western Canada)
144 Segre Place
Santa Cruz, CA 95060
Tel: (831) 426-4143
FAX: (831) 515-5444
blandy@mwjournal.com

International Sales
Richard Vaughan
International Sales Manager
16 Sussex Street
London SW1V 4RW, England
Tel: +44 207 596 8742
FAX: +44 207 596 8749
rvaughan@horizonhouse.co.uk

Germany, Austria, and Switzerland (German-speaking)
WMS.Werbe- und Media Service
Brigitte Beranek
Gerhart-Hauptmann-Street 33,
D-72574 Bad Urach
Germany
Tel: +49 7125 407 31 18
FAX: +49 7125 407 31 08
bberanek@horizonhouse.com

France
Gaston Traboulsi
Tel: 44 207 596 8742
gtraboulsi@horizonhouse.com

Israel
Dan Aronovic
Tel: 972 50 799 1121
aronovic@actcom.co.il

Korea
Young-Seoh Chinn
JES MEDIA, INC.
F801, MisahausD EL Tower
35 Jojeongdae-Ro
Hanam City, Gyeonggi-Do
12918 Korea
Tel: +82 2 481-3411
FAX: +82 2 481-3414
yschinn@horizonhouse.com

China
Shenzhen
Michael Tsui
ACT International
Tel: 86-755-25988571
FAX: 86-755-25988567
michaelt@actintl.com.hk

Shanghai
Linda Li
ACT International
Tel: 86-021-62511200
lindal@actintl.com.hk

Beijing
Cecily Bian
ACT International
Tel: +86 135 5262 1310
cecilyb@actintl.com.hk

Hong Kong, Taiwan, Singapore
Mark Mak
ACT International
Tel: 852-28386298
markm@actintl.com.hk

Japan
Katsuhiro Ishii
Ace Media Service Inc.
12-6, 4-Chome,
Nishiiko, Adachi-Ku
Tokyo 121-0824, Japan
Tel: +81 3 5691 3335
FAX: +81 3 5691 3336
amskatsu@dream.com

Ed Kiessling • Traffic Manager • 685 Canton Street, Norwood, MA 02062 • Tel: (781) 619-1963 FAX: (781) 769-6178 • ekiessling@mwjournal.com

FABS and LABS

IQE – The Origin of Most Compound Semiconductor Devices

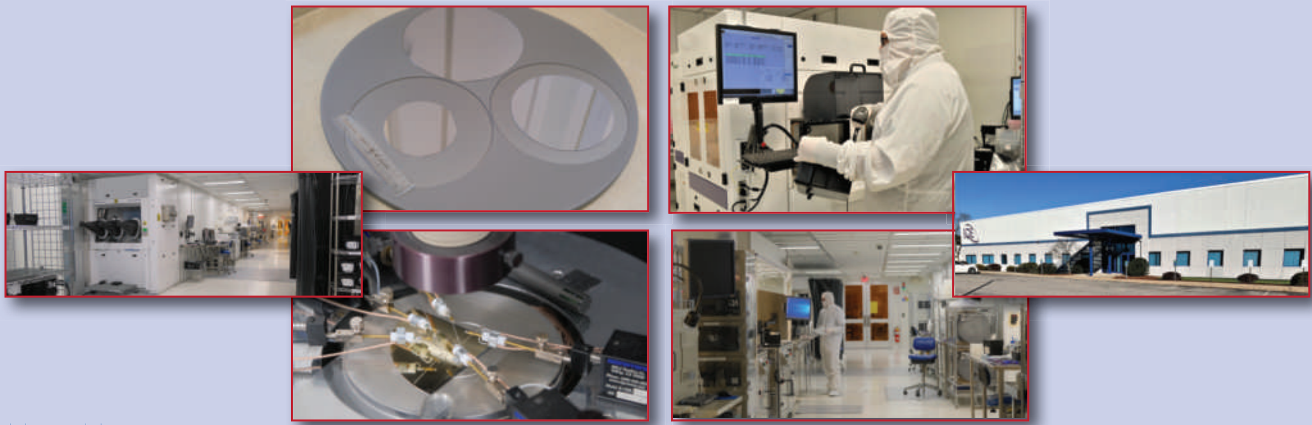

Most major smartphone launch events are soon followed by "teardown" reports describing how the latest semiconductor IC technologies have been implemented, including which companies won the prized design-ins for RF FEM, 3D sensing, display and power components. Semiconductor companies have created ICs that drive every facet of modern life by connecting us, energizing commerce, enabling education and much more. Many of these IC companies have become household names, but have you ever wondered about the origin of the semiconductor wafers that form the foundation of every electronic and optoelectronic device?

IQE plc is the leading global supplier of advanced compound semiconductor wafers and material solutions. Headquartered in Cardiff, Wales, and operating from manufacturing sites in the U.K., U.S., Taiwan and Singapore, this scale and global footprint allows IQE to ensure security of supply for customers in all parts of the world. IQE's 30-year leadership position is underpinned by a comprehensive product portfolio spanning nearly every major semiconductor material including GaAs, GaN, InP, GaSb, Si, SiGe and others.

IQE's Taunton, Massachusetts facility (IQE-MA) annually produces hundreds of thousands of leading-edge GaAs and GaN epitaxial wafers. Acquired from Kopin in 2013, the 65,000 ft^2 facility was built in 2001. IQE-MA supplies GaAs HBT, BiHEMT and BiFET wafers for 5G FEMs as well as GaAs vertical cavity surface emitting lasers (VCSELs) for 3D sensing, LiDAR and illumination. In 2020, IQE-MA completed an expansion of GaN manufacturing capacity to meet growing demand for 5G infrastructure and defense applications. This increased capacity has also been utilized for GaN-based emitters for high resolution displays including LED/laser development for emerging 5G, automotive, datacom and IoT applications.

The IQE-MA production floor consists of 8,500 ft^2 of Class 1000 cleanroom and is populated by epitaxial growth reactors and metrology equipment. Certain areas associated with wafer handling and QA/QC inspection are provisioned to Class 10. The GaAs and GaN growth reactors use a process known as metalorganic chemical vapor deposition (MOCVD) that produces highly ordered, single crystalline semiconductor materials with precise control of layer thicknesses and alloy compositions. The MOCVD reactors are configured for high throughput with servicing from a maintenance chase while always loading/unloading wafer product from the cleanroom side. IQE-MA is QMS-certified to ISO 9001:2015. Environmental, health and employee safety are top priorities and are certified to ISO 14001:2015.

The IQE-MA facility employs device fabrication and test capability, not for the production of device-level products, but to enable IQE to sample device performance from batches of as-grown wafers before shipping to customers. This capability has proven invaluable for control of production epitaxial processes and helps streamline product development. If IQE can demonstrate, via internal device fabrication and test, the benefits of a change to an epitaxial structure, it can reduce the number of fab cycles required at customer sites. This, in turn, reduces product development schedules and improves time-to-market. Device fabrication steps such as photolithography, wet processing, dielectric deposition and etching take place in a class 1000 cleanroom. Device test (I-V & C-V) and semiconductor materials characterization (such as XRD, AFM, SEM, Hall and photoluminescence) complete the full suite of materials and device capabilities.

A major part of ubiquitous wireless connectivity is enabled by IQE epitaxial wafers. IQE materials are the basis of devices employed for Wi-Fi, RF infrastructure, satcom, automotive, defense, gesture/facial recognition, cloud/networking/IoT, healthcare, industrial and many other applications. Utilizing state-of-the-art facilities such as IQE-MA, IQE has firmly established its position as the world's largest pure-play compound semiconductor epitaxial wafer supplier.

www.iqep.com

WERLATONE®

WE ARE HIGH POWER

NEW E-PLANE COMBINERS

Higher CW Power & Increased Duty Cycle Relative to Radial Combiners

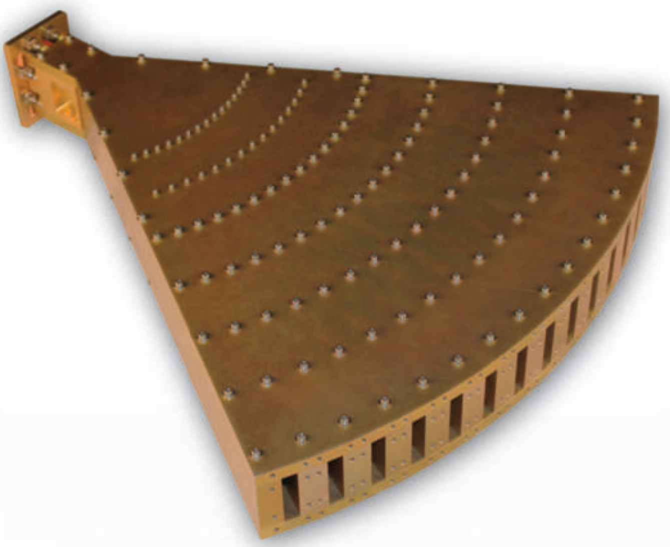

C-Band
E-Plane 16-Way Combiner
5300 - 5900 MHz
12,000 W CW, 2.5 MW Peak
WR159 Output, Half Height WR159 Inputs

- Combine Multiple High Power Solid State Power Amplifiers
- Planar Structures
- N-Way Architectures
- Coaxial or Waveguide Inputs
- Extremely Low Insertion Loss
- Scalable for S, C, X, Ku, Ka Bands
- Patented Werlatone Technology

*** CW & Peak Power of E-Plane Limited by Power Handling of Waveguide Output Connector Rating.**

Frequency	Output Waveguide	Radial Combiners	E-Plane Combiners
S-Band	WR284	≈ 2.0 kW CW	**≈ 36.0 kW CW**
C-Band	WR159	≈ 1.6 kW CW	**≈ 12.0 kW CW**
X-Band	WR90	≈ 0.55 kW CW	**≈ 2.4 kW CW**
Ku-Band	WR62	≈ 0.42 kW CW	**≈ 1.4 kW CW**
Ka-Band	WR28	≈ 0.02 kW CW	**≈ 0.4 kW CW**

Werlatone, Inc. 17 Jon Barrett Road Patterson, NY 12563 845-278-2220 sales@werlatone.com www.werlatone.com